Intelligent Multi-Sensor Measurements to Enhance Vehicle Navigation and Safety Systems

DTFH61-07-H-00026

- LiDAR Lane Detection
- Camera Lane Detection
- Sensor Integration

Motivation for Research

- 53% of U.S. highway fatalities in 2008 due to unintended lane departure accidents.
- Potential to save almost 20,000 lives.
- Goal : prevent lane departure fatalities by fusing multiple vehicle sensors

•From Google Images

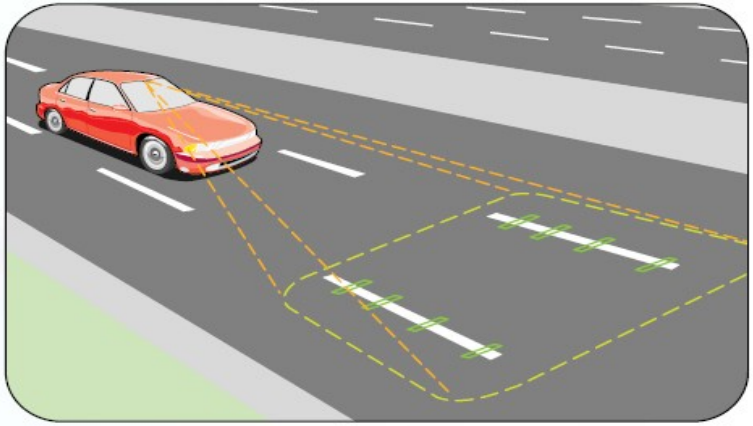

•From www.iteris.com

Approach

- The goal of this project is to design a system that can track lateral lane position on a highway
- 3 types of vehicle sensors to detect lane position
  - GPS/Map
  - Camera
  - (Light Detection and Ranging) LiDAR
- Fused sensors to take advantage of the strengths of each sensor to provide a more robust solution

Sensors

www.novatel.com

www.xbow.com

- Novatel Propak®-V3
  - GPS Receiver
  - 2Hz Update Rate
  - Provided Raw Measurements
- Crossbow 440 IMU
  - IMU
  - 50 Hz Update Rate
  - 3 Accelerometers / 3 Gyros
- Ibeo ALASCA XT
  - 4 layer simultaneous scanning
  - 3.2 ° vertical field of view
  - Capable of .25 ° resolution
  - Rotation frequency 8-40Hz
- Camera
  - Quickcam Pro 9000 webcam
  - Low cost, low resolution

Sensor Integration - Track Survey

- In order to use GPS to measure lane position, an accurate map of the lane must constructed.
- For our project, we surveyed the NCAT test track in Opelika, AL.

Results

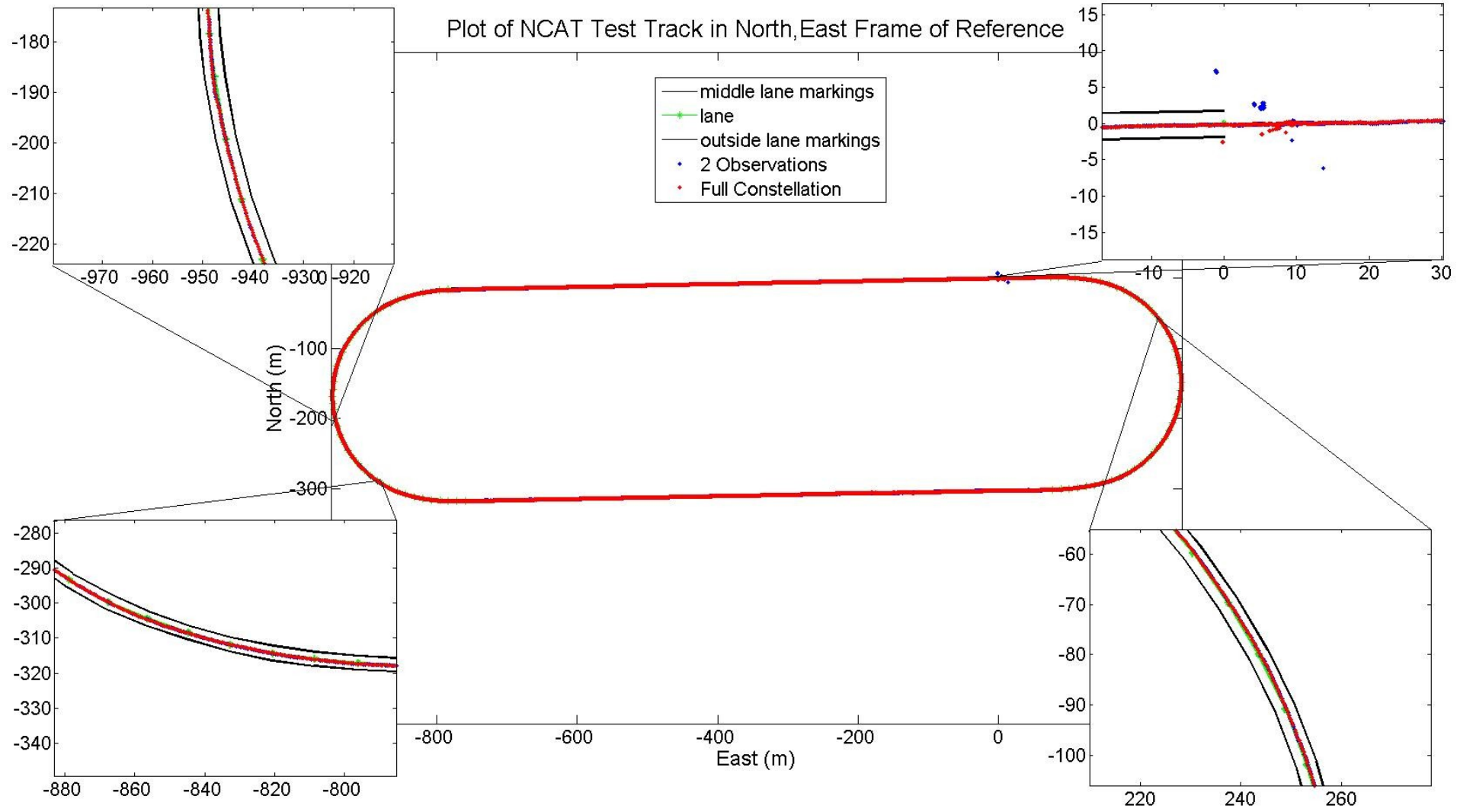
Plot of NCAT Test Track in North,East Frame of Reference
middle lane markings
lane
outside lane markings
2 Observations
Full Constellation
North (m)
East (m)
-180
-190
-200
-210
-220
-970 -960 -950 -940 -930 -920
15
10
5
0
-5
-10
-15
-10 0 10 20 30
-100
-200
-300
-800 -600 -400 -200 0
-280
-290
-300
-310
-320
-330
-340
-880 -860 -840 -820 -800
-60
-70
-80
-90
-100
220 240 260

Dissemination of Results

- Published Papers

- Allen, J. and Bevly D. “Use of Vision Sensors and Lane Maps to Aid GPS/INS under a Limited GPS Satellite Constellation.” In *Proceedings of the ION GNSS*, 2009.

- John Allen, Jordan Britt, Chris Rose, David Bevly, “Intelligent Multi-Sensor Measurements to Enhance Vehicle Navigation and Safety Systems, The Institute of Navigation 2009 International Technical Meeting, January 2009.

- Allen, J. and Bevly D. “Relating Local Vision Measurements to Global Navigation Satellite Systems Using Waypoint Based Maps.” *IEEE PLANS*, 2010.

- Britt, Jordan H., Bevly, David M., "Lane Tracking using Multilayer Laser Scanner to Enhance Vehicle Navigation and Safety Systems," *Proceedings of the 2009 International Technical Meeting of The Institute of Navigation*, Anaheim, CA, January 2009, pp. 629-634.

- Jordan Britt,, David Bevly “LiDAR Calibration Method for Vehicle Safety Systems”, SAE World Congress Intelligent Vehicle Initiative (IVI) Technology Advanced Controls and Navigation, April 2010.

- Britt, J.; Broderick, D. J.; Bevly, D. & Hung, J., “Lidar attitude estimation for vehicle safety systems”, *Position Location and Navigation Symposium (PLANS), 2010 IEEE/ION*, 2010, 1226 -1231

- Thesis – Jordan Britt, *Lane Detection Calibration and Attitude Determination with a Multilayer LiDAR for Vehicle Safety Systems*, 2010

- D.J. Broderick, J. Britt, J. Ryan, D.M. Bevly, J.Y. Hung, “Simple Calibration for Vehicle Pose Estimation Using Gaussian Processes,” *Proceedings of the 2011 International Technical Meeting of The Institute of Navigation, San Diego, CA*, January 2011.

- Rose, C. and Bevly, D. “Camera and Inertial Measurement Unit Sensor Fusion for Lane Detection and Tracking using Polynomial Bounding Curves.” In *Proceedings of the ION GNSS*, 2009.

- Rose, C. and Bevly, D. “Vehicle Lane Position Estimation with Camera Vision using Bounded Polynomial Interpolated Lines.” In *Proceedings of the ION Technical Meeting, 2009*.

- Thesis – Christopher Rose, *Lane Level Localization with Camera and Inertial Measurement Unit using an Extended Kalman Filter*, 2010

Dissemination of Results

- Presentations
  - Mid-point presentation to FHWA at Turner Fairbanks
  - Presentation to Nissan at Auburn AL.
  - Presentation to Honda at Auburn AL.
  - EAR kickoff Presentation to Automotive Advisory Board at Auburn, AL.
  - Presentation at TRB at Washington D.C.

Closing Comments

- Questions?

AUBURN
UNIVERSITY

Camera-based Lane Detection

Christopher Rose
David Bevly

Motivation

- We can save lives.
  - In 2008 52% of all highway fatalities occurred from unintended lane departure
    - Nearly 20,000 deaths
  - In 2006 it was 58%, comprising nearly 25,000 deaths
  - In short: more fatalities than any other crash type occur due to single vehicle road departures

Overview – Camera Lane Detection

- Introduction
  - Background
- Vision System
  - Image Processing
  - Line Processing
  - Linear Kalman Filter
  - Calculations
  - Vision System Experimental Results
- Vision/INS/Velocity Integration
  - State Structure
  - Time Update
  - Measurement Update
  - Vision/IMU/Velocity Experimental Results
- Conclusions
  - Future Work

Introduction

- Lane departure warning systems are already present in commercial vehicles; however, these systems are limited by the quality of the images obtained from cameras. Use of other sensors in addition to vision can provide the position within the lane even when lane markings are not visible.

Background

- C.R. Jung
  - Linear-parabolic model to create an LDW system using lateral offset based on near-field and far-field
- Y. Feng
  - Improved Hough transform for detection of road edge and establishment of an area of interested based on the prediction result of a Kalman filter
- E.C. Yeh
  - Obtained heading and lateral distance from single camera images
- D.A. Schwartz
  - Clothoid model for the road is unsuitable for sensor fusion
- T.J. Broida
  - 3-d motion estimation with a monocular camera

Contributions

- Specific contributions include:
  - Use of vision and inertial data specifically for lateral position estimation in the lane
  - Tracking of the lane in the image using only inertial data when the image fails to detect lines

Vision System

Vision Algorithm

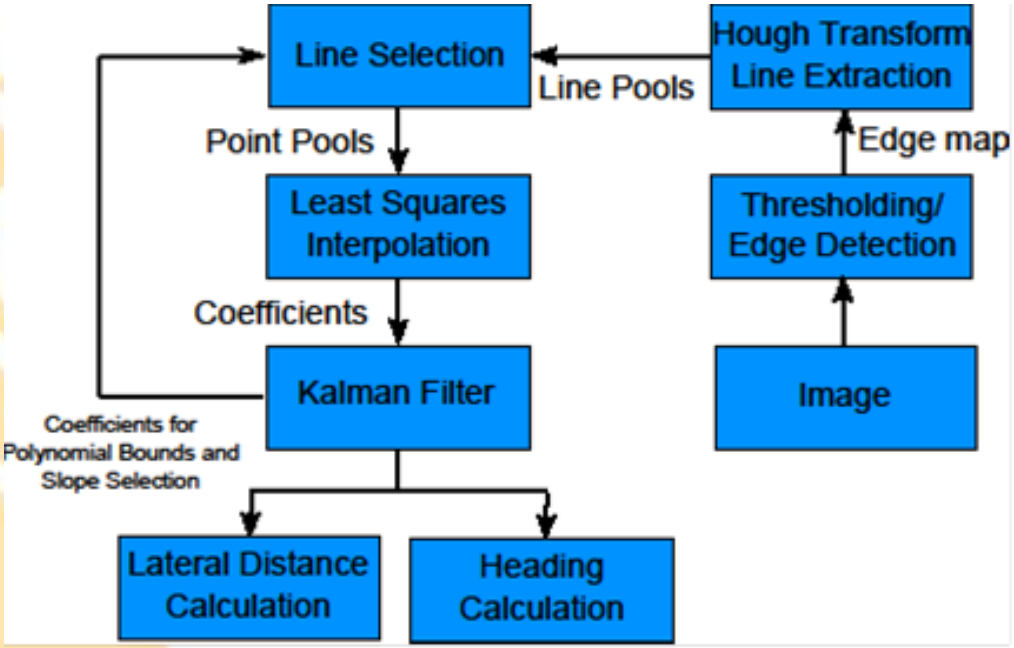

Constant Threshold

- Constant thresholds can provide feature extraction for unchanging or similar environments
  - Thresholds for one scene can fail for changing environments and lighting conditions

Dark Scene

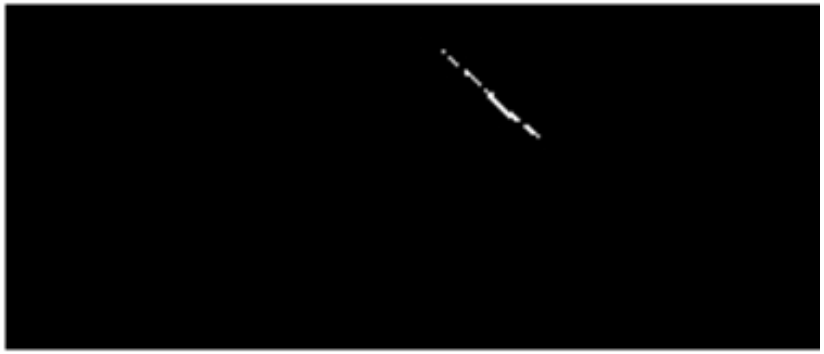

Constant Threshold (T=210)

Dynamic Threshold

- Dynamic Threshold
  - With a dynamic threshold, lane markings are detected in the image even with different lighting conditions
  - Threshold changes with respect to the statistics of the image

$$T = \mu + K\sigma$$

T: new threshold

μ: mean of grayscale values

K: expected noise

Dynamic Threshold

- Dynamic threshold – lane markings are detected in the image even with different lighting conditions

Night Scene

Dynamically Thresholded Image

Edge Detection

- Canny edge detection
  - Extracts the edges of the thresholded image

Day Scene

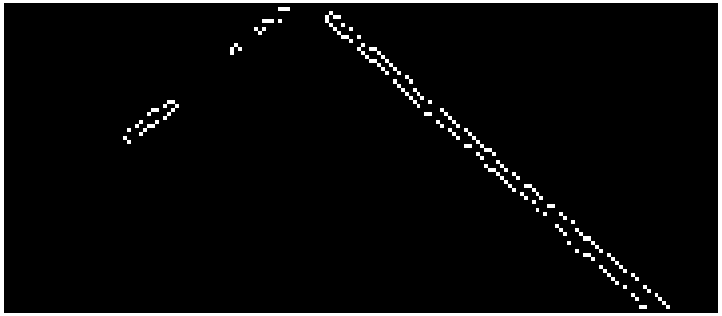

Edge Map

Hough Transform

- Hough Transform
  - Extracts, merges, and ignores lines from images
  - Uses the probabilistic Hough transform

Hough Lines

Line Selection

- Lines are classified as either left or right lane marking lines using their slope.
- Two further checks are used
  - Polynomial boundary checking
  - Slope checking

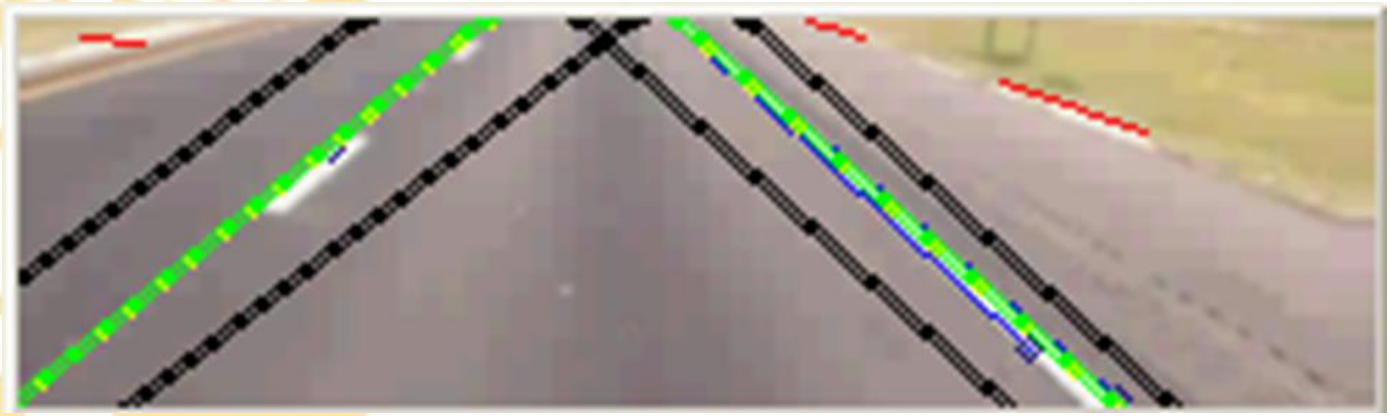

Polynomial Boundary Checking

Three points on each polynomial bound are calculated:

Right Polynomial Bound Calculation

$$x_{rb} = x_{est} + r\sin(\tan^{-1}(2ax_{est} + b))$$
$$y_{rb} = y_{est} - r\cos(\tan^{-1}(2ax_{est} + b))$$

Left Polynomial Bound Calculation

$$x_{lb} = x_{est} + r\sin(\tan^{-1}(2ax_{est} + b))$$
$$y_{lb} = y_{est} - r\cos(\tan^{-1}(2ax_{est} + b))$$

Least squares polynomial interpolation gives the coefficients of each polynomial bound.

Slope Checking

- The slope form each line from the Hough transform is compared with the slope from the last estimated lane marking. If within a given tolerance and if the line is within the polynomial bound, the endpoint and the midpoint of the line is added to the point pool.

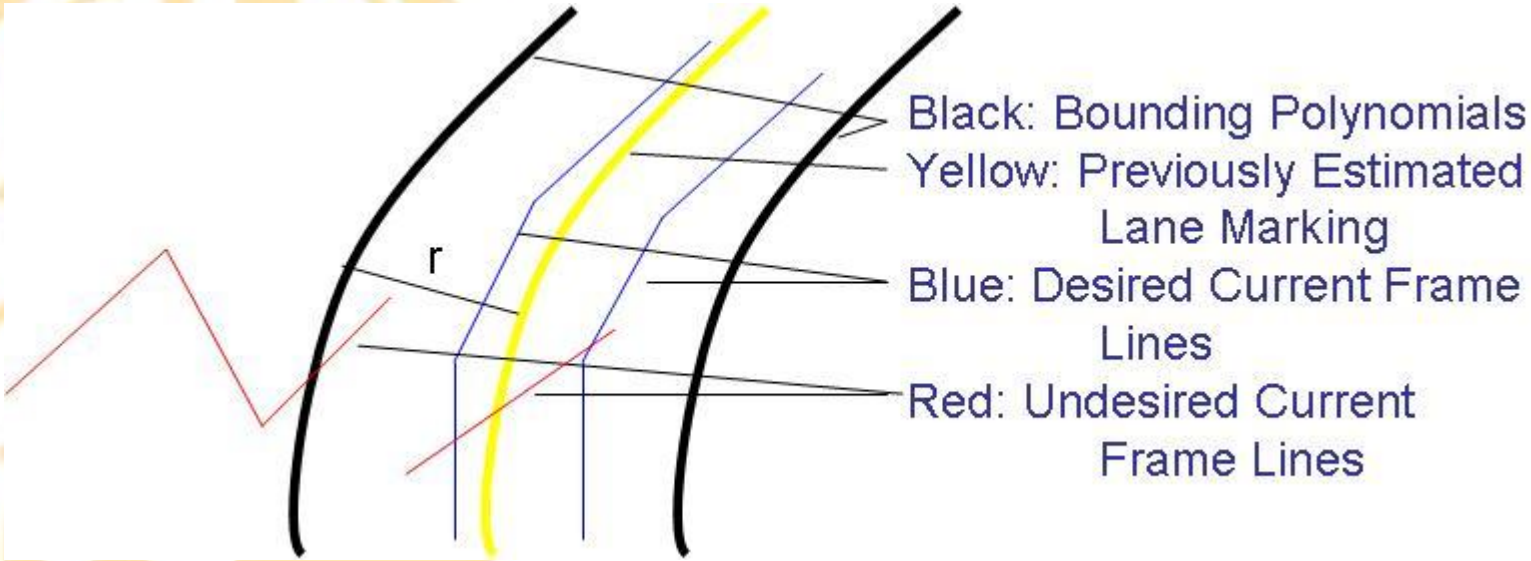

Least Squares Polynomial Interpolation

- Each lane is modeled with a polynomial equation:

$$y = ax^2 + bx + c$$

- Least squares polynomial interpolation is used to generate the coefficients of the model

$$\beta = (f'f)^{-1}f'y$$

where

$$f = \begin{bmatrix} 1 & x_1 & {x_1}^2 \\ 1 & x_2 & {x_2}^2 \\ \vdots & \vdots & \vdots \\ 1 & x_{n-1} & {x_{n-1}}^2 \\ 1 & x_n & {x_n}^2 \end{bmatrix} \qquad y = \begin{bmatrix} y_1 \\ y_2 \\ \vdots \\ y_{n-1} \\ y_n \end{bmatrix} \qquad \beta = [c \quad b \quad a]$$

Kalman filter

- Kalman filter
  - Reduce erroneous lane marking estimates
  - Measurement update corrects coefficients using the coefficients from the 2nd order polynomial interpolation

$$\hat{x} = \begin{bmatrix} a_L & b_L & c_L & a_R & b_R & c_R \end{bmatrix}$$

Lateral Distance Calculation

- Lateral distance is calculated when a lane marking is found

$$d_r = n\left(\frac{-b + \sqrt{4ay + b^2 - 4ac}}{2a}\right)$$

$$d_l = n\left(\frac{-b - \sqrt{4ay + b^2 - 4ac}}{2a}\right)$$

a,b,c: coefficient of the estimated polynomial model
y: image row for measurement
n: conversion factor

The conversion factor serves as the conversion from image to world space

$$n = \frac{w}{p}$$

w = width (m) of a typical lane
p = pixel count of the lane (image space)

Heading Calculation

- Heading is determined based on
  - Vanishing point of measured lane markings
  - Vanishing point of the camera

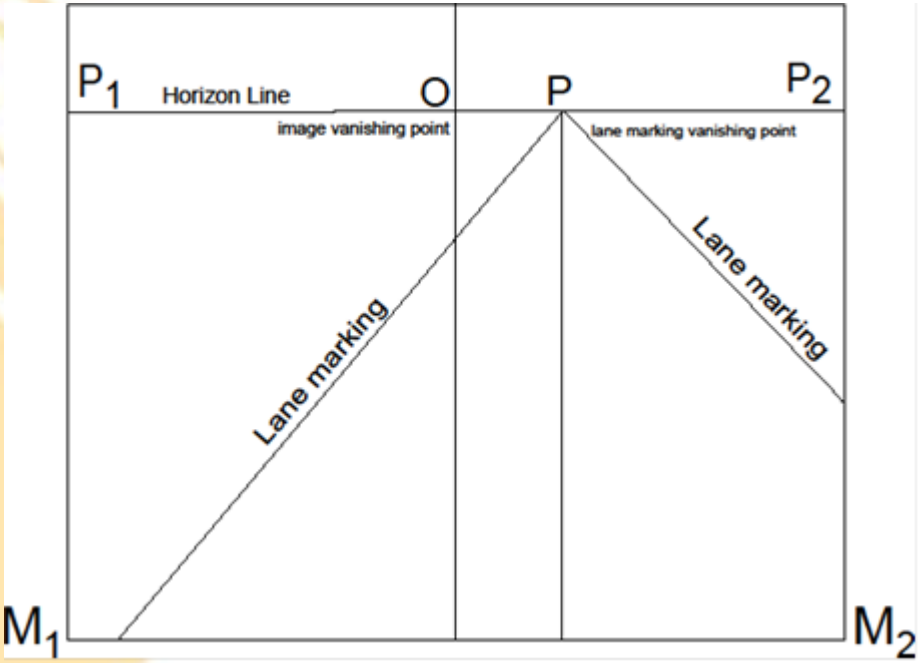

Heading Calculation

$$\psi = \tan^{-1}\left(OP\frac{\tan\frac{\Theta}{2}}{OP_2}\right)$$

OP: distance (pixels) from center point to vanishing point
OP_2: distance (pixels) from center point to image edge
Θ: visual angle
Ψ: heading angle

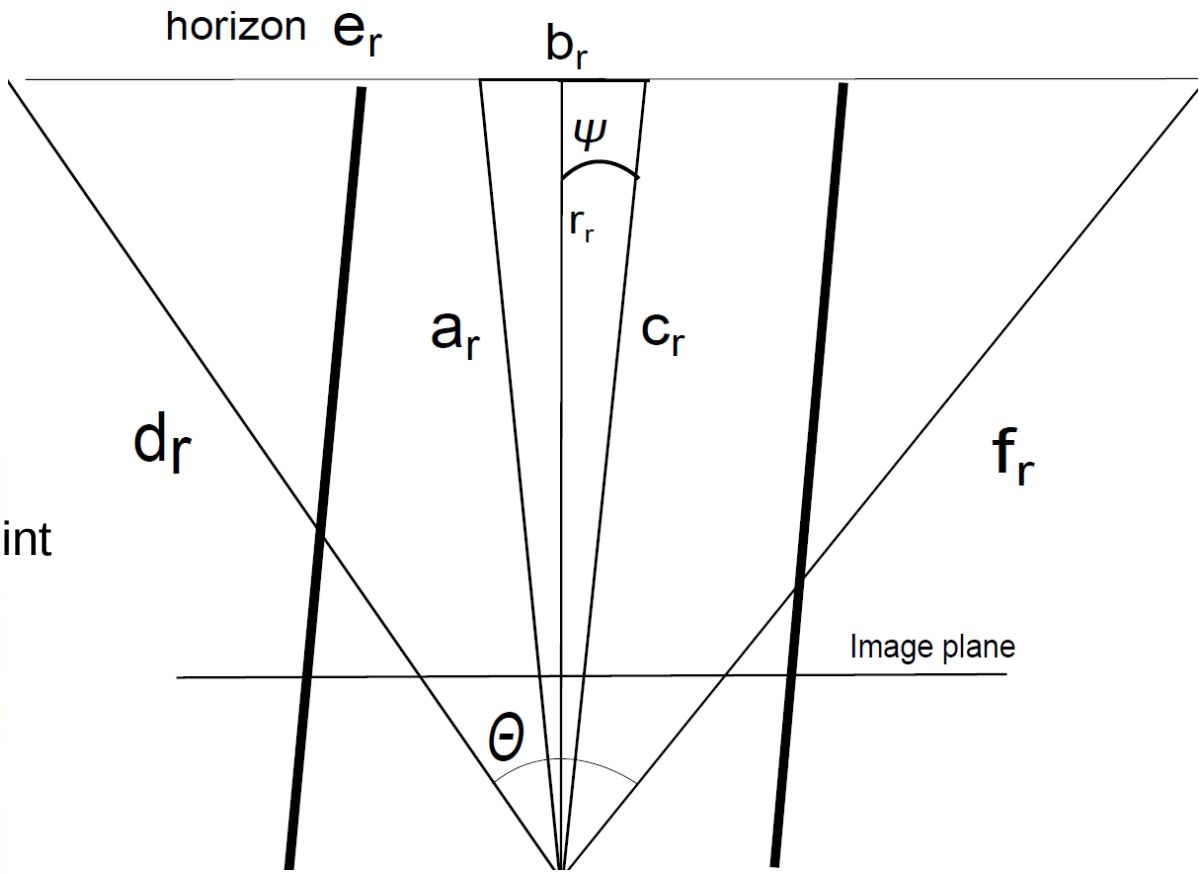

Bird's eye view of road

Performance in Varying Environments - City

Performance in Varying Environments

	Dusk	Night	Rain Dusk	Rain Night
Average Absolute Error (m)	0.2379	0.0307	0.0327	0.0512
RMS Error(m)	0.4214	0.0401	0.094	0.1253
std of Error	0.3526	0.0402	0.0887	0.1149
var of Error	0.1243	0.0016	0.0079	0.0132
% Detection	0.4801	0.9	0.1808	0.1947

Experimental Results

- Test Run
  - Hyundai Sonata driven around the right lane
  - NCAT test track
  - RTK GPS truth data

Truth Lateral Distance vs. Calculated Lateral distance

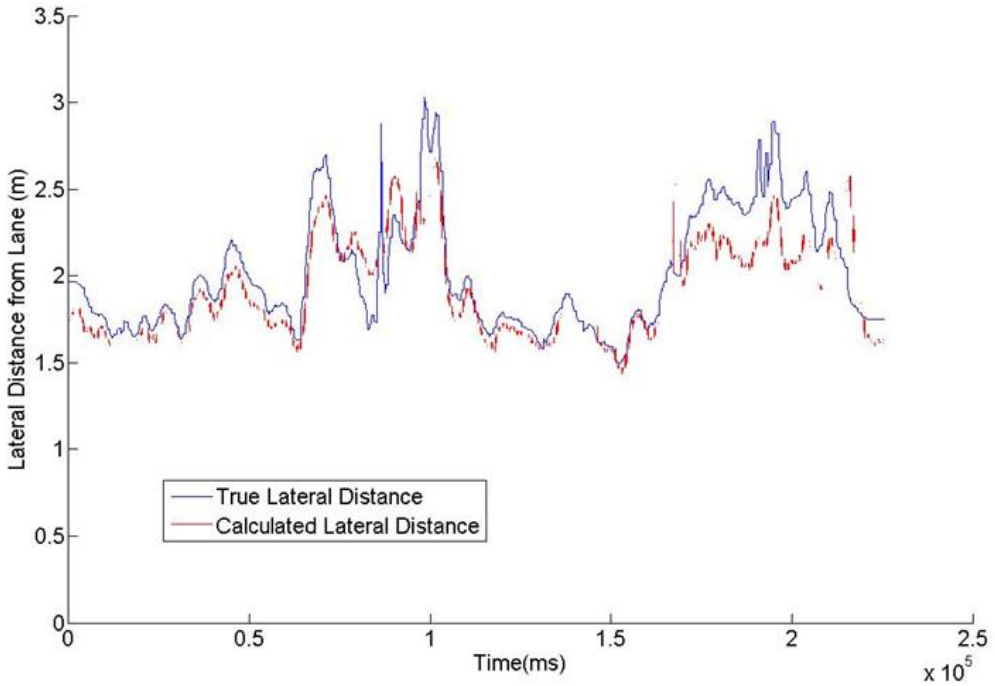

Heading Results

Two “spike” regions are the curves of the track

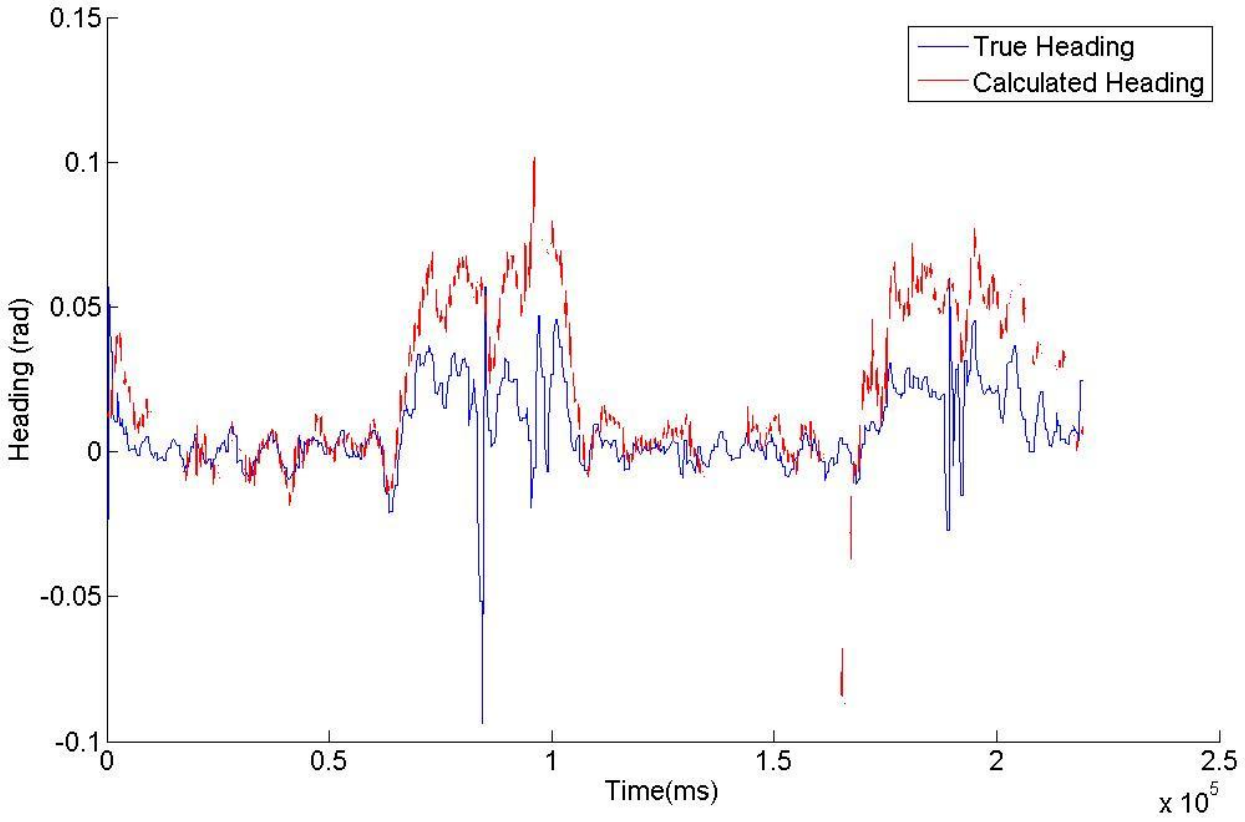

True Heading vs. Calculated Heading

Vision/INS/Velocity Integration

- Various problems can hinder lane detection
  - Environment
  - Eroded lane marking lines
  - Objects on road
- Integration of other sensors can provide lateral distance in the road when camera vision fails
- Extended Kalman filter used for sensor fusion

Vision/IMU/Velocity Integration

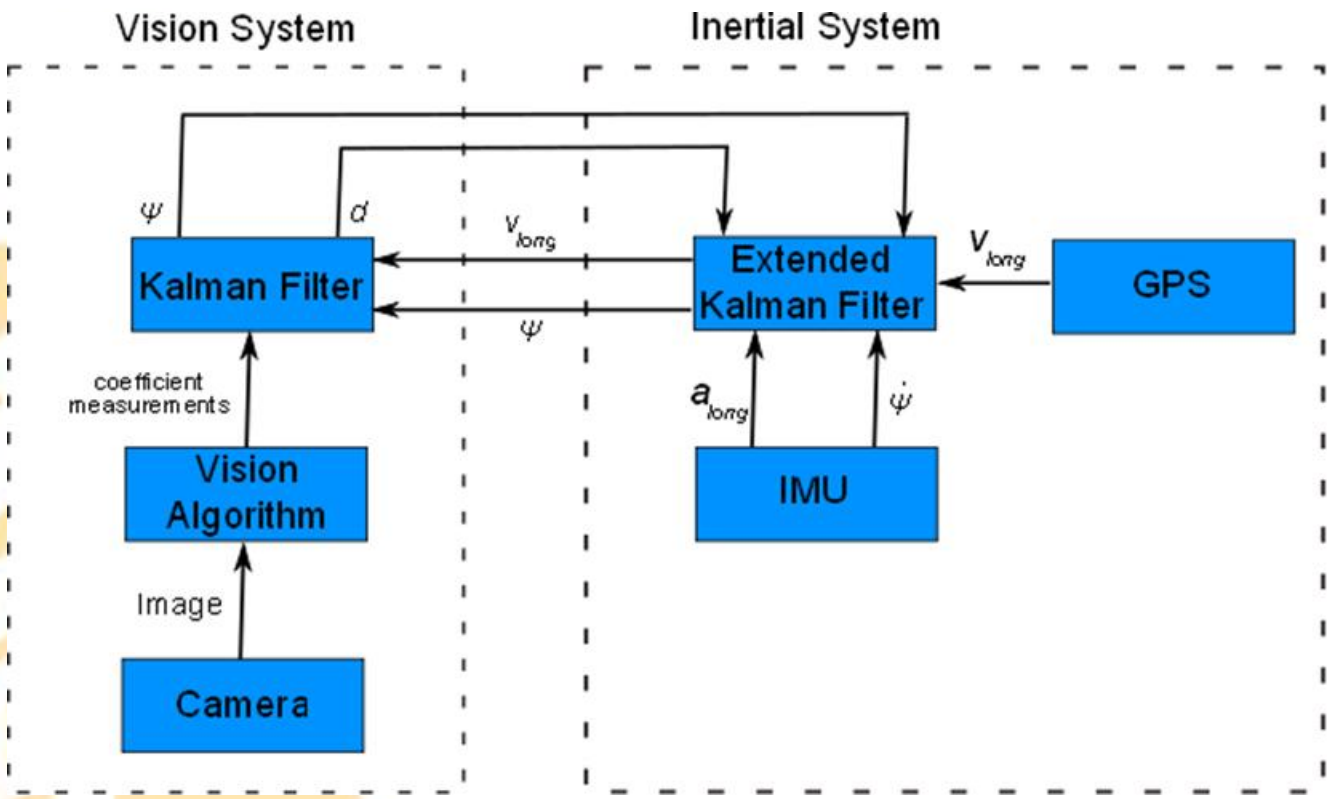

- GPS used for velocity
- Wheel odometry, radar, etc. can also be used

Road Frame

- Road Frame
  - Positive x-axis pointing down the road on the right lane marking
  - Y-axis points perpendicularly to the right
  - Z-axis points down and perpendicular to the road plane

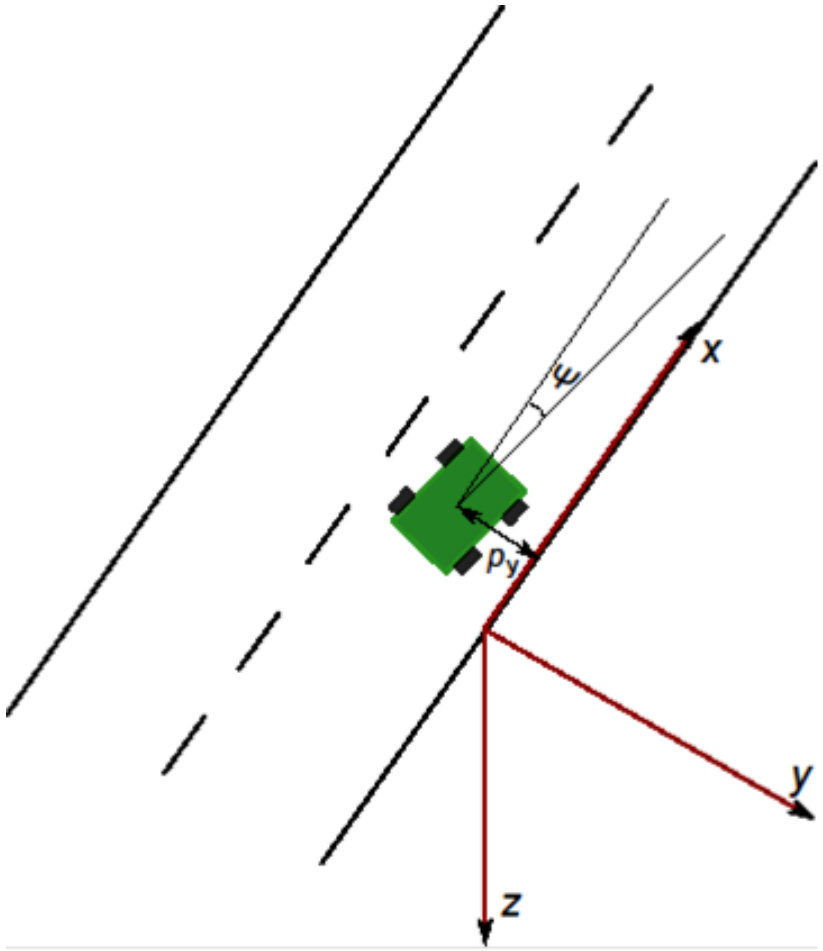

States

- State vector

$$\hat{x} = \begin{bmatrix} p_y & v_x & b_x & \psi & b_\psi \end{bmatrix}^T$$

p_y: lateral distance
v_x: longitudinal velocity
b_x: longitudinal acceleration bias
ψ: yaw
b_ψ: yaw rate bias

Time Update – Nonlinear equations

- Inputs:
  - $\dot{\psi}$: yaw rate
  - a_{long}: longitudinal acceleration
- States included are
  - b_{ψ}
  - b_{long}
  - v_x
  - ψ

Equations of Motion

- Propagation of states through time
  - Runge-kutta approximates solution
  - Noise is assumed to be zero

$$\dot{p_x} = v_x \sin(\psi)$$
$$\dot{v_y} = a_{long} - b_{long}$$
$$\dot{b_{long}} = 0$$
$$\dot{\psi} = \dot{\psi} - b_{\psi}$$
$$\dot{b_{\psi}} = 0$$

- Time update can use the heading and longitudinal velocity to estimate the location of the lane markings
  - m: pixels shifted in image space
  - r: radians per pixel shift

$$m = \frac{v_x \sin\psi \, dt}{n} \qquad r = \frac{2q}{w}$$

Time Update

- New coefficients of lane model for lateral motion

$$b = \frac{b}{1 - brm}$$

$$c = \frac{c}{1 - brm}$$

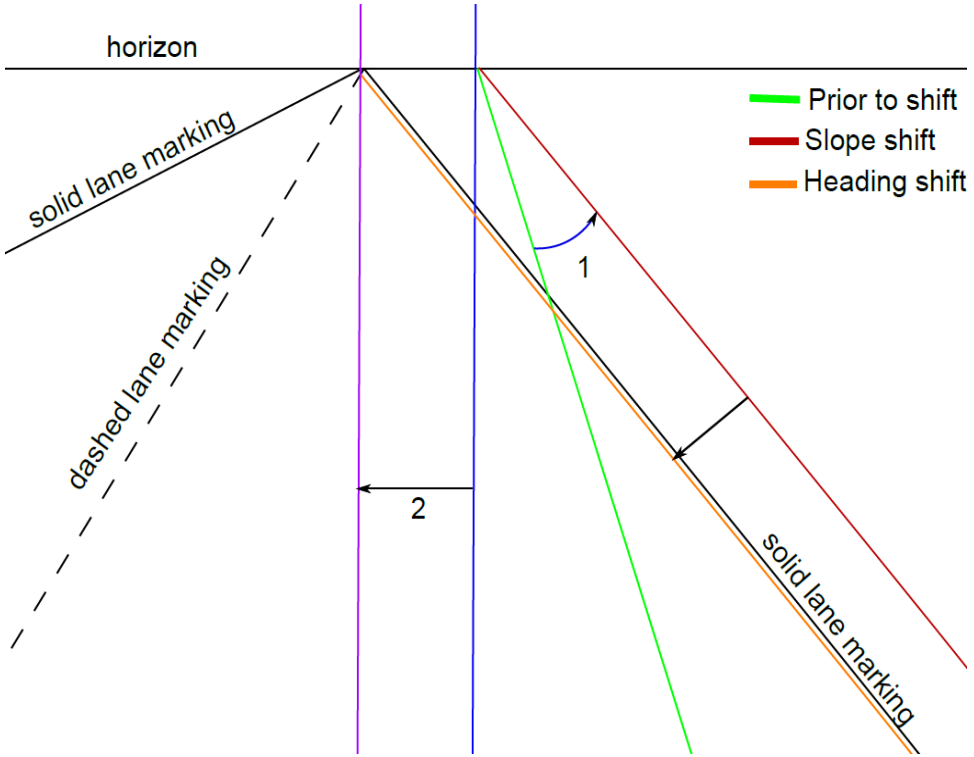

Measurement Update

- Measurement Update
  - Correction of states with camera and velocity (from GPS) measurement
  - Correct for drift from IMU
  - Measurements
    - Lateral distance (camera)
    - Heading (camera)
    - Longitudinal velocity (GPS)

Vision/IMU/Velocity Experimental Results

- New test run
  - Approximate straight road conditions of a highway
  - Taken at night under low light conditions
  - Faded section in first half
  - Double lane change maneuver in second
  - IMU: Crossbow 440 IMU
  - Speed: 30 mph

Lateral Position Estimate

Estimated Lateral Distance vs. True Lateral Distance

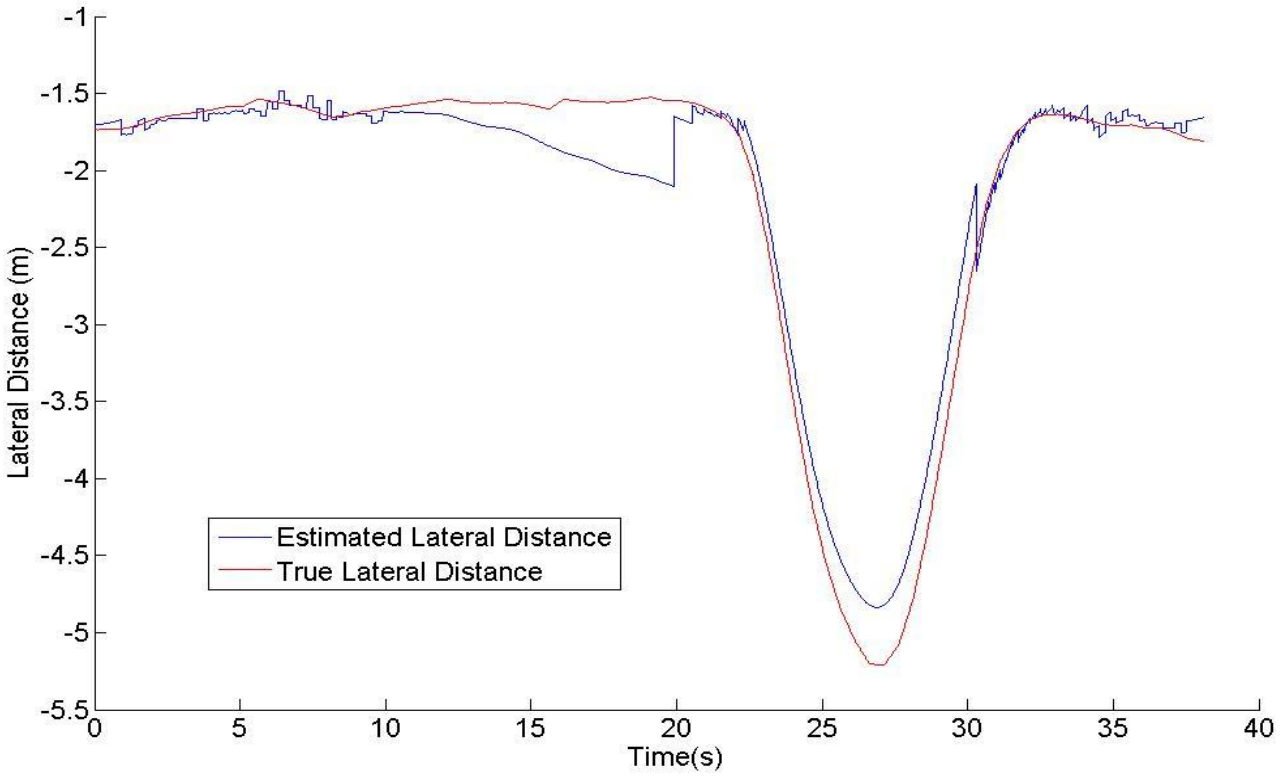

5s – 20s: faded lane markings
25s – 30s: double lane change

Heading Estimate

Estimated Heading vs. True Heading

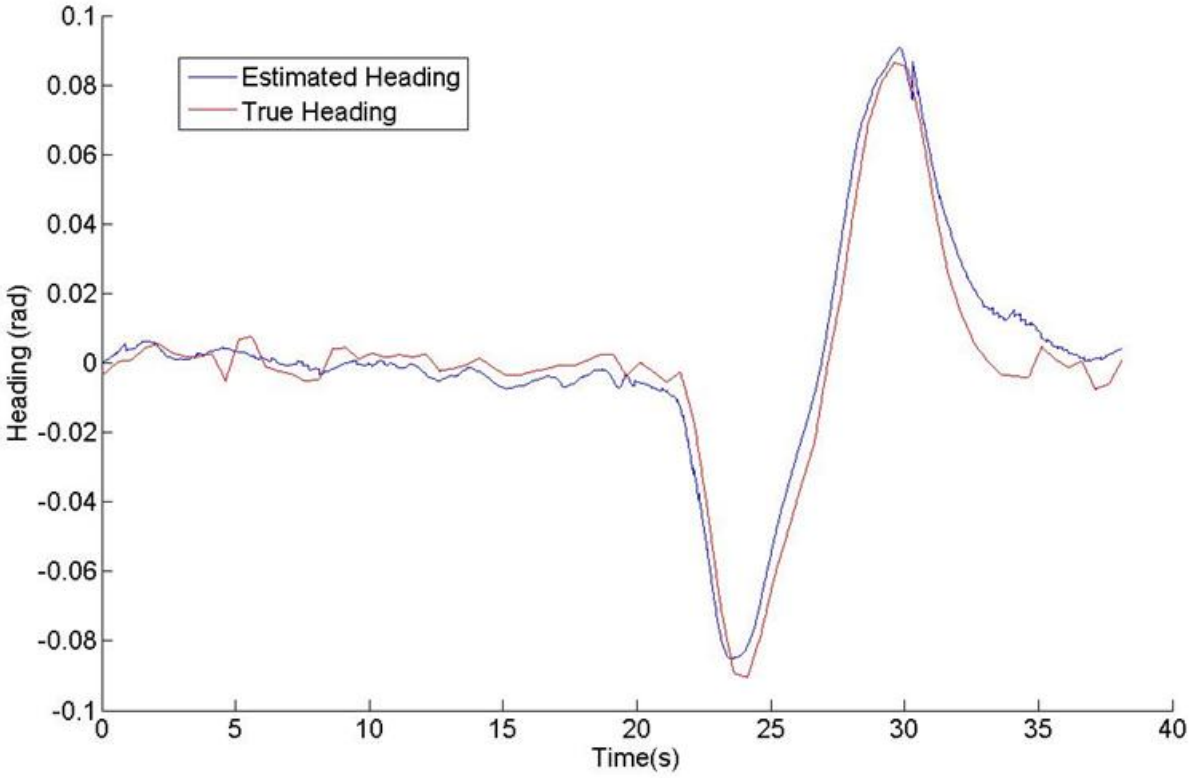

5s – 20s: faded lane markings
25s – 30s: double lane change

Conclusions

- Two systems are presented for estimating lateral distance in the lane
  - Vision only
  - Vision/IMU/Velocity
- Experimental results were compared with truth data to verify the vision/IMU algorithms. Lane model estimation was verified through observation.

Future Work

- Future work
  - Real time implementation of vision/IMU system
  - Extension of system to curved roads using coefficients to compensate for non-inertial frame
  - Compensation of lateral lane measurement on curved roads due to forward movement

Lane Detection, Calibration, and Attitude Determination with a Multi-Layer Lidar for Vehicle Safety Systems

Jordan Britt	:Auburn University
Dr. John Hung	:Auburn University
Dr. David Bevly	:Auburn University
Dr. Thaddeus Roppel	:Auburn University

AUBURN UNIVERSITY

AVLAB

Overview : Lane Detection

AUBURN UNIVERSITY

- Problem Introduction
- Motivation
- Background
- Proposed Method
- Testing
- Results
- Conclusions
- On to attitude determination

Problem Introduction

- Attempt to detect lane markings using a 3D lidar to prevent unintended lane departures
- Should be capable to adapting to changing road conditions

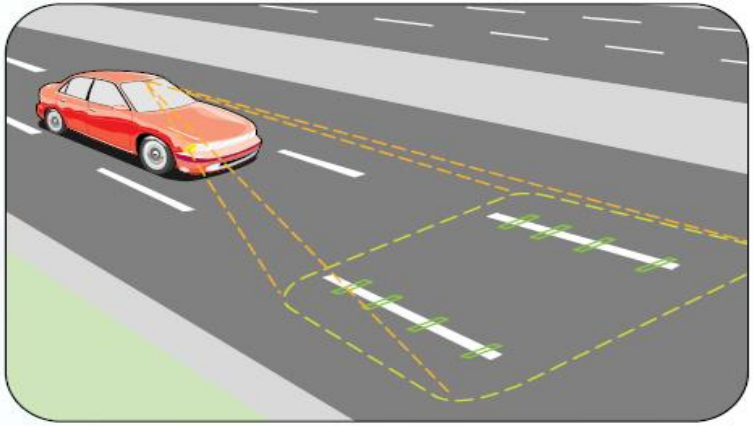

From www.iteris.com

Motivation

- We can save lives.
  - In 2008 52% of all highway fatalities occurred from unintended lane departure
    - Nearly 20,000 deaths
  - In 2006 it was 58%, comprising nearly 25,000 deaths
  - In short: more fatalities than any other crash type occur due to single vehicle road departures

Background: Previous Work

- [23] J. Kibbel, W. Justus, and K. Furstenberg. Lane estimation and departure warning using multilayer laserscanner. In Proc. IEEE Intelligent Transportation Systems, pages 607-611, September 13-15, 2005.
  - Uses Ibeo, Large ROI 10-30m and 12m, and uses histogram for detection. No truth metric provided, but provides detection rates varying from 16-100%, Averaging at 87%.
- [13] K. Dietmayer, N. Kämpchen, K. Fürstenberg, J. Kibbel, W. Justus, and R. Schulz. Advanced Microsystems for Automotive Applications 2005. VDI-Buch. Springer Berlin Heidelberg, 2005.
  - Once again uses a large ROI 0-30m and 12m. Truth metric was driving straight for short periods of time and estimating lane width, accurate to 0.25m
- [24] P. Lindner, E. Richter, G. Wanielik, K. Takagi, and A. Isogai. Multi-channel lidar processing for lane detection and estimation. In Proc. 12th International IEEE Conference on Intelligent Transportation Systems ITSC '09, pages 16, October 47, 2009.
  - 6-layer lidar, uses a polar histogram. No truth data, but notes it works best on asphalt, and worst on concrete. Rain has an adverse affect on detection

Contributions

- Development of a novel lane extraction method, that is based on a MMSE to an ideal lane
- Provide truth measurements in the form of high accuracy GPS

Background : What is a LiDAR ?

- LiDAR : Light Detection and Ranging
- Similar in concept to sonar or radar, but uses light instead of sound or electromagnetic waves

1D	2D	3D
	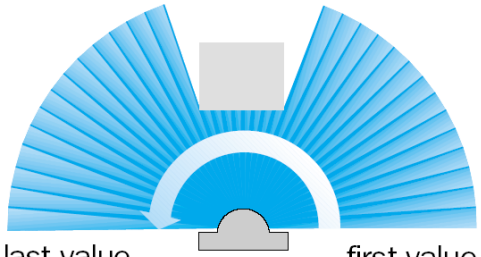	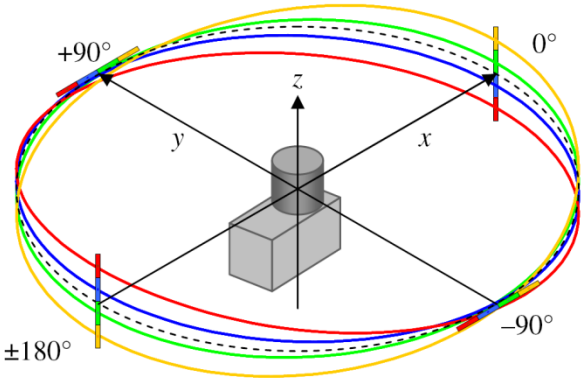

LiDAR : Reflectivity

- LiDAR provides distance as well as reflectivity, known as echo width
- Lines are detected on the premise that they are of high reflectivity than the road's surface

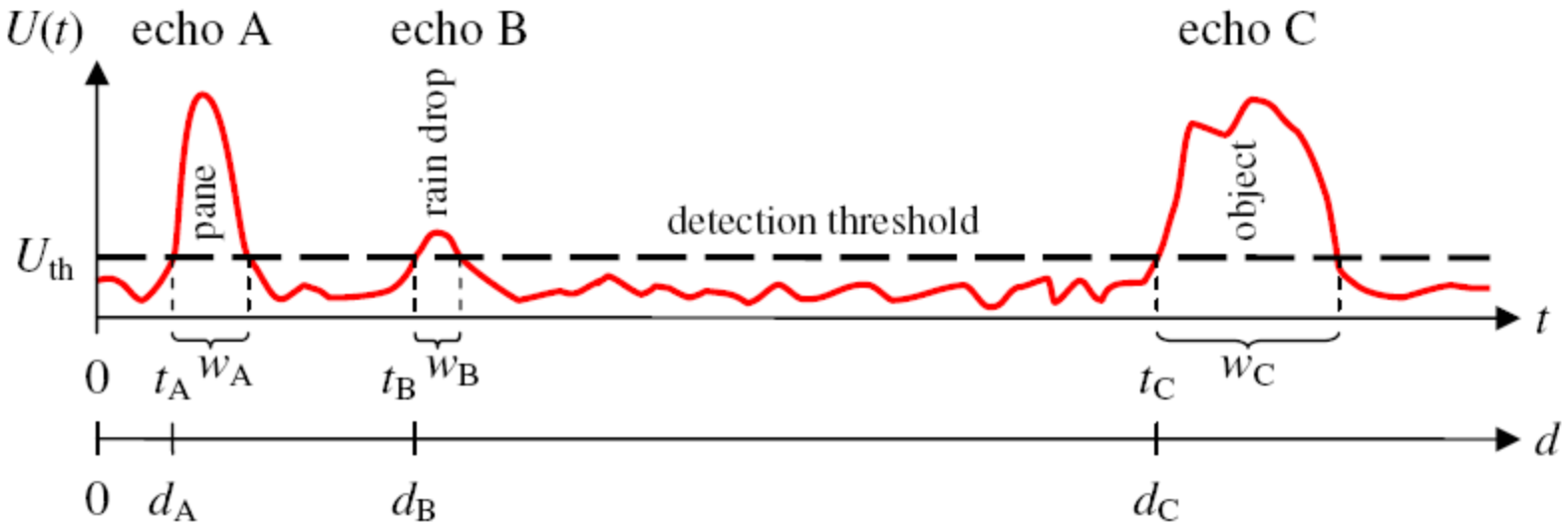

Hardware Overview

- Ibeo ALASCA XT
- 3D LiDAR
  - 4 layers
- 3.2 vertical field of view
- Capable of . 25 resolution (varies with scan angle)
- Data taken at 10Hz
- Multi-echo receivers

Mounting

- Mounted on roof rack of vehicle
  - Scans 1.7m in front of vehicle
  - Height of approx 1.5m
  - Pitched approximately -22
  - Resolution of 1.6 inches at lane markings

Calibrating the Lidar

- Calibrate the height and pitch of the LiDAR.
- Allows us to compensate for LiDAR mounting
- Determine resolution at lane markings

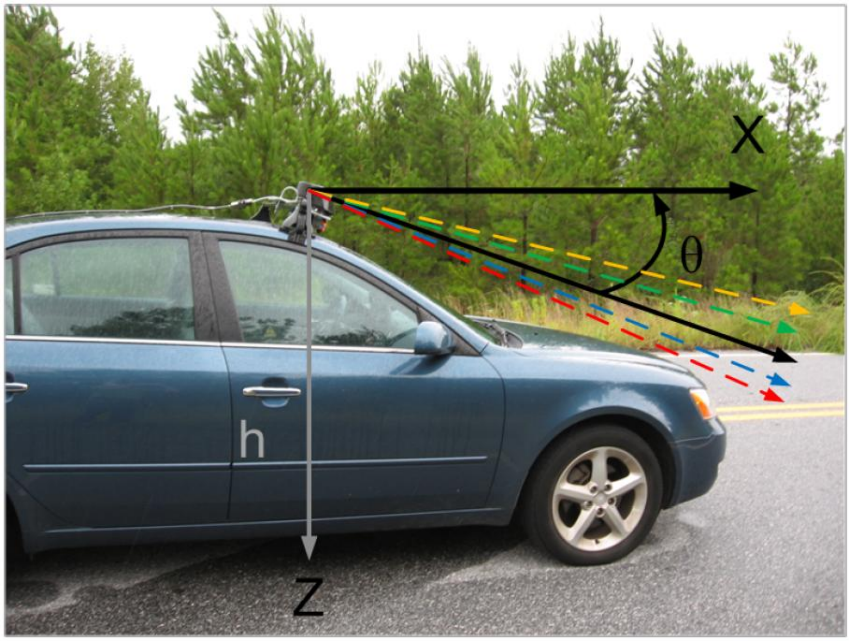

$$h_X = \rho_k \cos(\theta + \alpha_k),\ \gamma_k = 0°$$

$$\theta_{X,Y} = -Y_{\alpha_j} + \arctan((X_{\rho_i} \cos(X_{\alpha_i} - Y_{\alpha_j}) - Y_{\rho_j})/X_{\rho_i}/\sin(X_{\alpha_i} - Y_{\alpha_j})) - 90°\ \gamma_{i,j} = 0°$$

Detection Overview

- Bound the Search Area
- Generate an ideal scan to match actual lane markings
- Find the MMSE between the ideal scan and an actual scan
- Window the data
- Filter the data

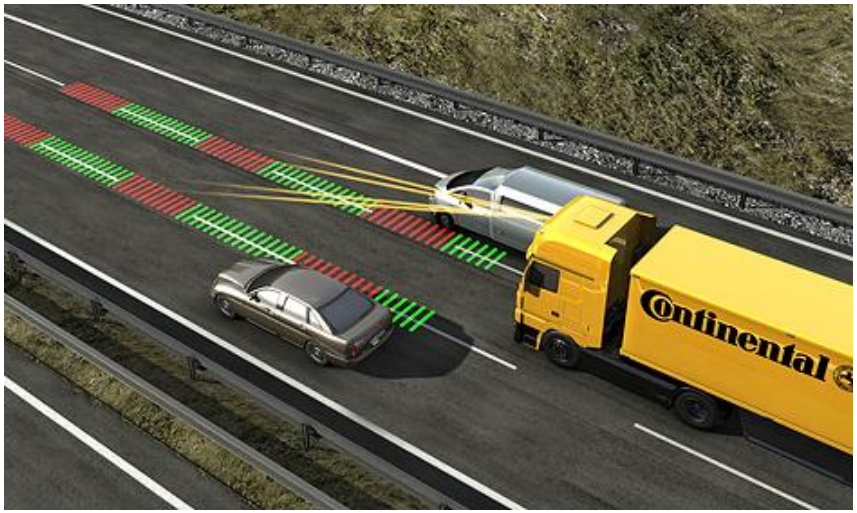

Courtesy: Google Images

Bounding the Search area

- Choose a bound to search for lanes within
- Chosen so that wherever the vehicle is in lane, it will see the lane markings
- Initially assumes a standard lane width of 12’

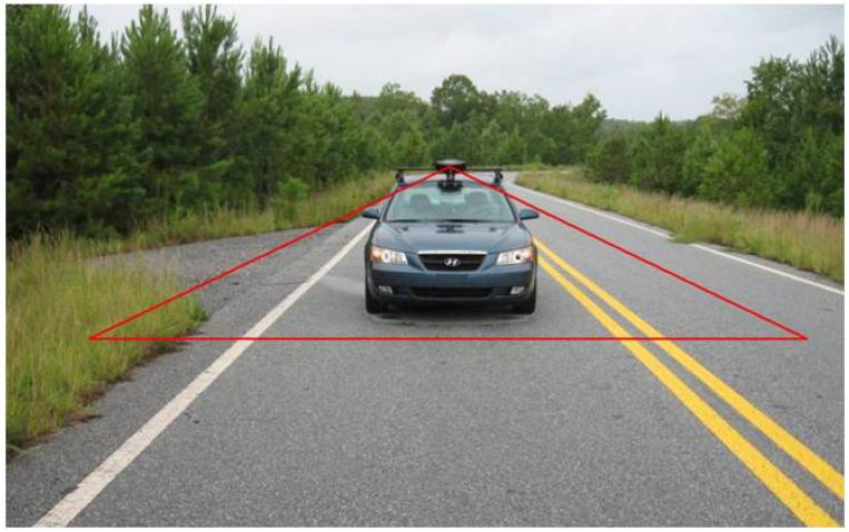

$$Angle\ Bound = \arctan\left(\frac{LW - \frac{VW}{2}}{\rho_k}\right),\ \gamma_k = 0°$$

An Ideal Scan

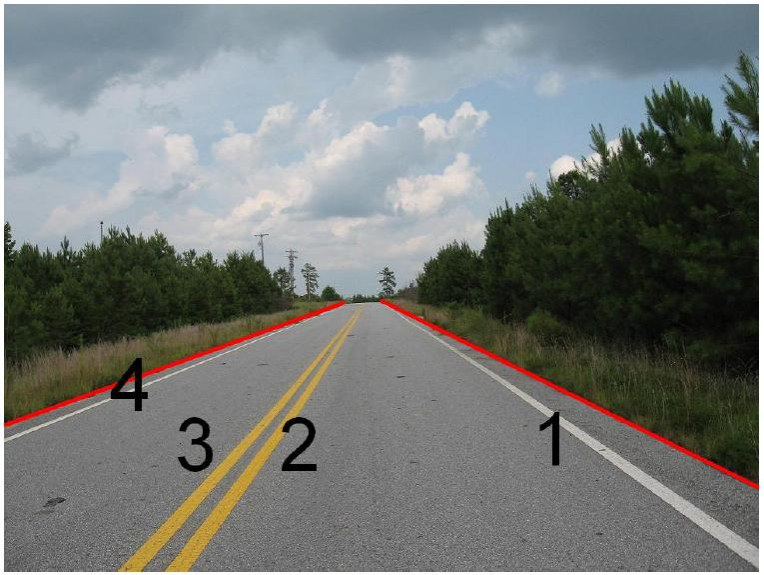

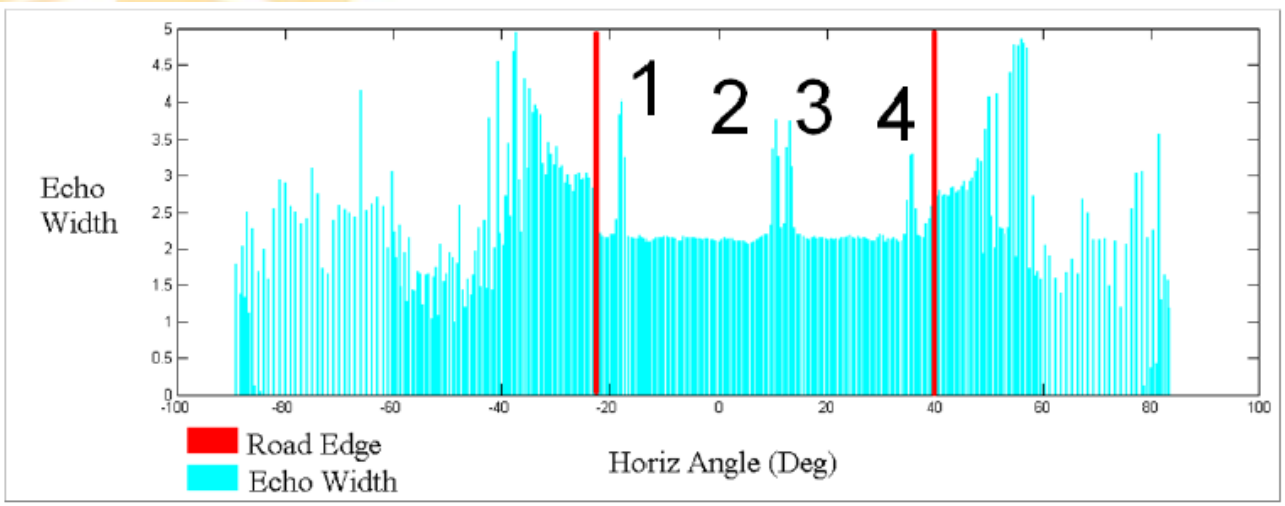

Non-Ideal Scan

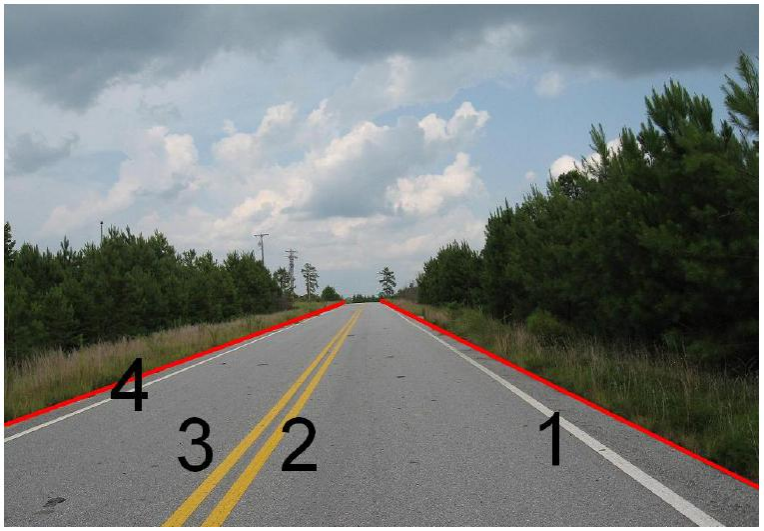

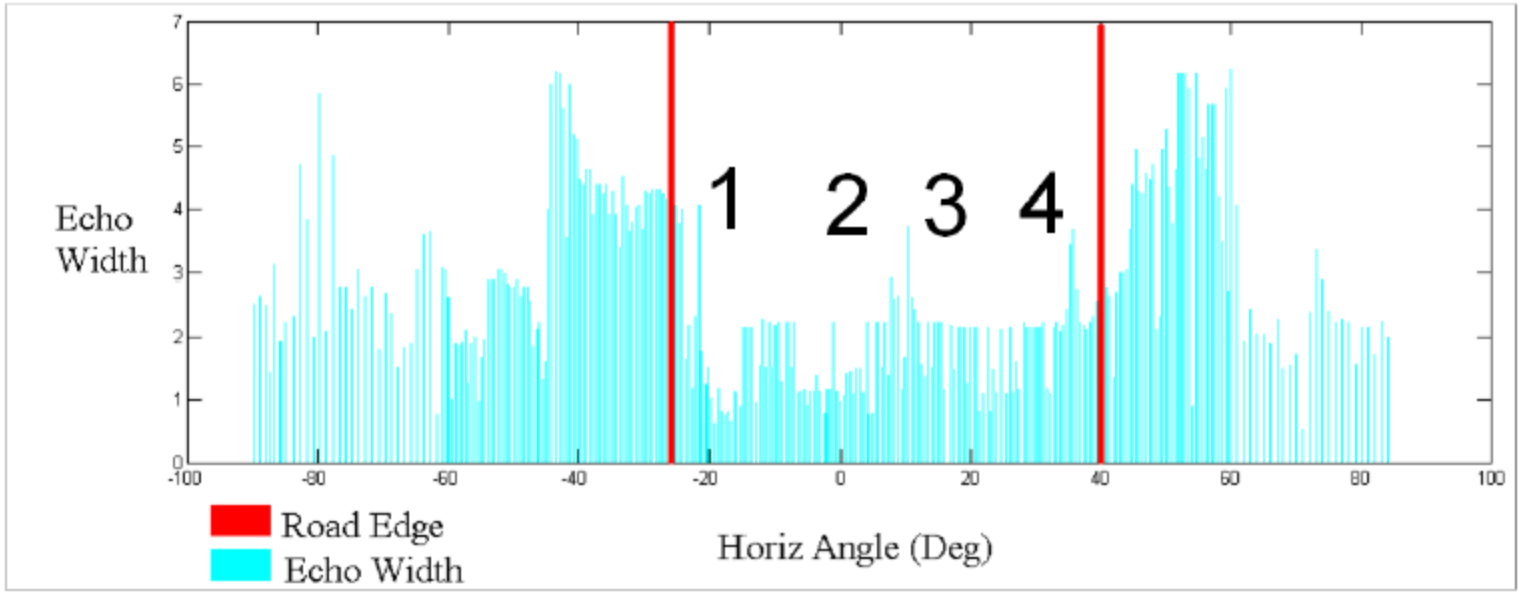

Creating an Ideal Scan

- Spikes represent the increase in reflectivity of the lane markings
- Flat area represents road's surface

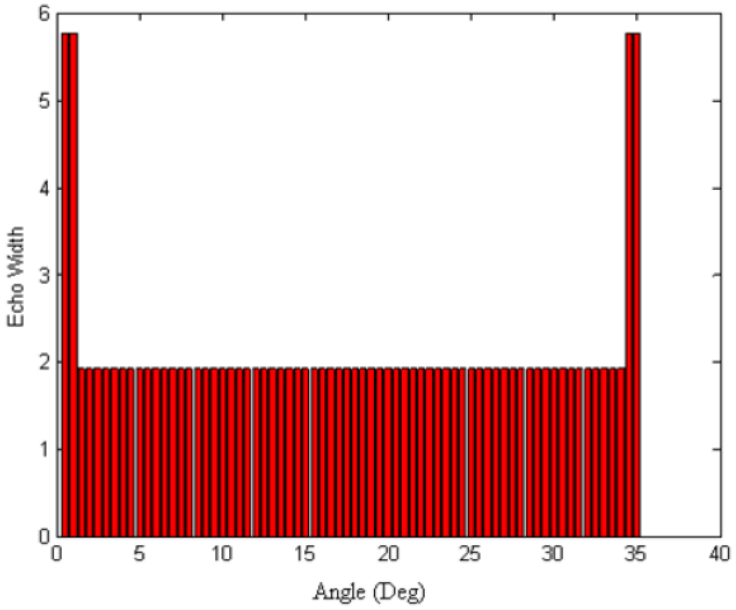

Match the ideal scan to actual data

- Average the reflectivity in front of the car to generate the flat portion of the scan
- Increase this average by 75% to generate lane markings
- Hence the ideal scan changes depending on the surface

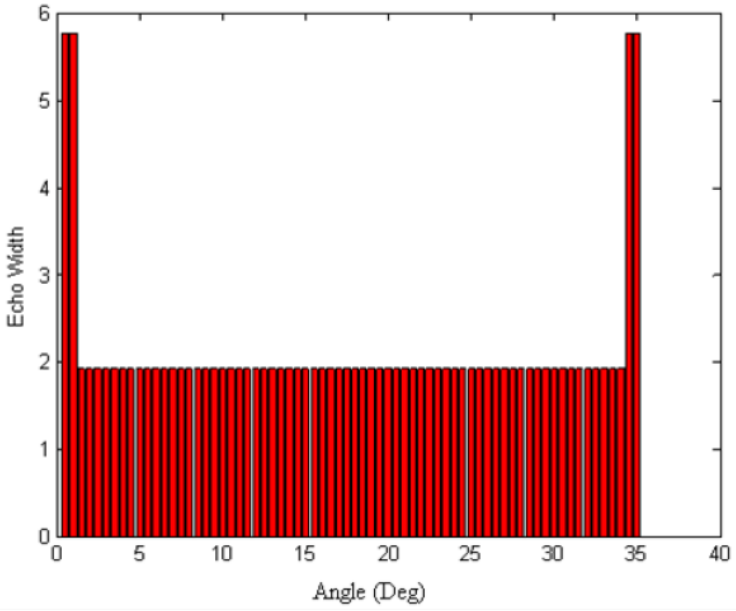

Match the ideal scan to actual data

- Allow size of the ideal scan to change size from some minimum lane width to some maximum lane width
- Find the MMSE of the ideal scan to the real data over the entirety of the search space
- Repeat for each layer

Match Ideal scan to data

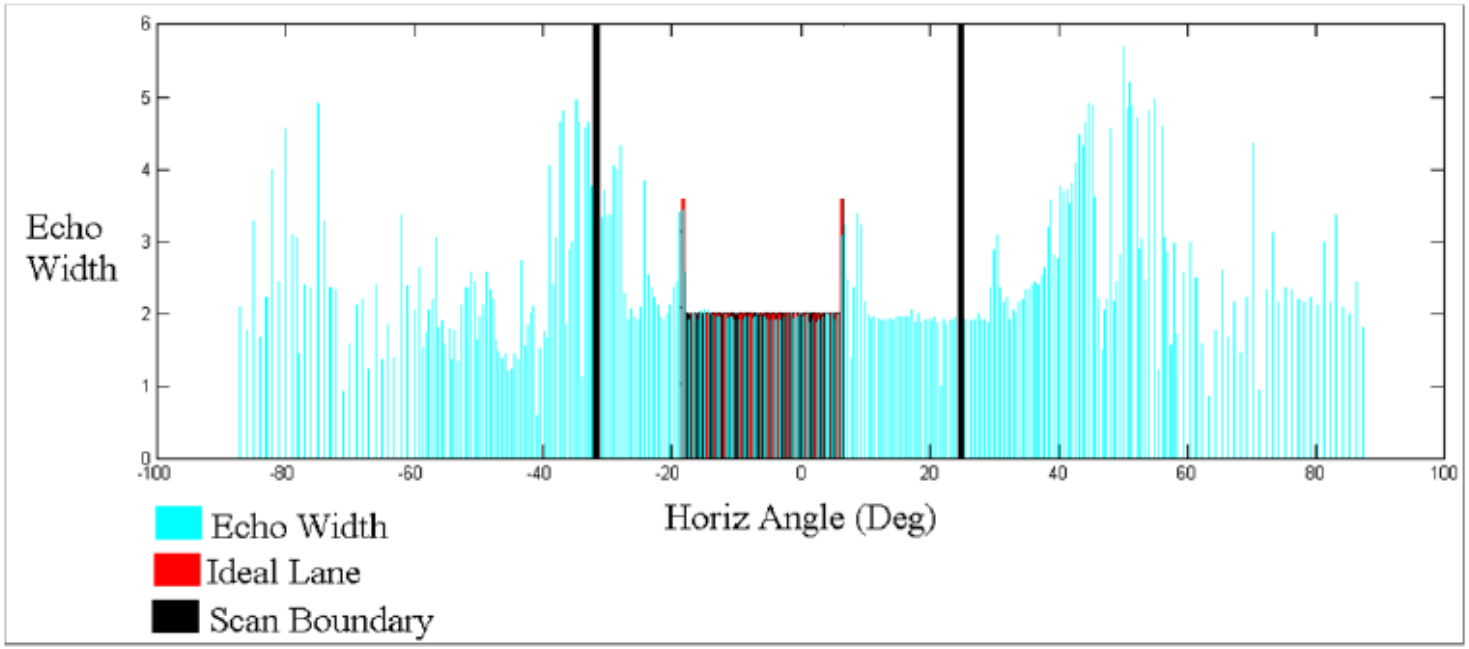

$$lane = min\left(\sum_{a=\gamma_{LB}}^{\gamma_a=0^\circ}\ \sum_{b=a+w_{min}}^{(a+w_{max})\leq\gamma_{RB}} \sqrt{\frac{\sum_{k=a}^{min(b,\gamma_{IRS})}(\gamma_{ILS+k}-\gamma_{LB+k})^2}{b-a}}\right)$$

Narrow the Search: Windows

- Window is a 4 bound around where lane marking was found
- Simply narrows the search space
- If no lane marking is found for two scans resume the origional search space
- In case of conflict choose closest window

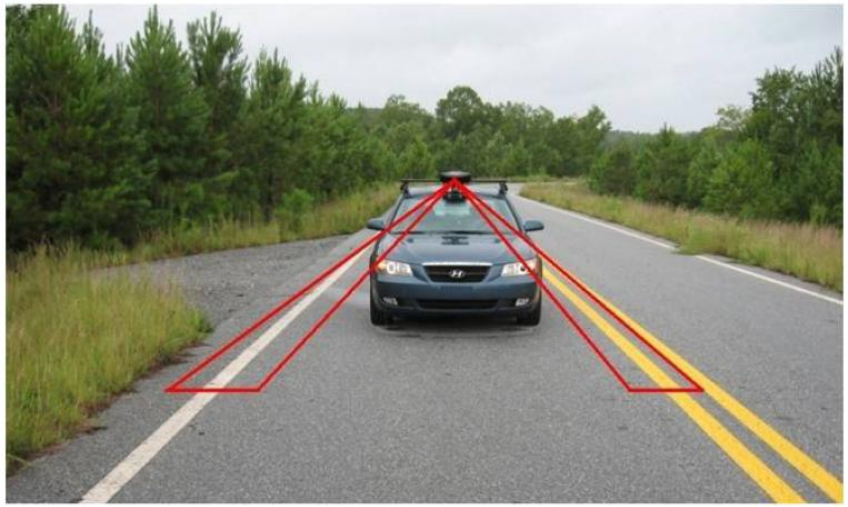

Filtering the Data

- Weighted average of L and R distances are computed
- These distances are then used to compute the distance from the center of the lane
- Finally, this distance is filtered using a single state Kalman filter to smooth data

Testing

- Driving at NCAT test track, and comparing reported LiDAR position to a surveyed map of the track.
- Driving on various roads with know lane width, and comparing estimated lane width to actual lane width as in [23] and [13]

NCAT Testing

- Mean error : 0.1193m
- Var of error: 0.0536m

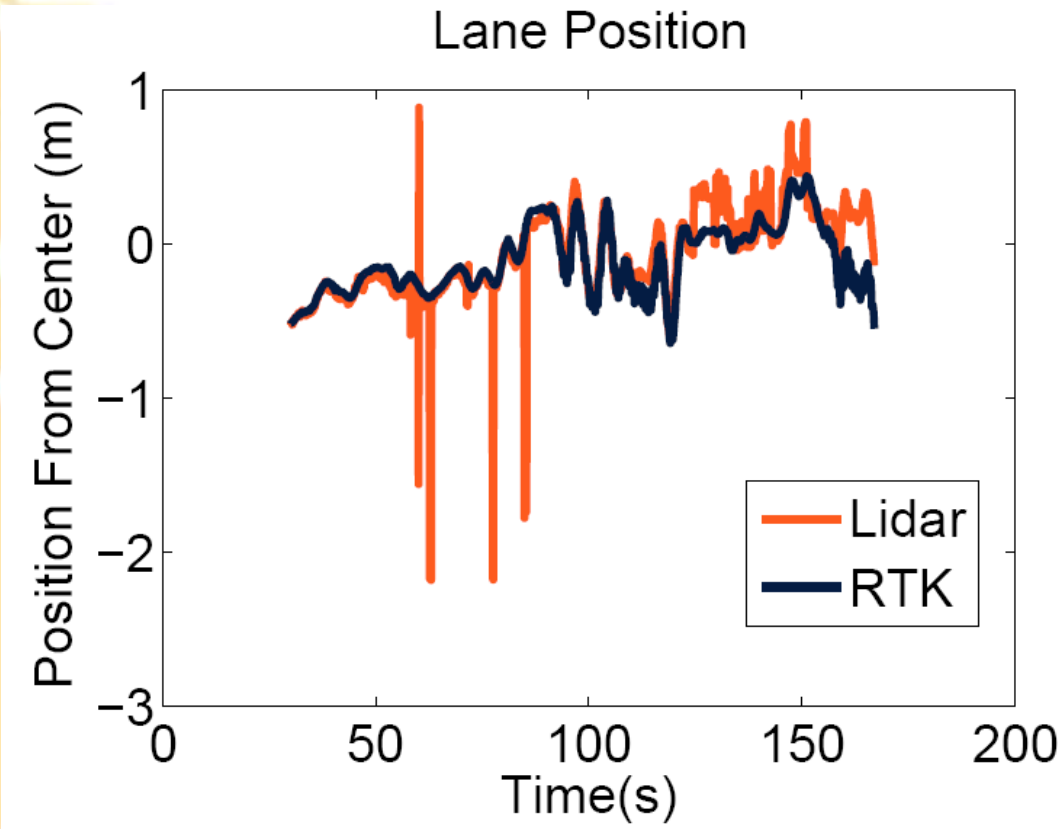

Lane Width Estimations

1. Highway
2. Double yellow on L, solid white on R
3. Gravel on road surface
4. Grass closely bordering roadway

Table 3.3: Results of Scenario Tests

	Avg. Lane Width Error (m)	Std of Error (m)	Detection (%)
Scenario 1	0.075	0.233	94.7
Scenario 2	0.042	0.272	81.7
Scenario 3	0.129	0.215	97.4
Scenario 4	0.169	0.329	76.86

Comparison to Literature

- [13] claimed by driving perfectly straight, their system was accurate to within 0.25m,
  - The presented algorithm is accurate to 0.12m
- [23] Lane width estimation, maximum error was 0.24m with a minimum detection rate of 16%
  - The presented algorithm maximum error was .269m with a minimum detection rate of 76%

Sources of Error

- Grass closely bordering roadway
- Sunlight directly shinning on LiDAR
- Dead bugs
- Rain

Conclusions

- Lane extraction algorithm does not appear to be effected by changes in lighting.
- Accurate to within the width of a lane marking
- Capable of extracting both solid and dashed lane markings

LiDAR Calibration and Attitude Determination

Overview

- Problem Introduction
- Motivation
- Background
- Hardware Overview
- Assumptions
- LiDAR Calibration
- Vehicle Attitude Estimation
- Results
- Conclusions

Problem Introduction

- Determine how the LiDAR is mounted in relation to the vehicle's axes.
- Determine vehicle pitch and roll.

Motivation

- It is critical to have sensor measurements aligned properly to vehicle, especially for LDW, E-Braking, ACC
- Determination of vehicle roll relative to the roadway could aid in roll-over estimation and prevention.

Background: Previous Work

- [37] Toshihiro Tsumura, Hiroshi Okubo, and Nobuo Komatsu. A 3-d position and attitude measurement system using laser scanners and corner cubes. IEEE/RSJ International Conference on Intelligent Robots and Systems, pages 604-611, 1993.
  - Calibrate uses prior surveyed points
- [5] Matthew Antone and Yuli Friedman. Fully automated laser range calibration.
- [7] Frank S. Barickman. Lane departure warning system research and test development. Transportation Research Center Inc., (07-0495), 2007.
  - Calibrate using known geometric structures
- [38] Zhenqi Zhu, Qing Tang, Jinsong Li, and Zhongxue Gan. Calibration of laser displacement sensor used by industrial robots. Optical Engineering, 43(1):12-13, 2004.
  - Calibrates using known motion of robitic arm

Background : LiDAR Attitude

- Many calibration and LiDAR attitude estimation algorithms rely on:
  - Beacons
  - Scanning objects with known geometry
  - Previously mapped environments
- Often not feasible for quick or in the field calibration

Contributions

- Development of a 3D LiDAR calibration and attitude determination scheme.
- Capable of calibrating “quickly”
- Capable of determining attitude with sub-degree accuracy.

Assumptions

- Vehicle is on a planar surface
  - Road, Garage, Hanger, Factory Floor
- Vehicle is capable of performing a pure pitch maneuver
- Vehicle is equipped with forward looking 3D LiDAR that can measure the planar surface
- LiDAR remains fixed on the vehicle once calibrated

Assumptions Continued

- Vehicle and lidar operating in the NED coordinate frame
- All LiDAR measurements originate at the same physical location
- All rotations assume right-handed convention

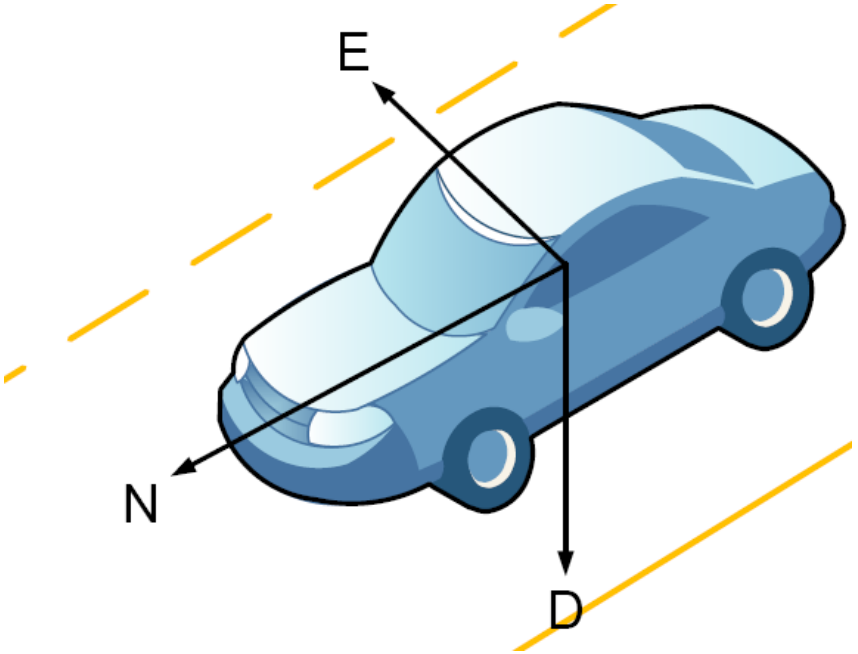

Senor Used

- IBEO ALASCA XT
  - Automotive Grade LiDAR
  - 4 layers at diverging vertical angles
  - Data collected at 10Hz with 0.25 resolution
  - All points originate at same location

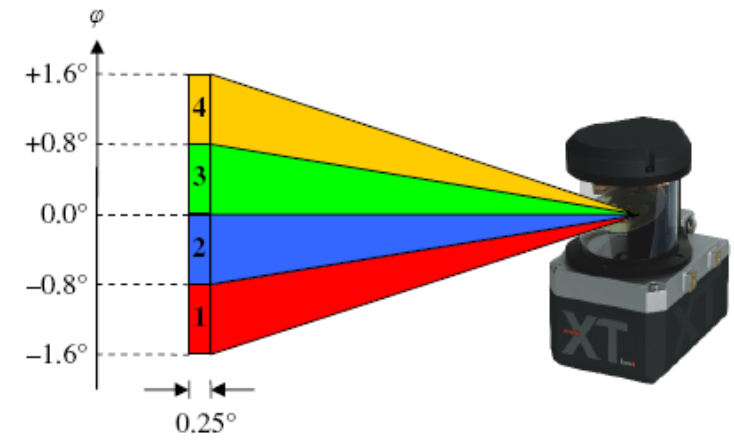

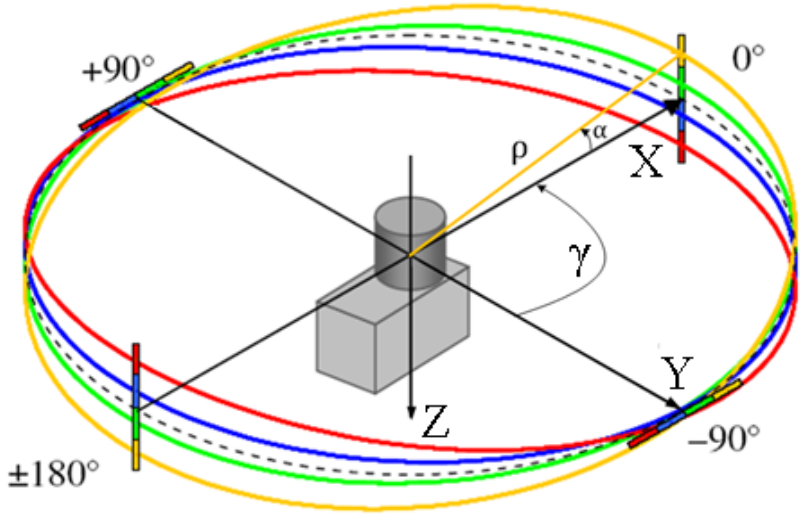

Images courtesy

Algorithm Overview

- Develop an equation to describe the Euler angles relating the LiDAR measurements to a vehicle on a level plane.
- LiDAR data will be collected on a static vehicle in steady state.
- LiDAR data will then be taken on a dynamic vehicle and compared to the steady state data to estimate vehicle motion and/or calibration parameters

Determination of Yaw

- Yaw cannot be determined directly
- Must have additional dynamic
- Rotation about Z-axis

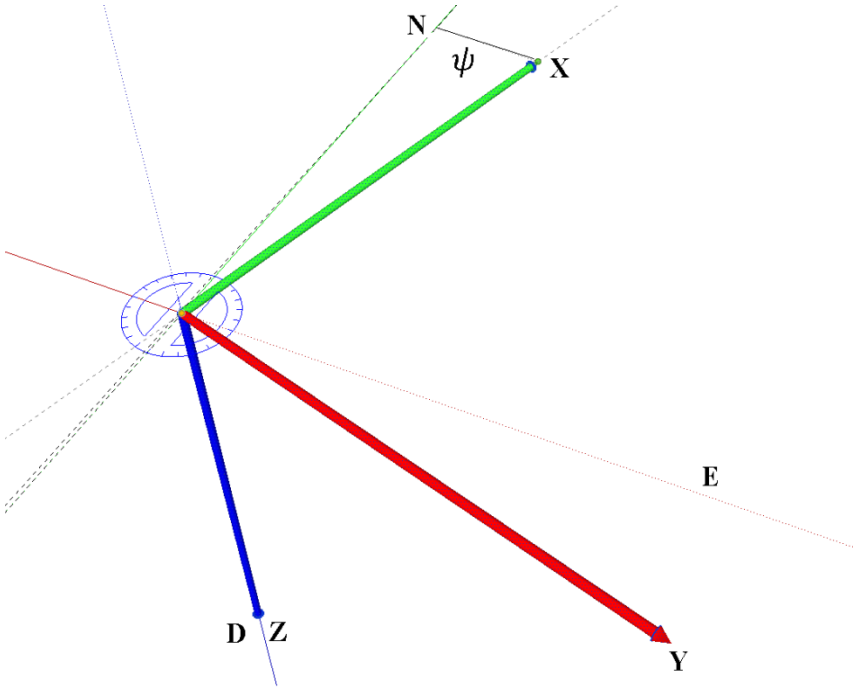

Determination of LiDAR Pitch

- Rotation about Y-axis

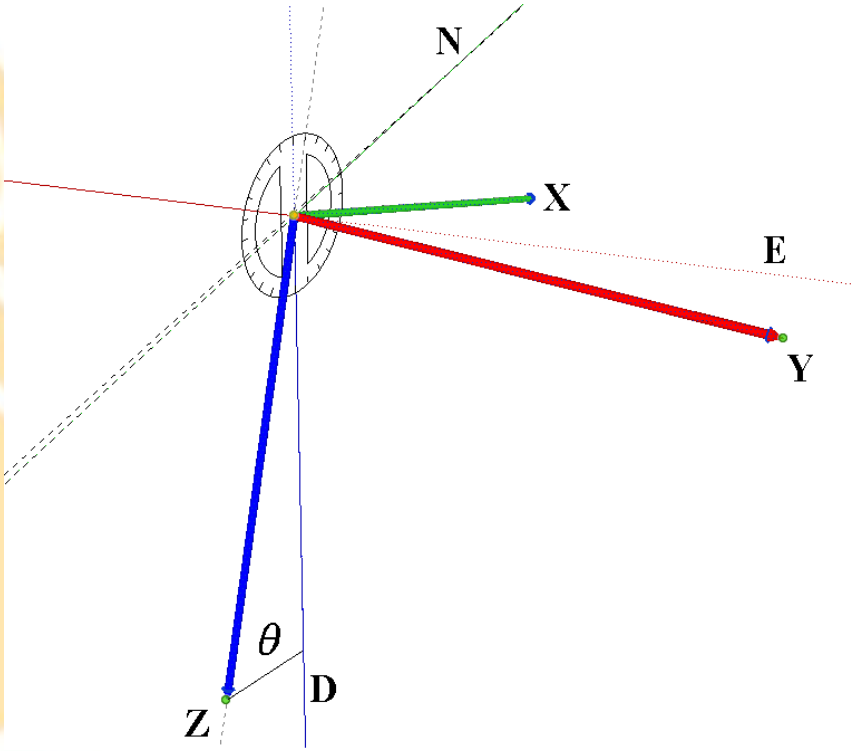

Determination of LiDAR Roll

- Rotation about X-axis

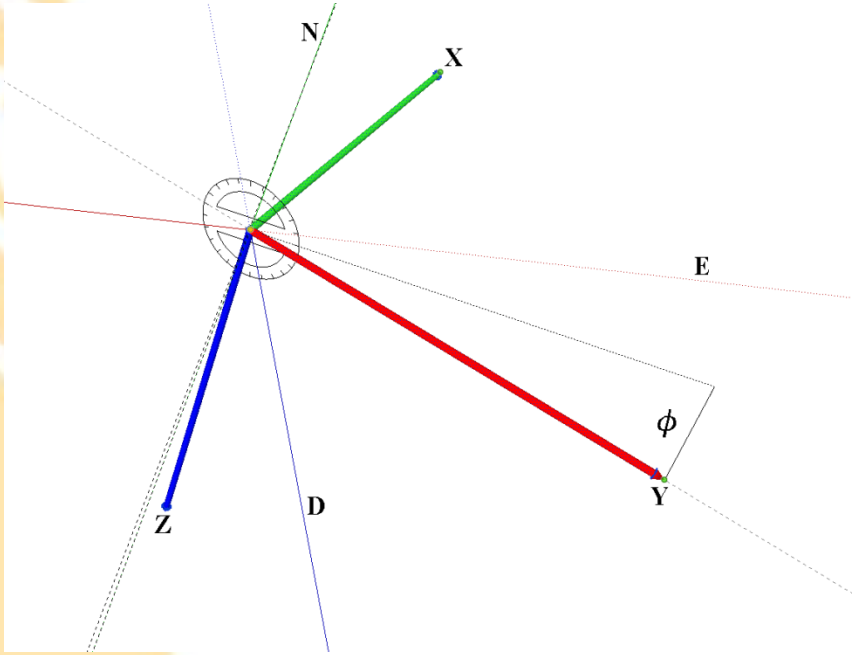

Determination of LiDAR Pitch & Roll :: Calibration Phase

- Because all points originate at the same location, we have an over determined system.
  - Note: pitch and roll are not a function of yaw.

$$NED_{lidar\_frame} = \begin{bmatrix} 1 & 0 & 0 \\ 0 & \cos(\phi) & \sin(\phi) \\ 0 & -\sin(\phi) & \cos(\phi) \end{bmatrix} \begin{bmatrix} \cos(\theta) & 0 & -\sin(\theta) \\ 0 & 1 & 0 \\ \sin(\theta) & 0 & \cos(\theta) \end{bmatrix} \begin{bmatrix} \cos(\psi) & \sin(\psi) & 0 \\ -\sin(\psi) & \cos(\psi) & 0 \\ 0 & 0 & 1 \end{bmatrix} \begin{bmatrix} x_n \\ y_n \\ z_n \end{bmatrix}$$

$$D_{\mathrm{n,lidar}} = -\sin(\theta)\, x_{\mathrm{n}} + \sin(\phi)\cos(\theta)\, y_{\mathrm{n}} + \cos(\phi)\cos(\theta)\, z_{\mathrm{n}}$$

$$\theta_{12} = \tan^{-1}\left(\frac{\sin(\phi)\, y_2 + \cos(\phi)\, z_2 - \sin(\phi)\, y_1 - \cos(\phi)\, z_1}{x_2 - x_1}\right)$$

$$\theta_{13} = \tan^{-1}\left(\frac{\sin(\phi)\, y_3 + \cos(\phi)\, z_3 - \sin(\phi)\, y_1 - \cos(\phi)\, z_1}{x_3 - x_1}\right)$$

$$\phi_{1213} = \tan^{-1}\left(\frac{(z_3 - z_1)(x_2 - x_1) + (z_1 - z_2)(x_3 - x_1)}{(y_1 - y_2)(x_3 - x_1) + (y_1 - y_3)(x_2 - x_1)}\right)$$

Determining LiDAR yaw

- The yaw is the relative yaw between the vehicle and LiDAR not global yaw.
- Vehicle must undergo a pure pitch dynamic.
  - Hence if the LiDAR and vehicle's axes are aligned with the vehicle's there should be no change in roll during this maneuver.
- We compare a pitched scan and static scan to determine this relative yaw

Determination of Vehicle Pitch & Roll

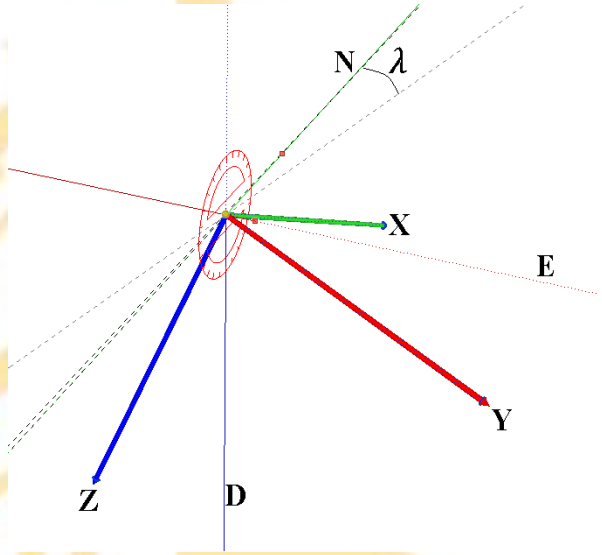

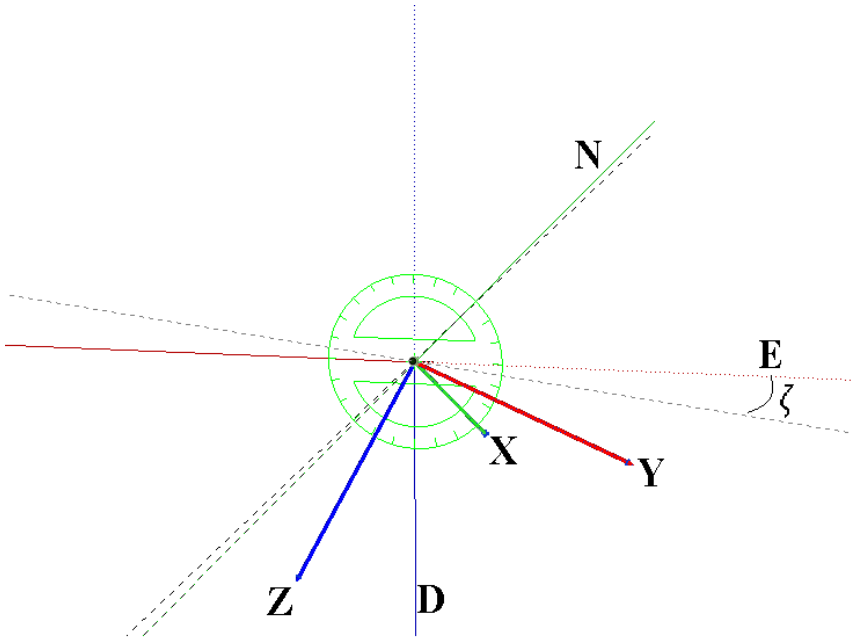

Perform some math

$$\begin{bmatrix} N_n \\ E_n \\ D_n \end{bmatrix} = \begin{bmatrix} \cos(\lambda) & 0 & -\sin(\lambda) \\ 0 & 1 & 0 \\ \sin(\lambda) & 0 & \cos(\lambda) \end{bmatrix}^T \begin{bmatrix} 1 & 0 & 0 \\ 0 & \cos(\zeta) & \sin(\zeta) \\ 0 & -\sin(\zeta) & \cos(\zeta) \end{bmatrix}^T$$

$$* \left(\begin{bmatrix} 1 & 0 & 0 \\ 0 & \cos(\phi) & \sin(\phi) \\ 0 & -\sin(\phi) & \cos(\phi) \end{bmatrix} \begin{bmatrix} \cos(\theta) & 0 & -\sin(\theta) \\ 0 & 1 & 0 \\ \sin(\theta) & 0 & \cos(\theta) \end{bmatrix} \begin{bmatrix} \cos(\psi) & \sin(psi) & 0 \\ -\sin(\psi) & \cos(\psi) & 0 \\ 0 & 0 & 1 \end{bmatrix} \right)^T \begin{bmatrix} x_n \\ y_n \\ z_n \end{bmatrix}$$

$$\begin{aligned} D_n = \sin(\lambda) & \left(\sin(\psi)\left(-z_n \sin(\phi) + y_n \cos(\phi)\right)\right. \\ & + \cos(\psi)\left(-x_n \cos(\theta) - y_n \sin(\phi)\sin(\theta) - z_n \cos(\phi)\sin(\theta)\right)\Big) \\ & + \cos(\lambda)\Big(\sin(\zeta)\left(y_n \sin(\phi)\sin(\theta)\sin(\psi) + x_n \cos(\theta)\sin(\psi)\right. \\ & + y_n \cos(\phi)\cos(\psi) + z_n \cos(\phi)\sin(\theta)\sin(\psi) - z_n \sin(\phi)\cos(\psi)\Big) \\ & + \cos(\zeta)\left(y_n \sin(\phi)\cos(\theta) - x_n \sin(\theta) + z_n \cos(\phi)\cos(\theta)\right)\Big) \end{aligned}$$

$$\begin{aligned} A_1 = & -y_1 \sin(\phi)\cos(\theta) + x_1 \sin(\theta) - z_1 * \cos(\phi) * \cos(theta) + z_2 \cos(\phi)\cos(\theta) \\ & + y_2 \sin(\phi)\cos(\theta) - x_2 \sin(\theta) \end{aligned}$$

$$\begin{aligned} B_1 = & \, y_3 \sin(\phi)\cos(\theta) - x_3 \sin(\theta) + z_3 \cos(\phi) * \cos(\theta) - y_1 \sin(\phi)\cos(\theta) + x_1 \sin(\theta) \\ & - z_1 \cos(\phi)\cos(\theta) \end{aligned}$$

$$D_1 = -z_2 \sin(\phi) + y_2 \cos(\phi) + z_1 \sin(\phi) - y_1 \cos(\phi)$$

$$E_1 = -z_3 \sin(\phi) + z_1 \sin(\phi) + y_3 \cos(\phi) - y_1 \cos(\phi)$$

$$\begin{aligned} G_1 = & -x_1 \cos(\theta) + z_2 \cos(\phi)\sin(\theta) - y_1 \sin(\phi)\sin(\theta) + y_2 \sin(\phi)\sin(\theta) + x_2 \cos(\theta) \\ & - z_1 \cos(\phi)\sin(\theta) \end{aligned}$$

$$\begin{aligned} A_2 = & -y_{11} \sin(\phi)\cos(\theta) + x_{11} \sin(\theta) - z_{11} * \cos(\phi) * \cos(theta) + z_{22} \cos(\phi)\cos(\theta) \\ & + y_{22} \sin(\phi)\cos(\theta) - x_{22} \sin(\theta) \end{aligned}$$

$$\begin{aligned} B_2 = & \, y_{33} \sin(\phi)\cos(\theta) - x_{33} \sin(\theta) + z_{33} \cos(\phi) * \cos(\theta) - y_{11} \sin(\phi)\cos(\theta) + x_{11} \sin(\theta) \\ & - z_{11} \cos(\phi)\cos(\theta) \end{aligned}$$

$$D_2 = -z_{22} \sin(\phi) + y_{22} \cos(\phi) + z_{11} \sin(\phi) - y_{11} \cos(\phi)$$

$$E_{11} = -z_{33} \sin(\phi) + z_{11} \sin(\phi) + y_{33} \cos(\phi) - y_{11} \cos(\phi)$$

$$\begin{aligned} G_2 = & -x_{11} \cos(\theta) + z_{22} \cos(\phi)\sin(\theta) - y_{11} \sin(\phi)\sin(\theta) + y_{22} \sin(\phi)\sin(\theta) + x_{22} \cos(\theta \\ & - z_{11} \cos(\phi)\sin(\theta) \end{aligned}$$

$$\begin{aligned} H_2 = & \, z_{33} \cos(\phi)\sin(\theta) + y_{33} \sin(\phi)\sin(\theta) + x_{33} \cos(\theta) - z_{11} \cos(\phi)\sin(\theta) \\ & - y_{11} \sin(\phi)\sin(\theta) - x_{11} \cos(\theta) \end{aligned}$$

Determination of Vehicle Pitch & Roll

- Note: Function of LiDAR yaw
- Use similar procedure.

$$\lambda_{1122} = \tan^{-1}\left(\frac{\cos(\zeta)\,A_{11} + \sin(\zeta)\,(\cos(\psi)\,D_{11} + \sin(\psi)\,G_{11})}{\cos(\psi)\,G_{11} - \sin(\psi)\,D_{11}}\right)$$

$$\lambda_{1133} = \tan^{-1}\left(\frac{\cos(\zeta)\,B_{11} + \sin(\zeta)\,(\cos(\psi)\,E_{11} + \sin(\psi)\,H_{11})}{\cos(\psi)\,H_{11} - \sin(\psi)\,E_{11}}\right)$$

$$\zeta_{11221133} = \tan^{-1}\left(\frac{\cos(\psi)\,(B_2G_2 - A_2H_2) + \sin(\psi)\,(-B_2D_2 + A_2E_2)}{\cos(\psi)^2\,(D_2H_2 - E_2G_2) + \sin(\psi)^2\,(-G_2E_2 + H_2D_2)}\right)$$

Determination of relative yaw

- Note: yaw is now reduced to LiDAR pitch and roll measurements.
- Setting the static vehicle roll calculation and the pitched vehicle roll calculation equal to one another, yields:

$$\psi = \tan^{-1}\left(\frac{(B_2G_2 - A_2H_2)(D_1H_1 - E_1G_1) - (B_1G_1 - A_1H_1)(D_2H_2 - E_2G_2)}{(-B_1D_1 + A_1E_1)(D_2H_2 - E_2G_2) - (-B_2D_2 + A_2E_2)(D_1H_1 - E_1G_1)}\right)$$

Considerations

- Singularities
  - Cannot report meaningful data if pointed straight down
- Larger separation the better
  - Due to numerical issues and noise, the LiDAR measurements should have a large separation to guarantee the best results

Computing a Solution

- Unscented Transform used for error propagation estimation and propagation.
  - See thesis for details
- Kalman filter used for determining the final result.

Testing

- Laboratory testing
  - Benign environment with highly controlled maneuvers
- Vehicle testing (static)
  - Vehicle undergoes induced maneuvers
- Vehicle testing (dynamic)
  - Vehicle undergoes driving maneuvers

Test Setup: Laboratory

- 5 DOF Jig created
  - Simulates LiDAR pitch & roll, vehicle pitch & roll, and a yaw between them.
  - Hallway floor used to simulate planar surface.
- Relative angle measured using US-DIGITAL inclinometers (0.1) accuracy
- Preformed tests with a calibration scan and then a series of (vehicle) pitch and (vehicle) roll maneuvers

Test Results

- Total of ~200 tests preformed
- 50 LiDAR scans are analyzed at each test point
- 20 unique calibration points
- Pitch varies between 352.5 and 340.8
- Roll varies between 0.1 and 337.1

Pitch Errors

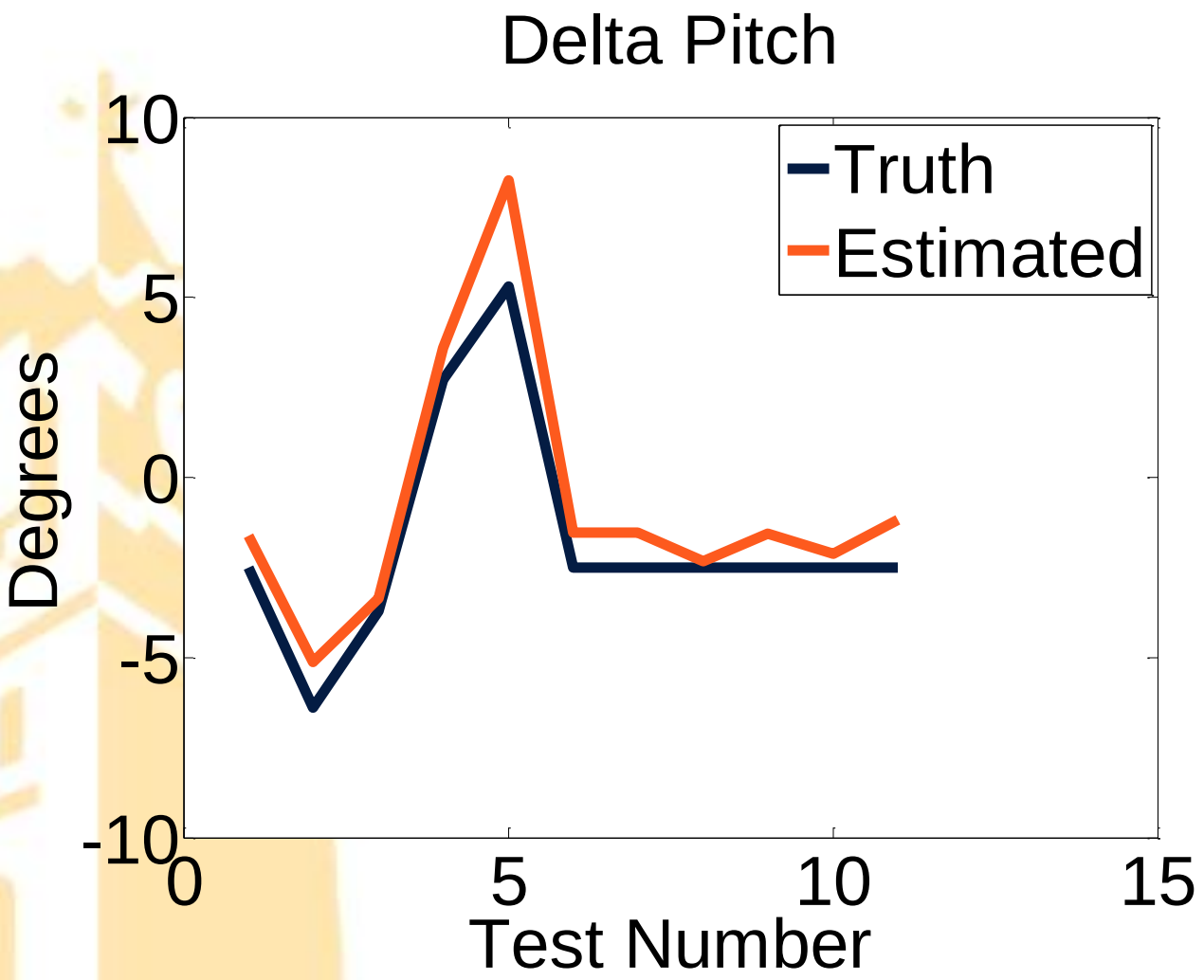

Roll Errors

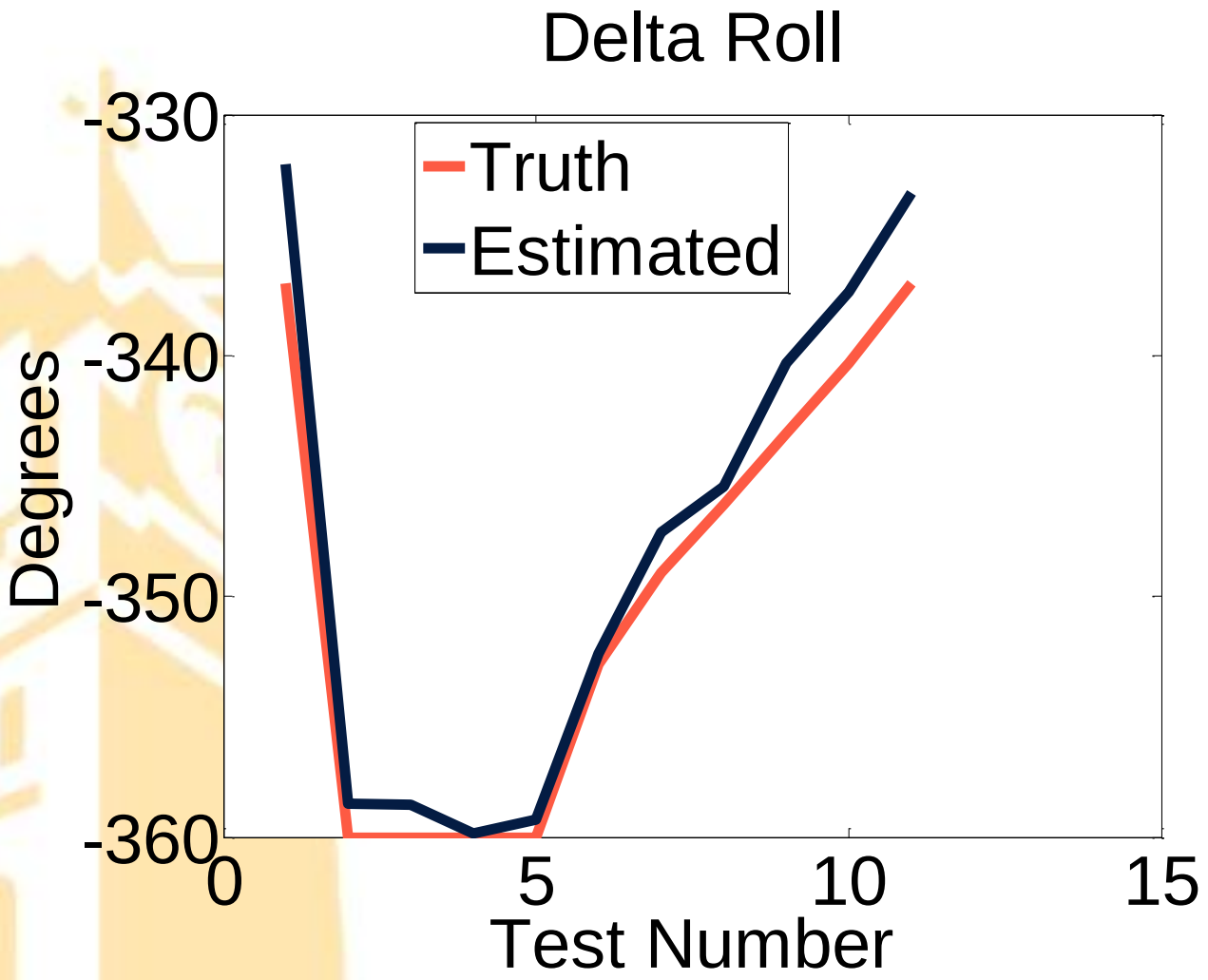
Delta Roll
Truth
Estimated
Degrees
-330
-340
-350
-360
0
5
10
15
Test Number

Results: Laboratory

- Results accurate to within 0.1 possible
- However after 200 tests the average error was:
  - Pitch =1.6
  - Roll = 1.78

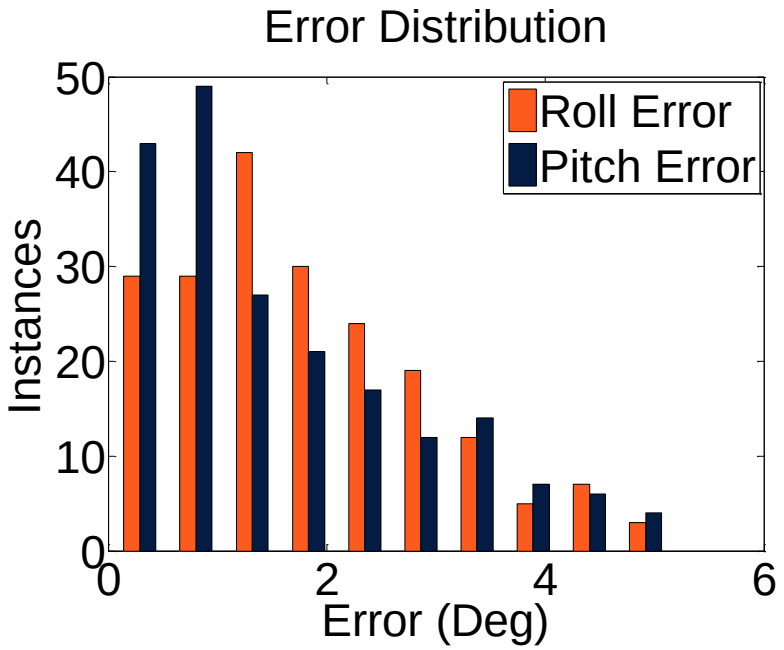

Test Procedure

Calibration:

- 50 Static Scans taken
- Vehicle was then driven and the brakes applied to induce vehicle pitch
- 50 static and one pitched scan of the brake test compared

Attitude Testing:

- Vehicle Position on flat level ground
- Vehicle underwent induced pitch and roll maneuvers.
  - Vehicle change in pitch = 1.46
  - Vehicle change in roll = 2.75

Truth & Comparative system :: Septentrio

- 3-antenna GPS system
- Provides vehicle pitch, roll, and yaw in Euler angle form.
- Accurate to ~0.6 for our given baseline

Pitch Comparison to Septentrio

Pitch:

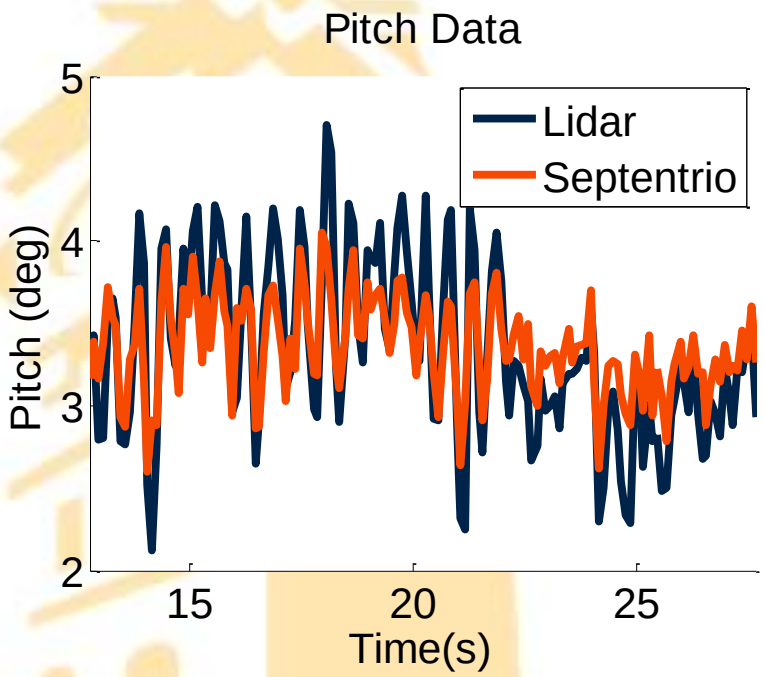

Roll:

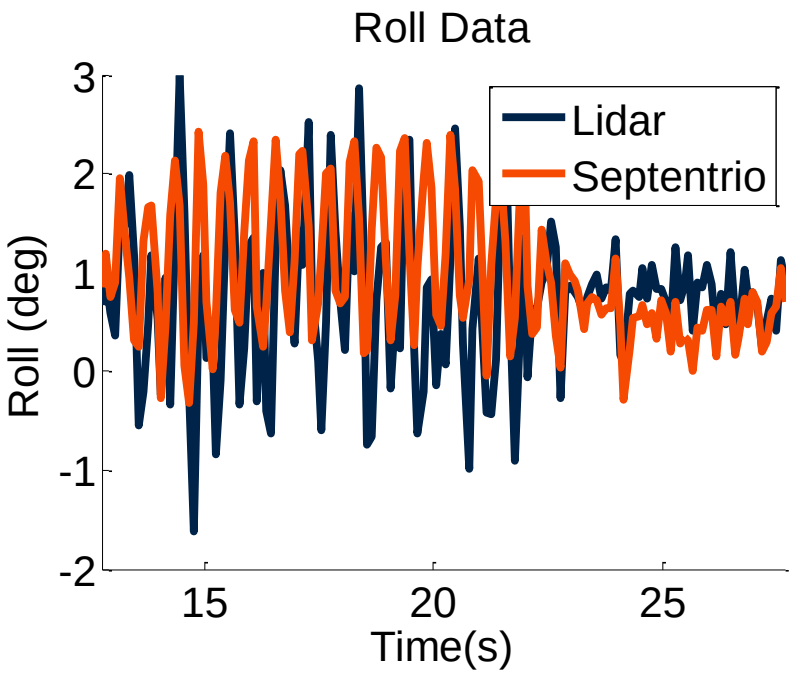

Results Vehicle(static)

- MSE Pitch = 0.1129
- MSE Roll = 0.7855

- Avg Error Pitch =0.28
- Avg Error Roll = 0.68

- Average Processing time per scan = 0.26s
- Average Calibration time = 66s

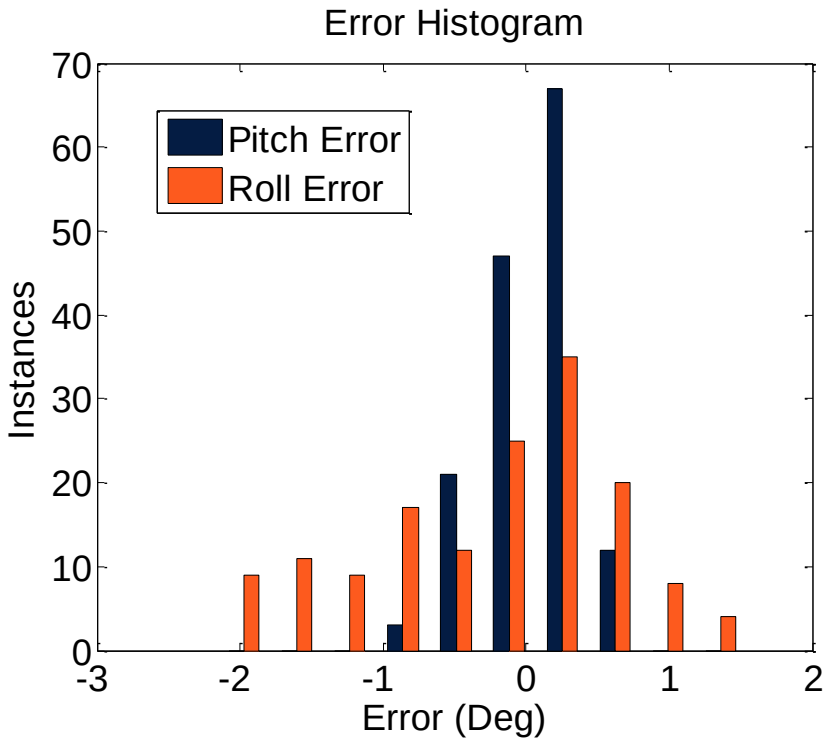

Test Procedure

Calibration:

- 50 Static Scans taken
- Vehicle was then driven and the brakes applied to induce vehicle pitch
- 50 static and one pitched scan of the brake test compared

Attitude Testing:

- Vehicle put through a series of dynamic maneuvers to induce vehicle pitch and roll
- Data analyzed only when in the maneuver

Dynamic Testing:

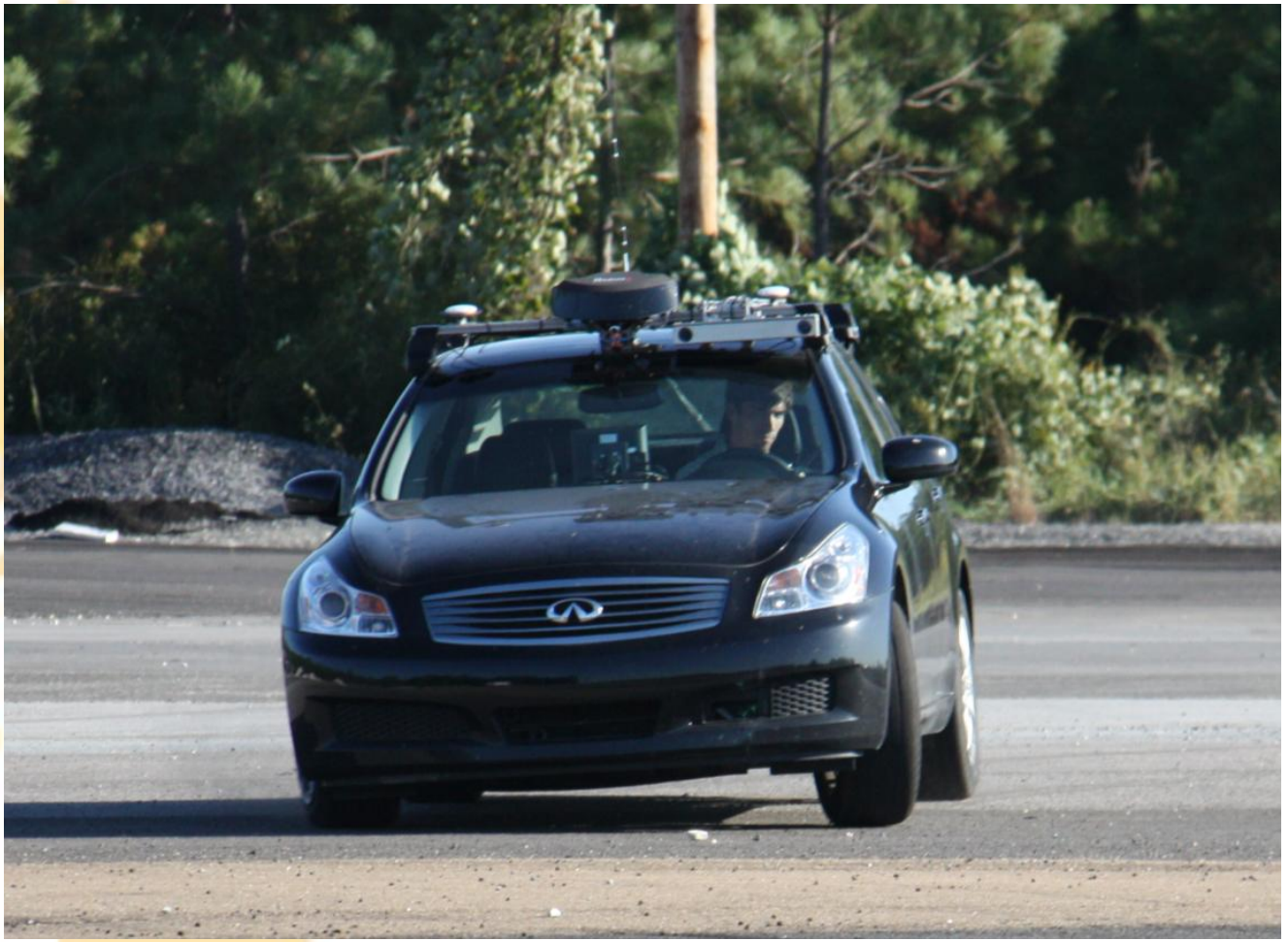

Pitch Comparison to Septentrio

Pitch:

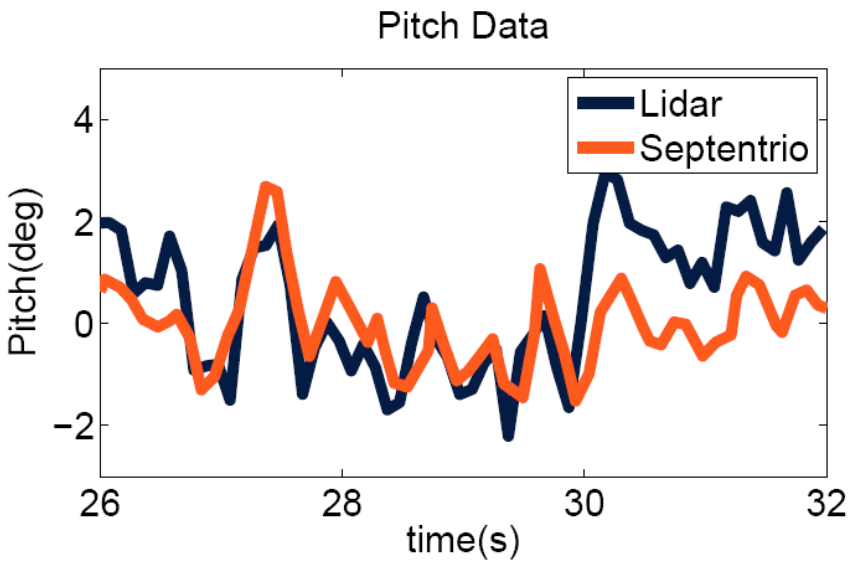

Roll:

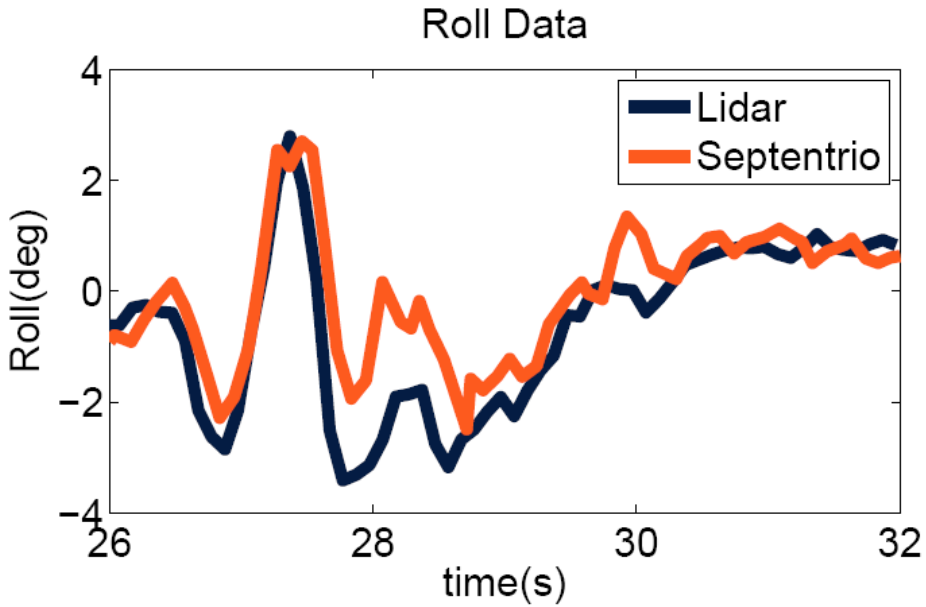

Results Vehicle(static)

- MSE Pitch = 2.054
- MSE Roll = 0.4617

- Avg Error Pitch =0.78
- Avg Error Roll = 0.31

- Average Processing time per scan = 0.06s
- Average Calibration time = 2.26s

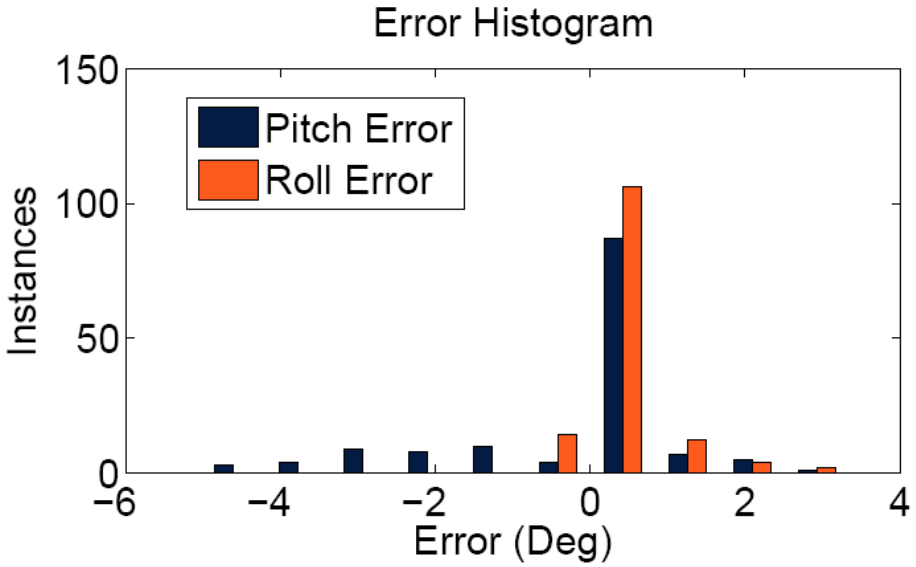

Results – Considerations

- Data was post processed
- No truth method used for determination of calibration success
- Error is merely comparative not absolute
  - Septentrio only accurate to ~0.6
  - No test preformed to determine the accuracy of the Septentrio's mounting on the vehicle

Conclusions

- Capable of determining vehicle pitch and roll to within sub-degree accuracy
- For meaningful calibration : vehicle's axes must be aligned with plane
- Highly non-linear problem
- Computationally complex
- Larger change in pitch dynamics the better for calibration

Future Work

- Determine how non uniform plane can be to yield accurate results

Questions or Comments?

Use of Vision Sensors and Lane Maps to Aid GPS-INS under a Limited GPS Satellite Constellation

AUBURN

UNIVERSITY

SAMUEL GINN
COLLEGE OF ENGINEERING

John Allen

Work Funded by FHWA

Outline

- Prior Work/Contributions
- Motivation
- Background
- Lane Map
- 6DOF Filter Setup and Results
- Limited GPS Satellite Observabilty and Results

Motivation

- Research has shown that nearly half of traffic fatalities occur due to an unintentional lane departure.
  - Lane departure warning (LDW) systems may prevent many of these accidents.
  - Current LDW systems use only vision sensors.
- GPS based navigation filters are prone to failure in urban environments.
- Goal of this thesis is to present a method of combining vision measurements and vehicle constraints to maintain observability of a GPS based navigation filter when only 2 GPS satellites are visible.
- An Extended Kalman Filter is used to combine measurements from a GPS receiver, LiDAR, camera, and IMU.
  - The navigation coordinate frame used is a Cartesian coordinate frame based off a waypoint map.

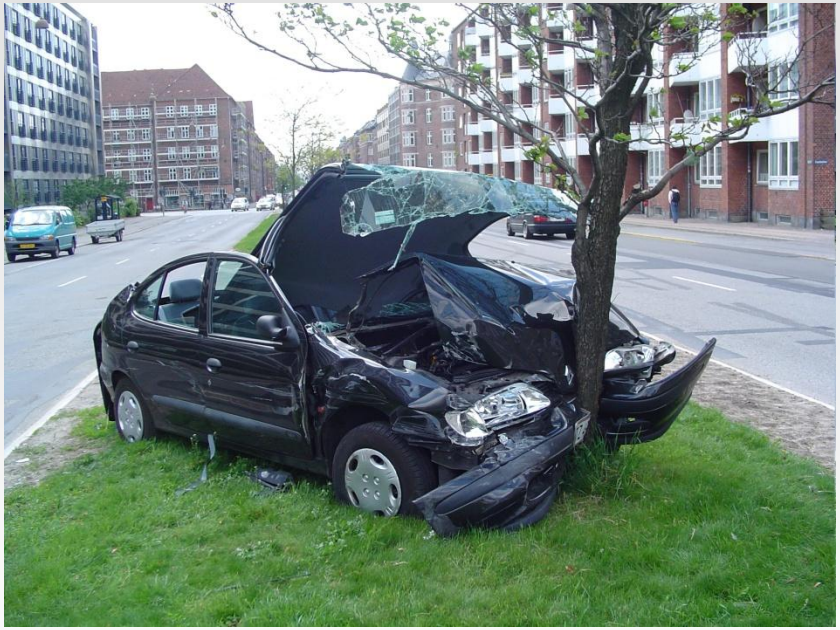

AUBURN UNIVERSITY

SAMUEL GINN COLLEGE OF ENGINEERING

Prior Work

- J. Clanton, “Gps and inertial sensors enhancement for vision-based highway lane tracking," Master's thesis, Auburn University, 2006.
- S. Mammar, S. Glaser, and M. Netto, “Time to line crossing for lane departure avoidance: a theoretical study and an experimental setting," vol. 7, no. 2, pp. 226-241, 2006.
- J. Kibbel, W. Justus, and K. Furstenberg, “Lane estimation and departure warning using multilayer laserscanner," in Proc. IEEE Intelligent Transportation Systems, pp. 607-611, 2005.

Contributions

- J. W. Allen and D. M. Bevly, “Use of vision sensors and lane maps to aid gps/ins under a limited gps satellite constellation," in 2010 ION GNSS Savannah, Georgia, 2010.
- J. W. Allen and D. M. Bevly, “Relating local vision measurements to global navigation satellite systems using waypoint based maps," in Proc. IEEE/ION Position Location and Navigation Symp. (PLANS), pp. 1204-1211, 2010.
- J. W. Allen, C. Rose, J. Britt, and D. M. Bevly, “Intelligent multi-sensor measurements to enhance vehicle navigation and safety systems," in 2009 International Technical Meeting. Anaheim, California, 2009.

Background

- Typical navigation filter setup
  - Filter is based in a navigation coordinate frame
  - IMU measurements are given in the body coordinate frame and must be rotated into the navigation coordinate frame.
  - Update measurements are given in the navigation coordinate frame.
- Vision measurements are not given in the navigation coordinate frame.

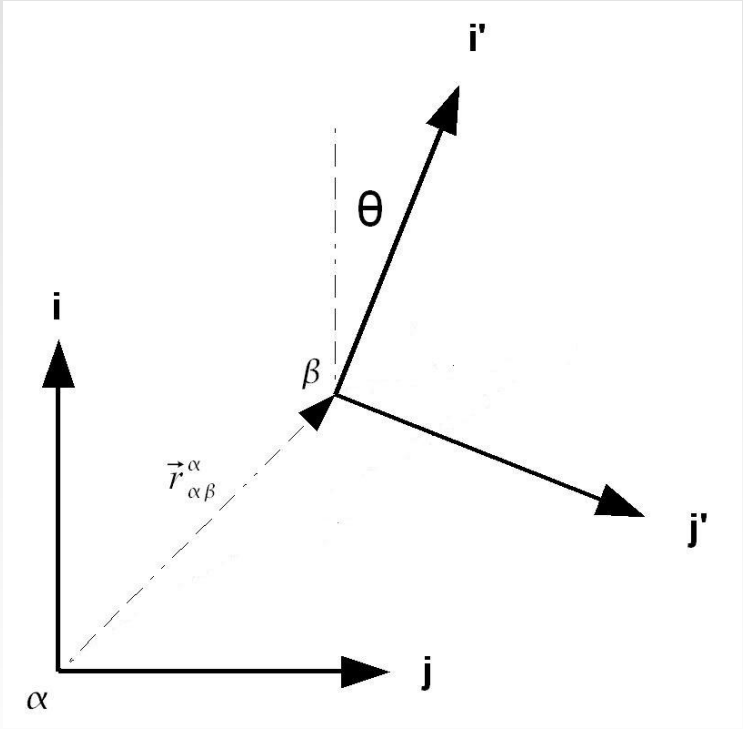

Background

- If measurements are not given in the navigation coordinate frame, they can be rotated and translated to the navigation coordinate frame.
- This will not work for a lane position measurement

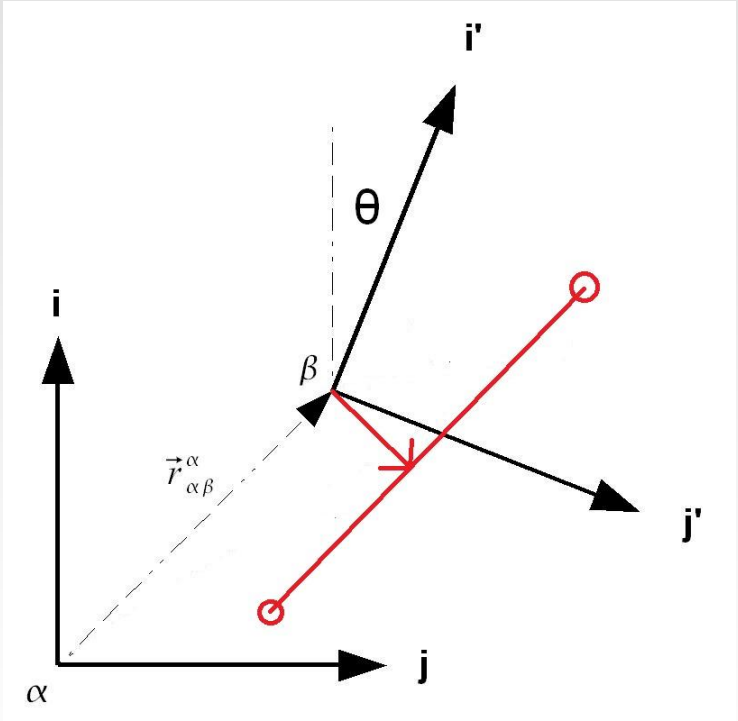

Background

- First approach was to construct a navigation filter with a navigation coordinate frame based on the way-point map.
- Ideally, we would like to add lane position measurements to typical types of navigation filters.

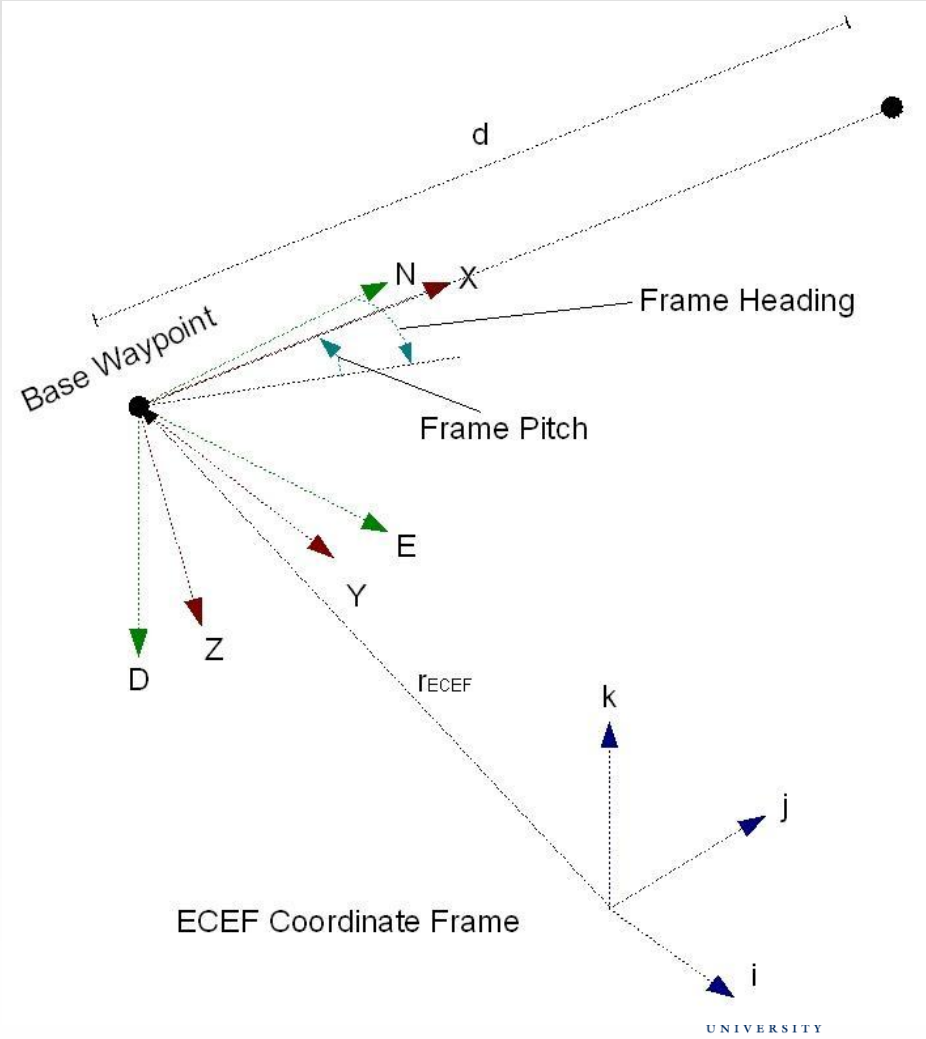

Rotation 2D

- 2D rotations are based on one rotation
- Rotation is about an axis that is perpendicular to the 2D coordinate frame

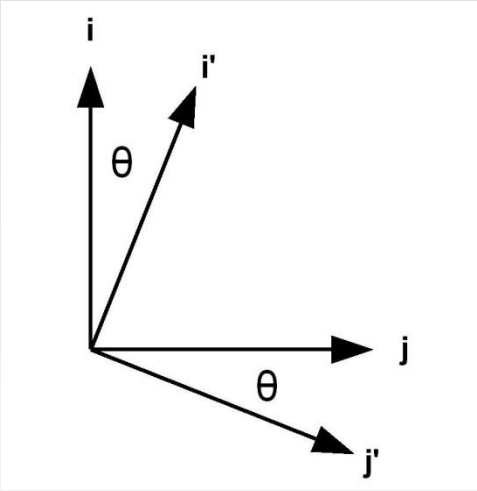

$$C_{(i,j)}^{(i',j')} = \begin{bmatrix} \cos(\theta) & \sin(\theta) \\ -\sin(\theta) & \cos(\theta) \end{bmatrix}$$

Rotation 3D

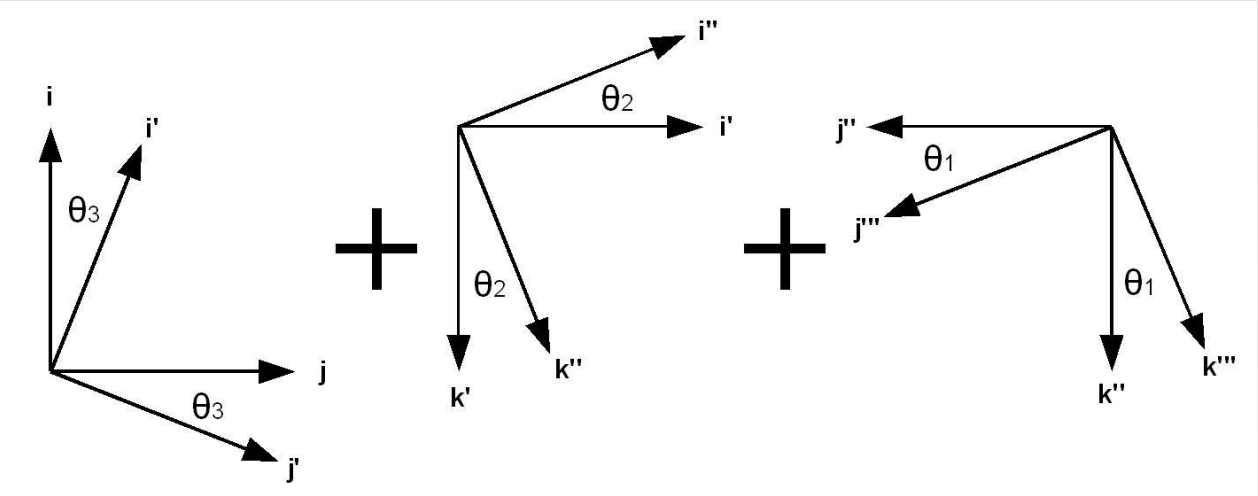

$$C_{(i,j)}^{(i''',j''')} = \begin{bmatrix} 1 & 0 & 0 \\ 0 & c_1 & s_1 \\ 0 & -s_1 & c_1 \end{bmatrix} \begin{bmatrix} c_2 & 0 & -s_2 \\ 0 & 1 & 0 \\ s_2 & 0 & c_2 \end{bmatrix} \begin{bmatrix} c_3 & s_3 & 0 \\ -s_3 & c_3 & 0 \\ 0 & 0 & 1 \end{bmatrix} = \begin{bmatrix} c_2c_3 & c_2s_3 & -s_2 \\ s_1s_2c_3 - c_1s_3 & s_1s_2s_3 + c_1c_3 & s_1c_2 \\ c_1s_2c_3 + s_1s_3 & c_1s_2s_3 - s_1c_3 & c_1c_2 \end{bmatrix}$$

Rotation and Translation

- Coordinates from 2 different coordinate frames can be mapped into each other.

$$\vec{r}^{\,\beta}_{\beta p} = C^{\beta}_{\alpha}\left[\vec{r}^{\,\alpha}_{\alpha p} - \vec{r}^{\,\alpha}_{\alpha\beta}\right]$$

$$\vec{r}^{\,\alpha}_{\alpha p} = C^{\alpha}_{\beta}\vec{r}^{\,\beta}_{\beta p} + \vec{r}^{\,\alpha}_{\alpha\beta}$$

$$\vec{v}^{\,\beta} = C^{\beta}_{\alpha}\vec{v}^{\,\alpha}$$

$$\vec{v}^{\,\alpha} = C^{\alpha}_{\beta}\vec{v}^{\,\beta}$$

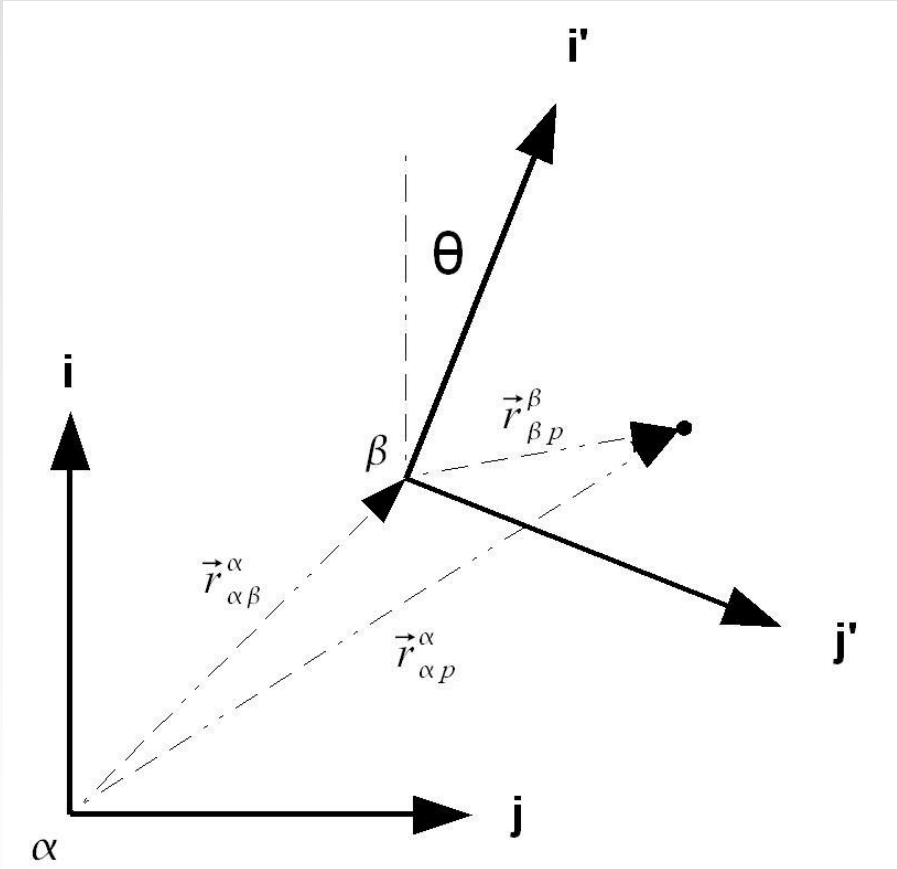

AUBURN UNIVERSITY
SAMUEL GINN COLLEGE OF ENGINEERING

Track Survey

- In order to use GPS to measure lane position, an accurate map of the lane must constructed.
- For our project, we surveyed the NCAT test track in Opelika, AL.

Google Earth

Track Survey

Track Map

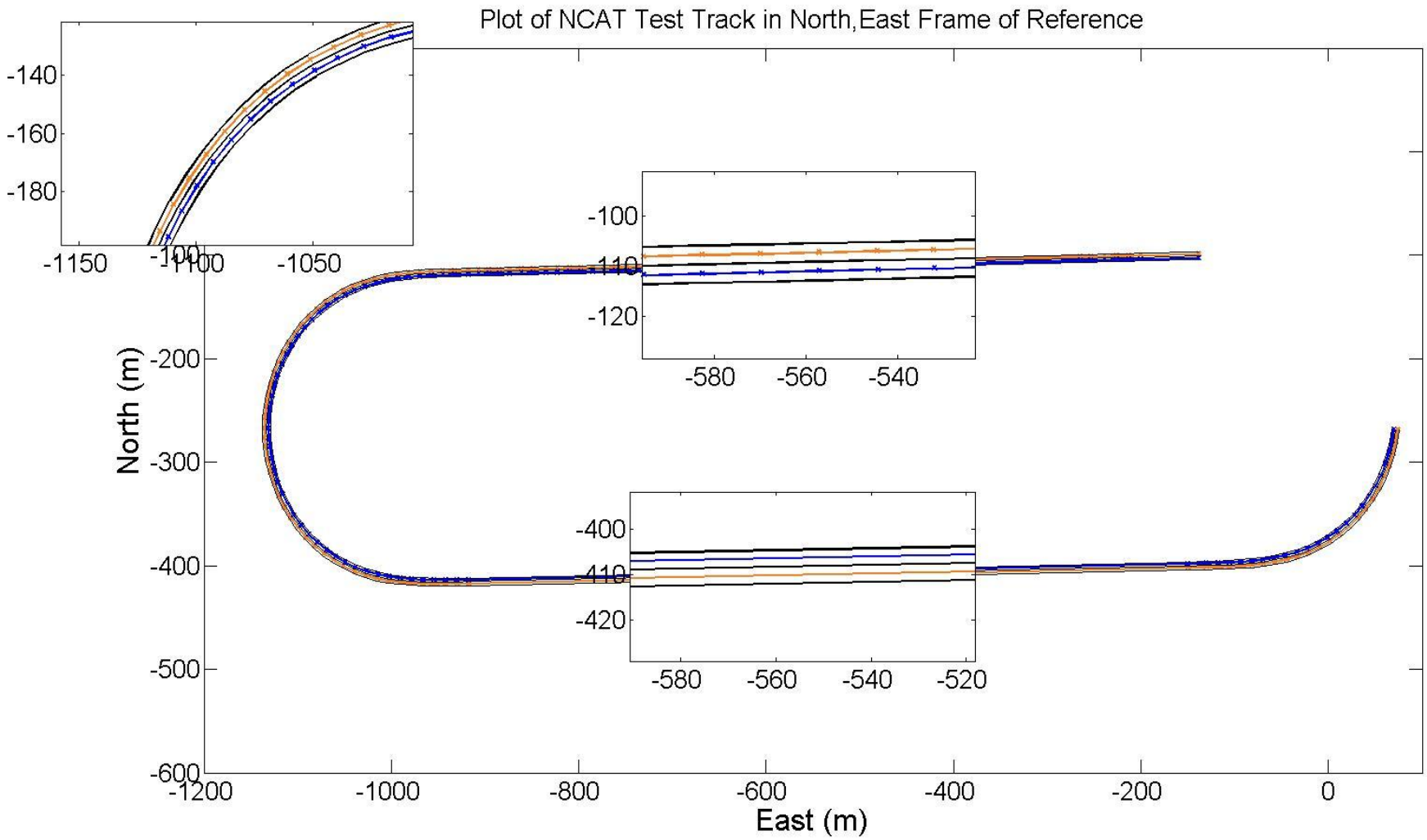
Plot of NCAT Test Track in North,East Frame of Reference
North (m)
East (m)
-140
-160
-180
-1150
-1100
-1050
-100
-110
-120
-580
-560
-540
-400
-410
-420
-520
-200
-300
-500
-600
-1200
-1000
-800
-600
-400
0

Track Map

- RTK GPS used to survey the track
- RTK provides a very accurate base line between base station and rover
- Survey should be saved as base-line vectors from a marked location in order to prevent global biasing

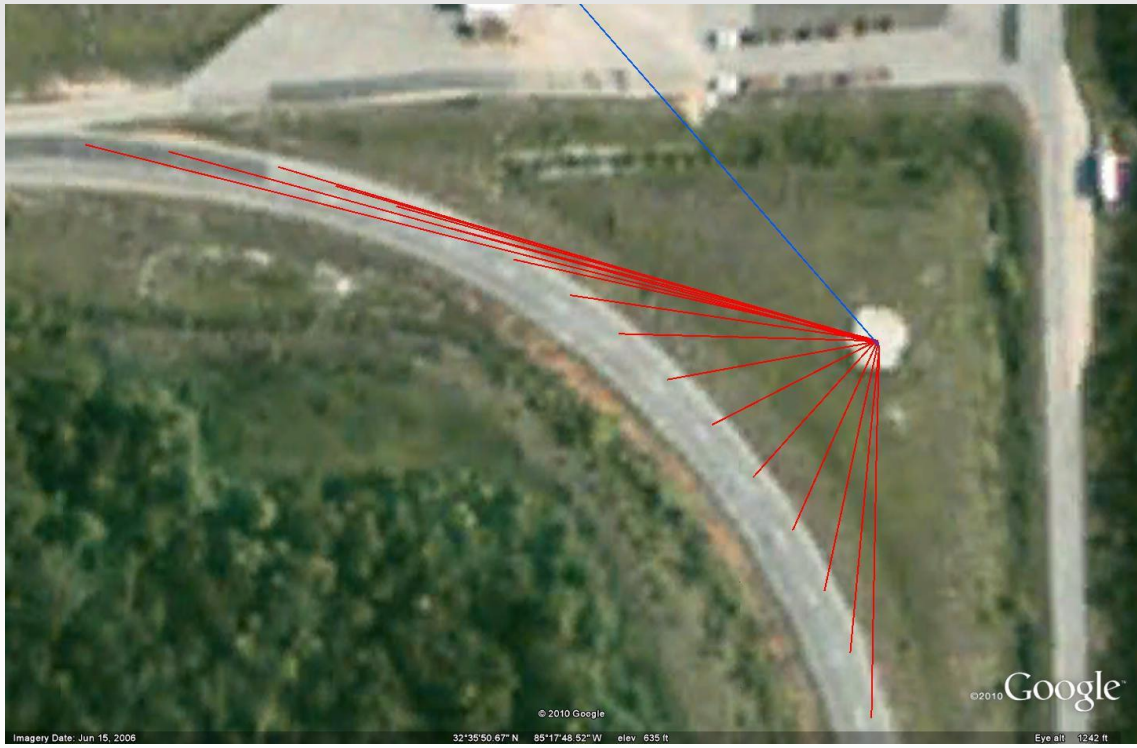

AUBURN UNIVERSITY
SAMUEL GINN COLLEGE OF ENGINEERING

Track Map

- Along with waypoint positions, road attitude is needed
- Attitude represents rotation from the ECEF (navigation) coordinate frame to the Road (measurement) coordinate frame
- Road coordinate frame
  - X axis points in the from last waypoint passed to next waypoint
  - Y axis points right when facing direction of travel
  - Z axis points down with respect to the x-y plane

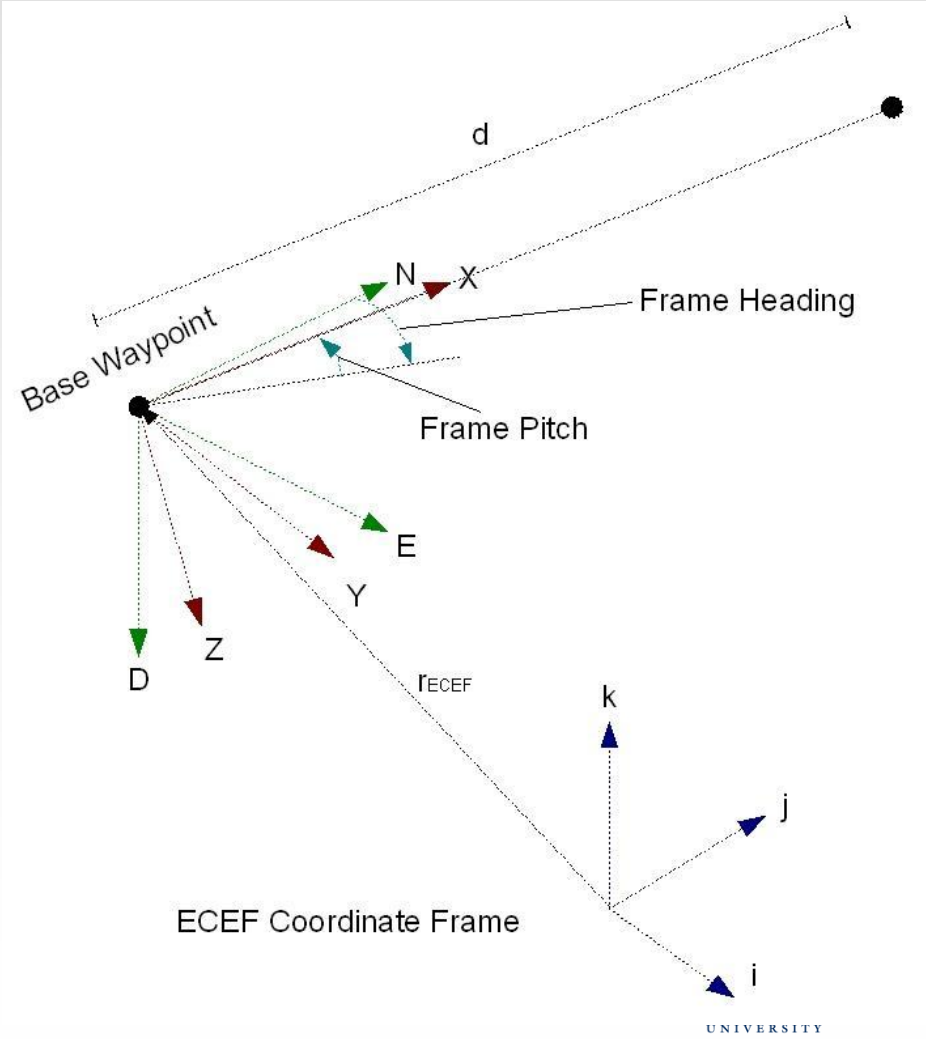

Track Map

- Can be thought of as 4 Euler rotations (longitude, latitude, road heading, and road pitch)
  - Longitude and Latitude can be determined from waypoint positions
  - Road heading and pitch can be determined by waypoint geometry.
- Wish to determine the 3 Euler angles that correspond to the 4 known rotations

$$Map\ Database = \begin{bmatrix} \vec{r}^{\,e}_{er,1} & \vec{\varphi}_1 & d_{r,1} \\ \vdots & \vdots & \vdots \\ \vec{r}^{\,e}_{er,m} & \vec{\varphi}_m & d_{r,m} \end{bmatrix}$$

6 DOF Filter Setup

- States: position, velocity, attitude, accel/gyro biases, clock drift/bias
- Navigation coordinate frame is the global (ECEF) coordinate frame
- GPS measurements are given in the global coordinate frame

$$x = \begin{bmatrix} \vec{r}^{\,e}_{eb} & \vec{v}^{\,e}_{eb} & \vec{a} & \vec{b}_f & \vec{b}_g & c\delta t & c\delta \dot{t} \end{bmatrix}^T$$

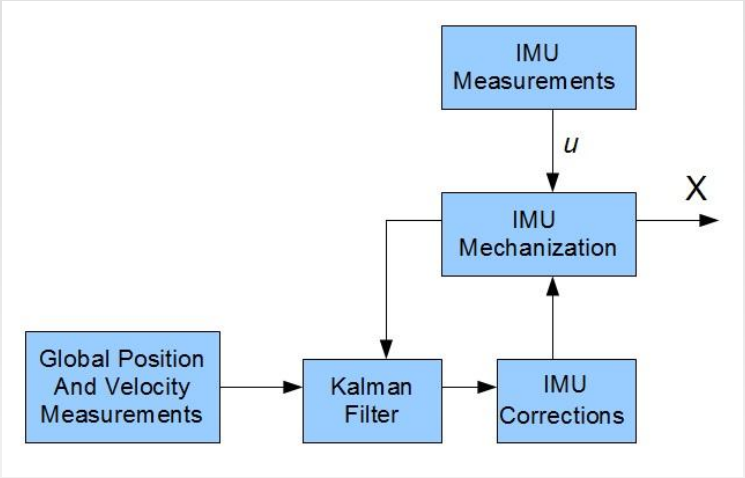

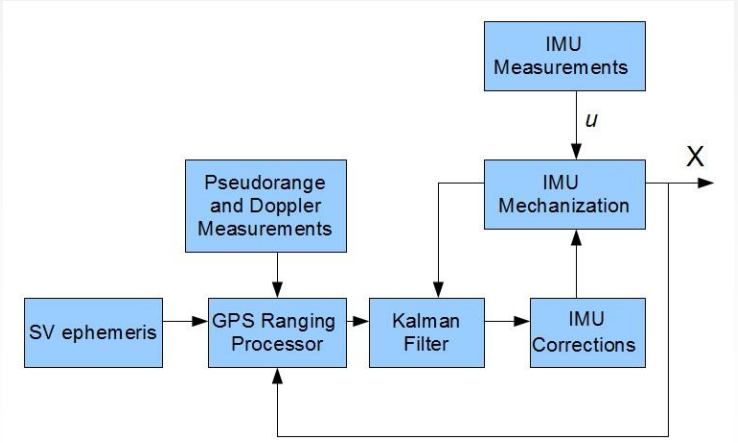

6 DOF Filter Setup

- Adding lane map results in the ability to use measurements in the road coordinate frame
  - Vision is used to measure position in one axis
  - Height above the road is constant allowing measurement of position in another axis

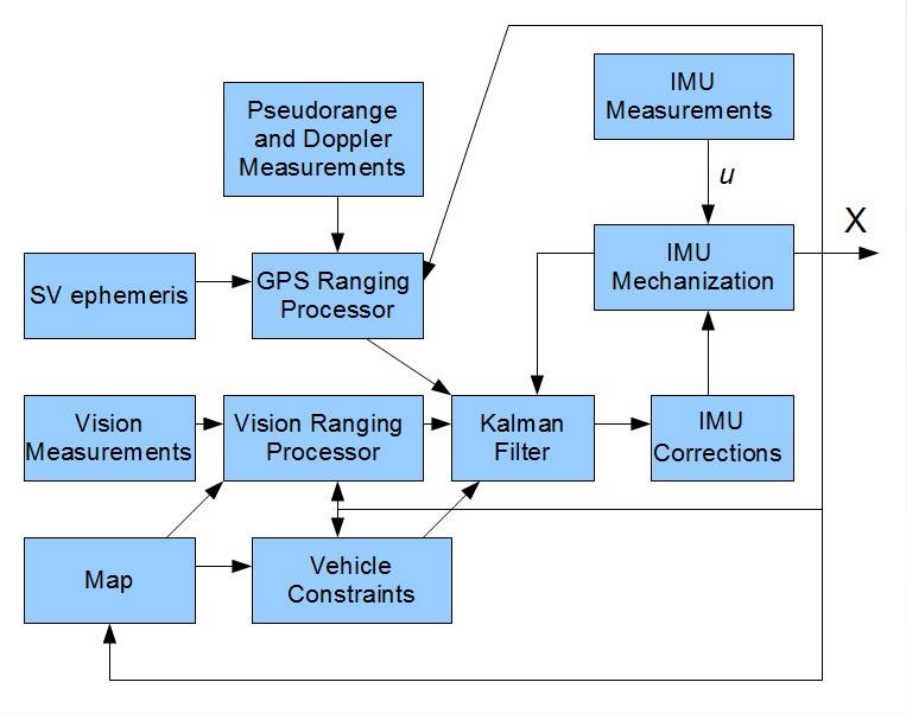

AUBURN UNIVERSITY
SAMUEL GINN COLLEGE OF ENGINEERING

Vision\Height Measurement Update

$$Map\ Database = \begin{bmatrix} \vec{r}^{\,e}_{er,1} & \vec{\varphi}_1 & d_{r,1} \\ \vdots & \vdots & \vdots \\ \vec{r}^{\,e}_{er,m} & \vec{\varphi}_m & d_{r,m} \end{bmatrix}$$

$$C^r_e = \begin{bmatrix} c_2c_3 & c_2s_3 & -s_2 \\ s_1s_2c_3 - c_1s_3 & s_1s_2s_3 + c_1c_3 & s_1c_2 \\ c_1s_2c_3 + s_1s_3 & c_1s_2s_3 - s_1c_3 & c_1c_2 \end{bmatrix}$$

$$\begin{bmatrix} \hat{x} \\ \hat{y} \\ \hat{z} \end{bmatrix} = C^r_e\left[\vec{r}^{\,e}_{eb} - \vec{r}^{\,e}_{er,i}\right]$$

$$h(x) = \begin{bmatrix} \hat{y} \\ \hat{h} \end{bmatrix} = \begin{bmatrix} C^r_{e\,(2,1)}\left(\vec{r}^{\,e}_{eb,1} - \vec{r}^{\,e}_{er,i,1}\right) + C^r_{e\,(2,2)}\left(\vec{r}^{\,e}_{eb,2} - \vec{r}^{\,e}_{er,i,2}\right) + C^r_{e\,(2,3)}\left(\vec{r}^{\,e}_{eb,3} - \vec{r}^{\,e}_{er,i,3}\right) \\ -C^r_{e\,(3,1)}\left(\vec{r}^{\,e}_{eb,1} - \vec{r}^{\,e}_{er,i,1}\right) - C^r_{e\,(3,2)}\left(\vec{r}^{\,e}_{eb,2} - \vec{r}^{\,e}_{er,i,2}\right) - C^r_{e\,(3,3)}\left(\vec{r}^{\,e}_{eb,3} - \vec{r}^{\,e}_{er,i,3}\right) \end{bmatrix}$$

$$e_1 = \left[C^r_{e\,(2,1)}, C^r_{e\,(2,2)}, C^r_{e\,(2,3)}\right]$$

$$e_2 = \left[-C^r_{e\,(3,1)}, -C^r_{e\,(3,2)}, -C^r_{e\,(3,3)}\right]$$

$$H(x) = \begin{bmatrix} e_1 & 0 & 0 & 0 & 0 & 0 & 0 \\ e_2 & 0 & 0 & 0 & 0 & 0 & 0 \end{bmatrix}$$

Vision\Height Measurement Update

$$Map\ Database = \begin{bmatrix} \vec{r}^{\,e}_{er,1} & \vec{\varphi}_1 & d_{r,1} \\ \vdots & \vdots & \vdots \\ \vec{r}^{\,e}_{er,m} & \vec{\varphi}_m & d_{r,m} \end{bmatrix}$$

$$C_e^r = \begin{bmatrix} c_2c_3 & c_2s_3 & -s_2 \\ s_1s_2c_3 - c_1s_3 & s_1s_2s_3 + c_1c_3 & s_1c_2 \\ c_1s_2c_3 + s_1s_3 & c_1s_2s_3 - s_1c_3 & c_1c_2 \end{bmatrix}$$

$$\begin{bmatrix} \hat{x} \\ \hat{y} \\ \hat{z} \end{bmatrix} = C_e^r\left[\vec{r}^{\,e}_{eb} - \vec{r}^{\,e}_{er,i}\right]$$

$$h(x) = \begin{bmatrix} \hat{y} \\ \hat{h} \end{bmatrix} = \begin{bmatrix} C^r_{e\,(2,1)}\left(\vec{r}^{\,e}_{eb,1} - \vec{r}^{\,e}_{er,i,1}\right) + C^r_{e\,(2,2)}\left(\vec{r}^{\,e}_{eb,2} - \vec{r}^{\,e}_{er,i,2}\right) + C^r_{e\,(2,3)}\left(\vec{r}^{\,e}_{eb,3} - \vec{r}^{\,e}_{er,i,3}\right) \\ -C^r_{e\,(3,1)}\left(\vec{r}^{\,e}_{eb,1} - \vec{r}^{\,e}_{er,i,1}\right) - C^r_{e\,(3,2)}\left(\vec{r}^{\,e}_{eb,2} - \vec{r}^{\,e}_{er,i,2}\right) - C^r_{e\,(3,3)}\left(\vec{r}^{\,e}_{eb,3} - \vec{r}^{\,e}_{er,i,3}\right) \end{bmatrix}$$

$$e_1 = \left[C^r_{e\,(2,1)}, C^r_{e\,(2,2)}, C^r_{e\,(2,3)}\right]$$

$$e_2 = \left[-C^r_{e\,(3,1)}, -C^r_{e\,(3,2)}, -C^r_{e\,(3,3)}\right]$$

$$H(x) = \begin{bmatrix} e_1 & 0 & 0 & 0 & 0 & 0 & 0 \\ e_2 & 0 & 0 & 0 & 0 & 0 & 0 \end{bmatrix}$$

Test Setup

- All test was done at the Nation Center for Asphalt Testing (NCAT) test track in Opelika, AL
  - 2 Lanes
  - 1.8 mile oval
  - 8 degrees of bank in the turns

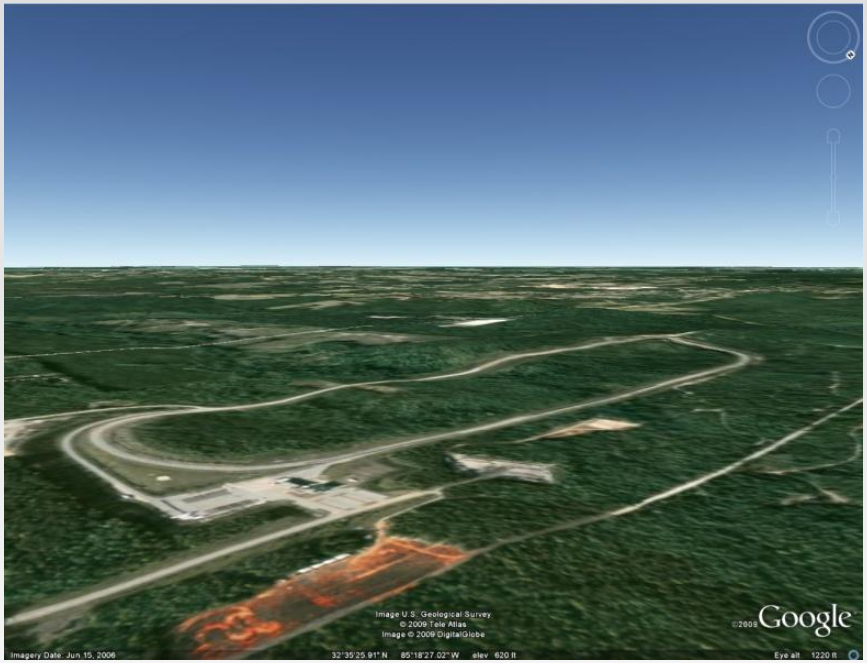

AUBURN UNIVERSITY
SAMUEL GINN COLLEGE OF ENGINEERING

Test Setup

- Results obtained by post processing real data.
- All data was collected at the NCAT test track
- Equipment Used:
  - Septentrio GPS receiver
  - Crossbow 440 IMU
  - IBEO ALASCA XT laser scanner
  - Logitch QuickCam Pro 9000

Results

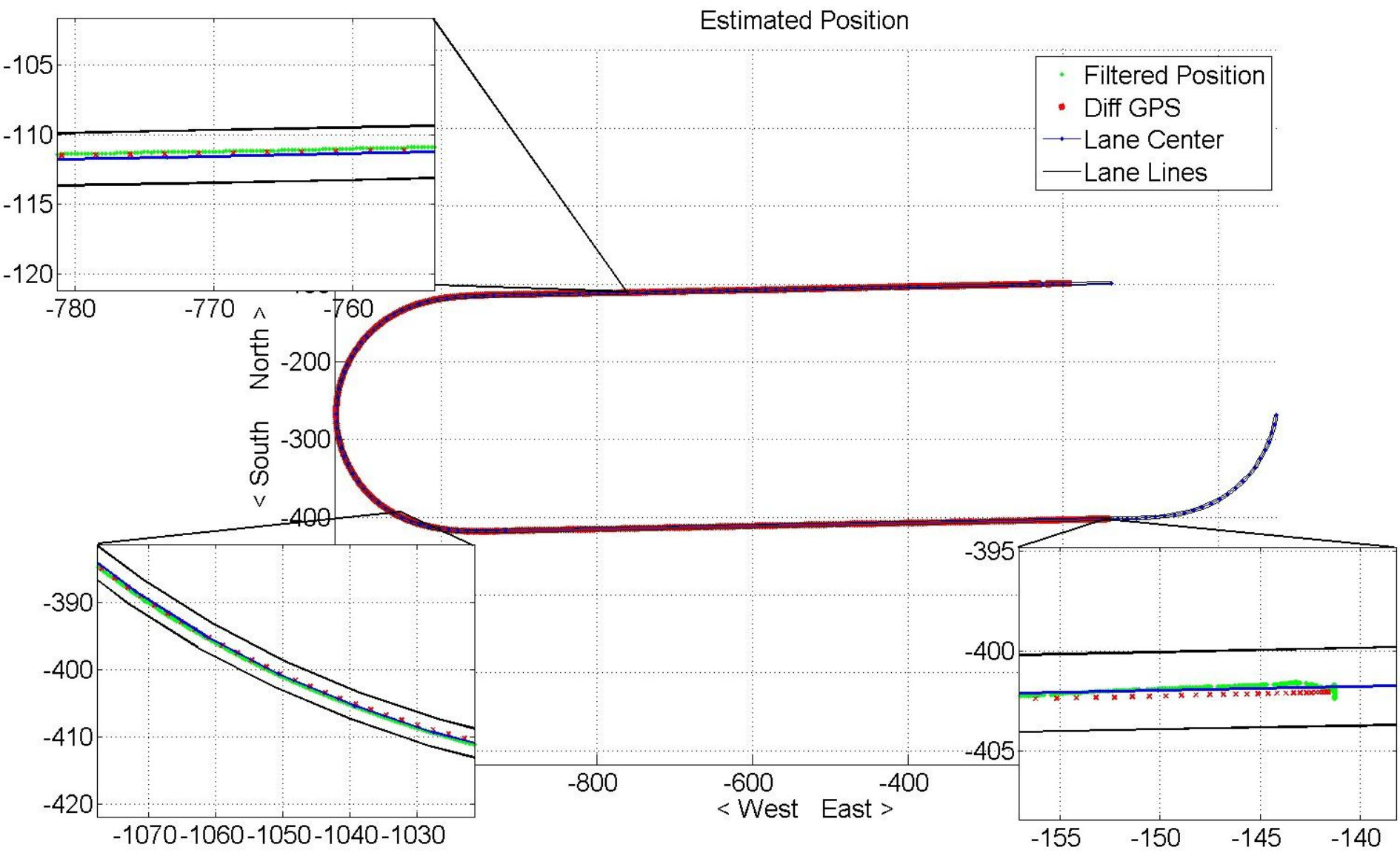
Estimated Position
Filtered Position
Diff GPS
Lane Center
Lane Lines
-105
-110
-115
-120
-780
-770
-760
< South North >
-200
-300
-400
-390
-400
-410
-420
-1070
-1060
-1050
-1040
-1030
-800
-600
-400
< West East >
-395
-400
-405
-155
-150
-145
-140

Results

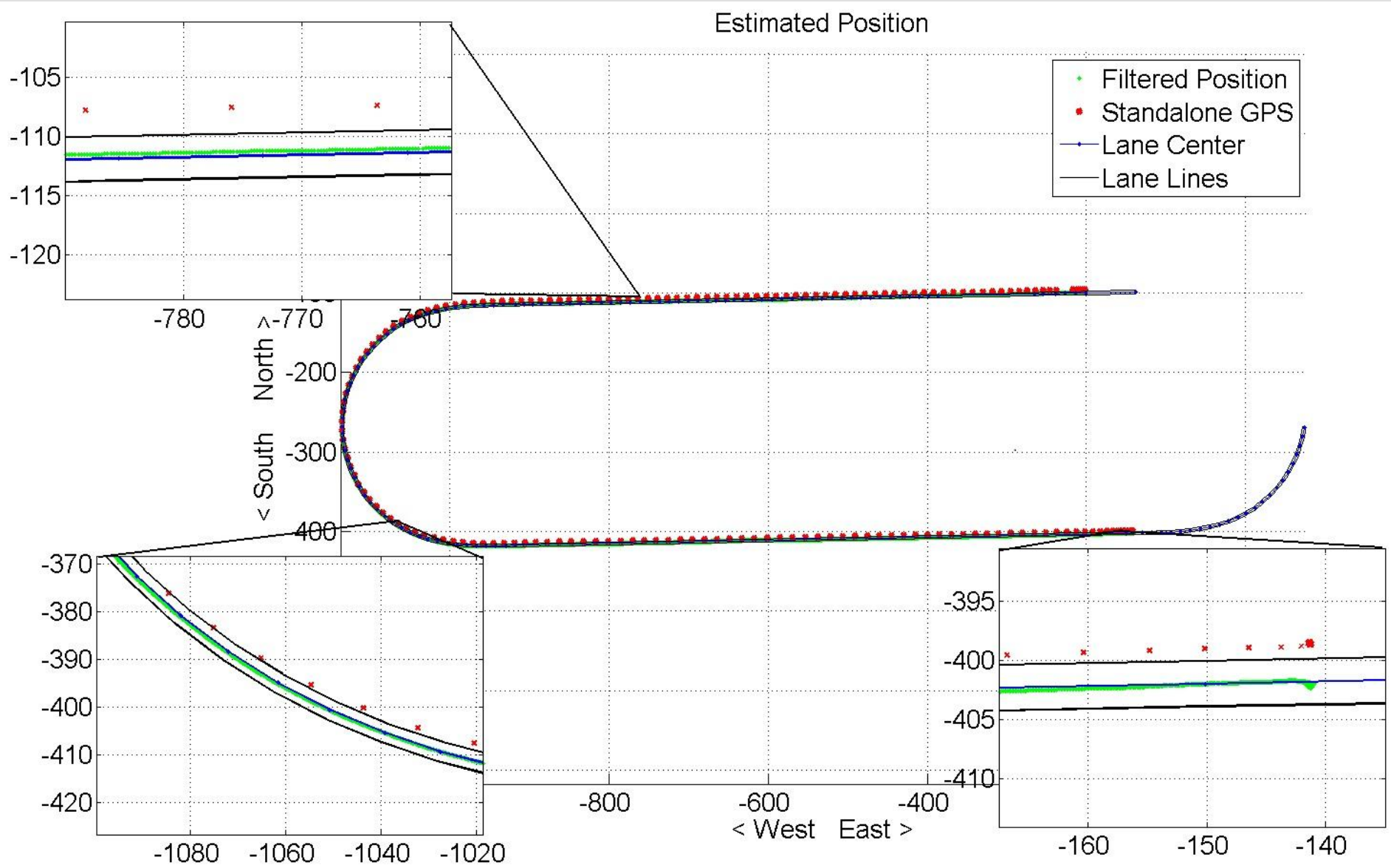
Estimated Position
Filtered Position
Standalone GPS
Lane Center
Lane Lines
-105
-110
-115
-120
-780
-770
-760
-200
-300
-400
< South North
-370
-380
-390
-400
-410
-420
-1080
-1060
-1040
-1020
-800
-600
-400
< West East >
-395
-400
-405
-410
-160
-150
-140


www.fraps.com
Failure Point
©2010 Google

Results

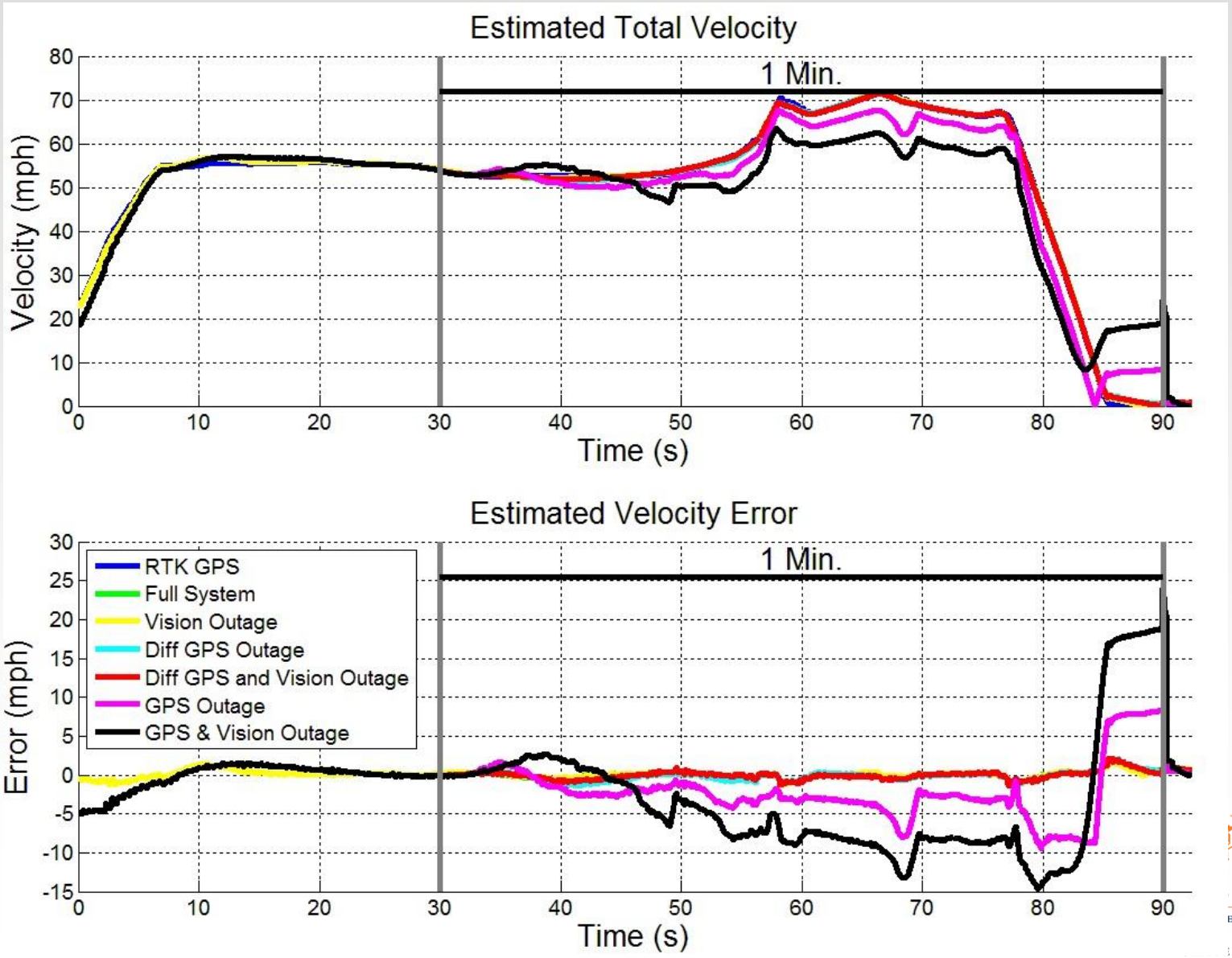

Results

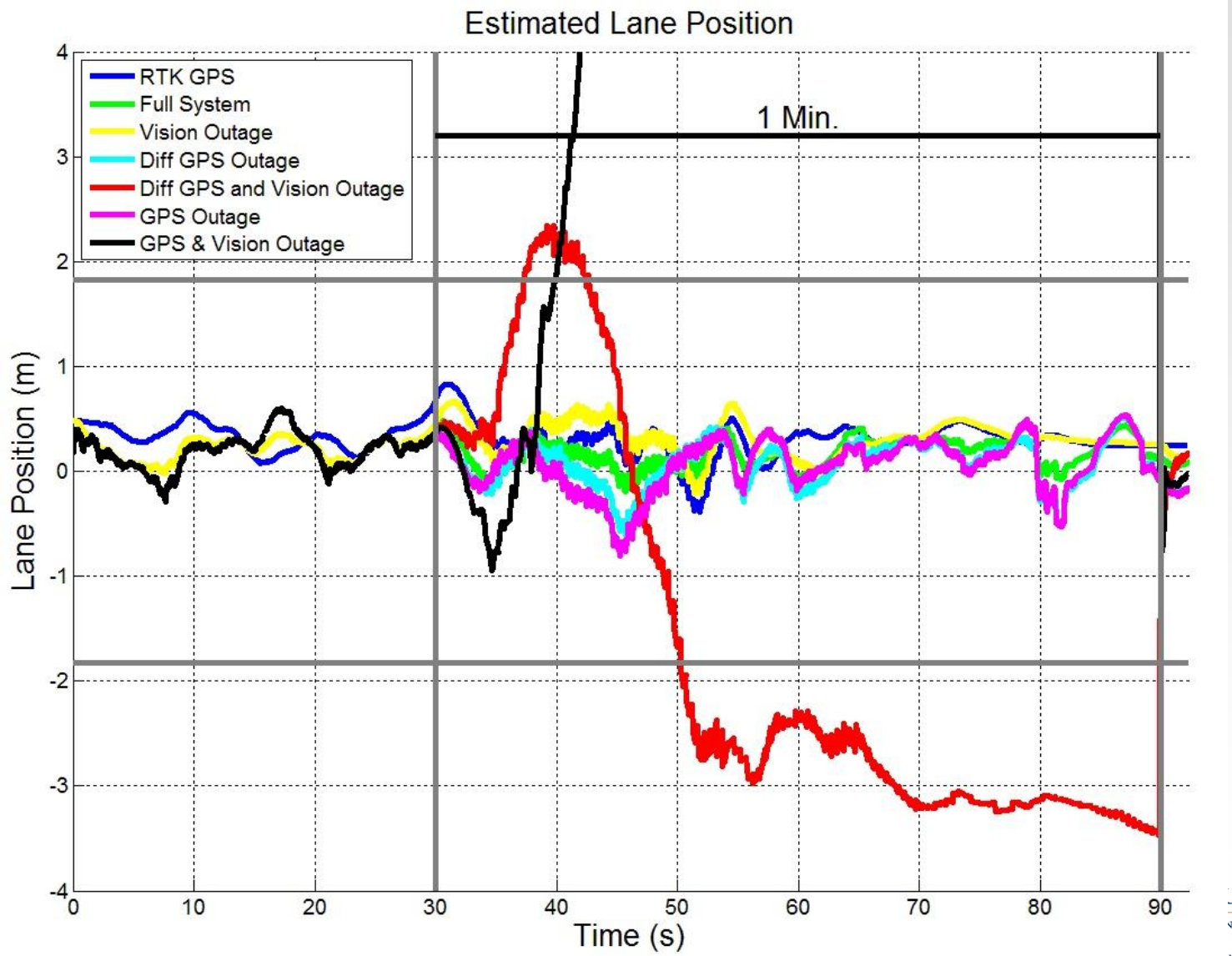

Results

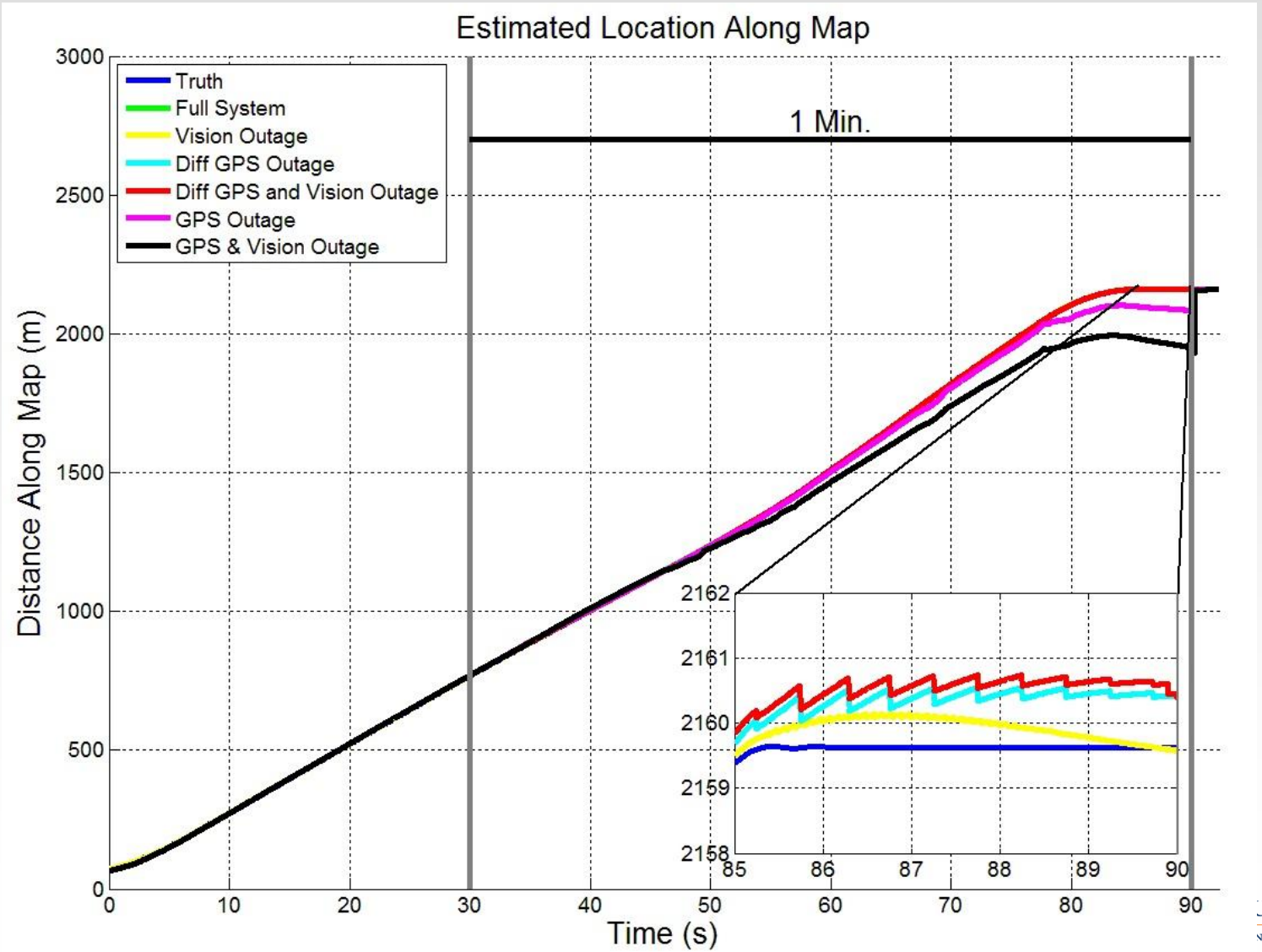

Results

- Availability of differential GPS or vision measurements will result in lane level accuracy.
  - Standalone GPS can not achieve lane level position without the aid of vision
- Longitudinal position remains accurate as long as GPS is available.
  - Vision can be used to maintain lane position with no GPS, however, this will result in longitudinal position drift

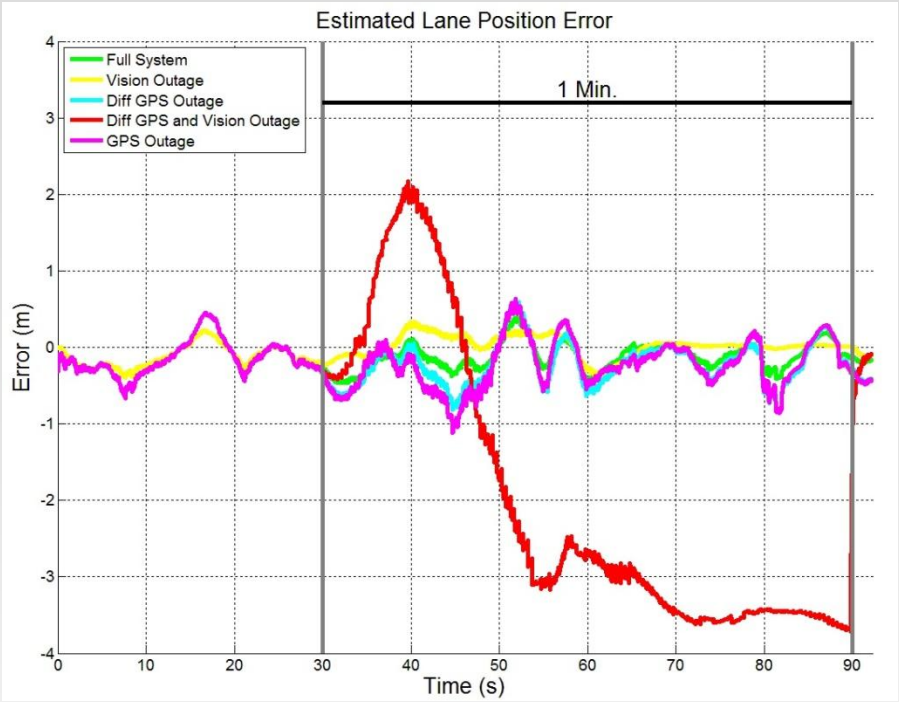

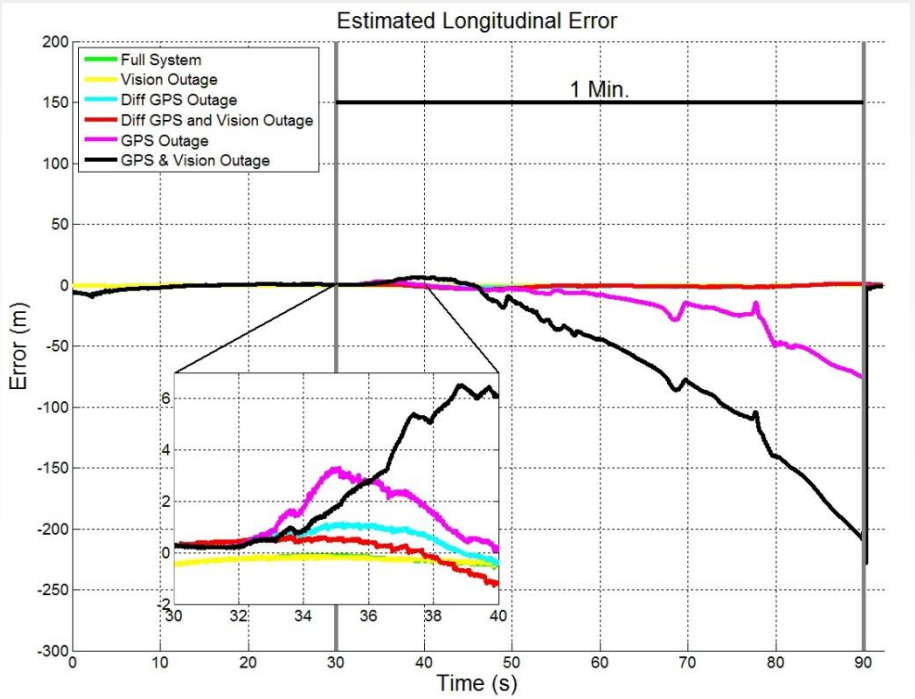

Observabilty Analysis

- 11 States
- These equation assume a steady state attitude
- G=gravity vector expressed in navigation coordinate frame
- u=IMU input
  - u_1-u_3=accelerometer inputs

states

$$X = \begin{bmatrix} x \\ y \\ z \\ \dot{x} \\ \dot{y} \\ \dot{z} \\ b_{ax} \\ b_{ay} \\ b_{az} \\ ct_u \\ \dot{ct_u} \end{bmatrix} = \begin{bmatrix} X_1 \\ X_2 \\ X_3 \\ X_4 \\ X_5 \\ X_6 \\ X_7 \\ X_8 \\ X_9 \\ X_{10} \\ X_{11} \end{bmatrix}$$

EOM

$$\dot{X}_{11\times1} = \begin{bmatrix} X_{4:6} \\ C_{\text{Body}}^{\text{Nav}}(u_{1:3} - X_{7:9}) - G - \Omega \\ 0_{1\times3} \\ X_{11} \\ 0 \end{bmatrix}$$

AUBURN UNIVERSITY
SAMUEL GINN COLLEGE OF ENGINEERING

Closely Coupled (4 Observations)

- rank(OBS)=11 if the unit vector to each SV is independent
- Requires at least 4 observations to be fully observable.

$$C=\begin{bmatrix} a_1 & b_1 & c_1 & 0 & 0 & 0 & 0 & 0 & 0 & 1 & 0 \\ 0 & 0 & 0 & a_1 & b_1 & c_1 & 0 & 0 & 0 & 0 & 1 \\ a_2 & b_2 & c_2 & 0 & 0 & 0 & 0 & 0 & 0 & 1 & 0 \\ 0 & 0 & 0 & a_2 & b_2 & c_2 & 0 & 0 & 0 & 0 & 1 \\ a_3 & b_3 & c_3 & 0 & 0 & 0 & 0 & 0 & 0 & 1 & 0 \\ 0 & 0 & 0 & a_3 & b_3 & c_3 & 0 & 0 & 0 & 0 & 1 \\ a_4 & b_4 & c_4 & 0 & 0 & 0 & 0 & 0 & 0 & 1 & 0 \\ 0 & 0 & 0 & a_4 & b_4 & c_4 & 0 & 0 & 0 & 0 & 1 \end{bmatrix}$$

unit vector to sv1=[a_1 b_1 c_1]
unit vector to sv2=[a_2 b_2 c_2]
unit vector to sv3=[a_3 b_3 c_3]
unit vector to sv4=[a_4 b_4 c_4]

$$A=\begin{bmatrix} O_{3\times3} & I_{3\times3} & O_{3\times3} & O_{3\times1} & O_{3\times1} \\ O_{3\times3} & O_{3\times3} & -C_{BODY}^{NAV} & O_{3\times1} & O_{3\times1} \\ O_{3\times3} & O_{3\times3} & O_{3\times3} & O_{3\times1} & O_{3\times1} \\ O_{1\times3} & O_{1\times3} & O_{1\times3} & 1 & 0 \\ O_{1\times3} & O_{1\times3} & O_{1\times3} & 0 & 0 \end{bmatrix}$$

$$OBS=\begin{bmatrix} C \\ CA \\ CA^2 \\ .... \\ CA^{13} \end{bmatrix}$$

AUBURN UNIVERSITY
SAMUEL GINN COLLEGE OF ENGINEERING

H Tightly Coupled (2 Observations)

$$H=\begin{bmatrix} a_1 & b_1 & c_1 & 0 & 0 & 0 & 0 & 0 & 0 & 0 & -1 & 0 \\ 0 & 0 & 0 & a_1 & b_1 & c_1 & 0 & 0 & 0 & 0 & 0 & -1 \\ a_2 & b_2 & c_2 & 0 & 0 & 0 & 0 & 0 & 0 & 0 & -1 & 0 \\ 0 & 0 & 0 & a_2 & b_2 & c_2 & 0 & 0 & 0 & 0 & 0 & -1 \\ 0 & 0 & 0 & 0 & 0 & 0 & 0 & 0 & 0 & 1 & 0 & 0 & 0 \end{bmatrix} \longrightarrow C=\begin{bmatrix} a_1 & b_1 & c_1 & 0 & 0 & 0 & 0 & 0 & 0 & 1 & 0 \\ 0 & 0 & 0 & a_1 & b_1 & c_1 & 0 & 0 & 0 & 0 & 1 \\ a_2 & b_2 & c_2 & 0 & 0 & 0 & 0 & 0 & 0 & 1 & 0 \\ 0 & 0 & 0 & a_2 & b_2 & c_2 & 0 & 0 & 0 & 0 & 1 \\ a_3 & b_3 & c_3 & 0 & 0 & 0 & 0 & 0 & 0 & 0 & 0 \\ a_4 & b_4 & c_4 & 0 & 0 & 0 & 0 & 0 & 0 & 0 & 0 \end{bmatrix}$$

rank(obs)=8

$$OBS=\begin{bmatrix} C \\ CA \\ CA^2 \\ .... \\ CA^{13} \end{bmatrix}$$

rank(obs)=13

AUBURN UNIVERSITY
SAMUEL GINN COLLEGE OF ENGINEERING

Observability Analysis (2 Observations)

	Elevation	Azimuth
SV1	60°	90°
SV2	30°	-90°

$$H = \begin{bmatrix} 0 & .5 & -.866 & 0 & 0 & 0 & 0 & 0 & 0 & 1 & 0 \\ 0 & 0 & 0 & 0 & .5 & -.866 & 0 & 0 & 0 & 0 & 1 \\ 0 & -.866 & -.5 & 0 & 0 & 0 & 0 & 0 & 0 & 1 & 0 \\ 0 & 0 & 0 & 0 & -.866 & -.5 & 0 & 0 & 0 & 0 & 1 \\ 0 & 1 & 0 & 0 & 0 & 0 & 0 & 0 & 0 & 0 & 0 \\ 0 & 0 & 1 & 0 & 0 & 0 & 0 & 0 & 0 & 0 & 0 \end{bmatrix}$$

- No x axis position or x axis velocity information is provided by the GPS observations. This causes a loss of observability.

$$OBS = \begin{bmatrix} C \\ CA \\ CA^2 \\ .... \\ CA^{13} \end{bmatrix}$$

rank(obs)=10

Observability Analysis (2 Observations)

	Elevation	Azimuth
SV1	45°	0°
SV2	45°	180°

$$H = \begin{bmatrix} .707 & 0 & -.707 & 0 & 0 & 0 & 0 & 0 & 0 & 1 & 0 \\ 0 & 0 & 0 & .707 & 0 & -.707 & 0 & 0 & 0 & 0 & 1 \\ -.707 & 0 & -.707 & 0 & 0 & 0 & 0 & 0 & 0 & 1 & 0 \\ 0 & 0 & 0 & -.707 & 0 & -.707 & 0 & 0 & 0 & 0 & 1 \\ 0 & 1 & 0 & 0 & 0 & 0 & 0 & 0 & 0 & 0 & 0 \\ 0 & 0 & 1 & 0 & 0 & 0 & 0 & 0 & 0 & 0 & 0 \end{bmatrix}$$

- No y axis position or y axis velocity information is provided by the GPS observations: however, the system is still observable because the vision measurements provide information in the y axis.

$$OBS = \begin{bmatrix} C \\ CA \\ CA^2 \\ .... \\ CA^{13} \end{bmatrix}$$

rank(obs)=13

NCAT Test Track

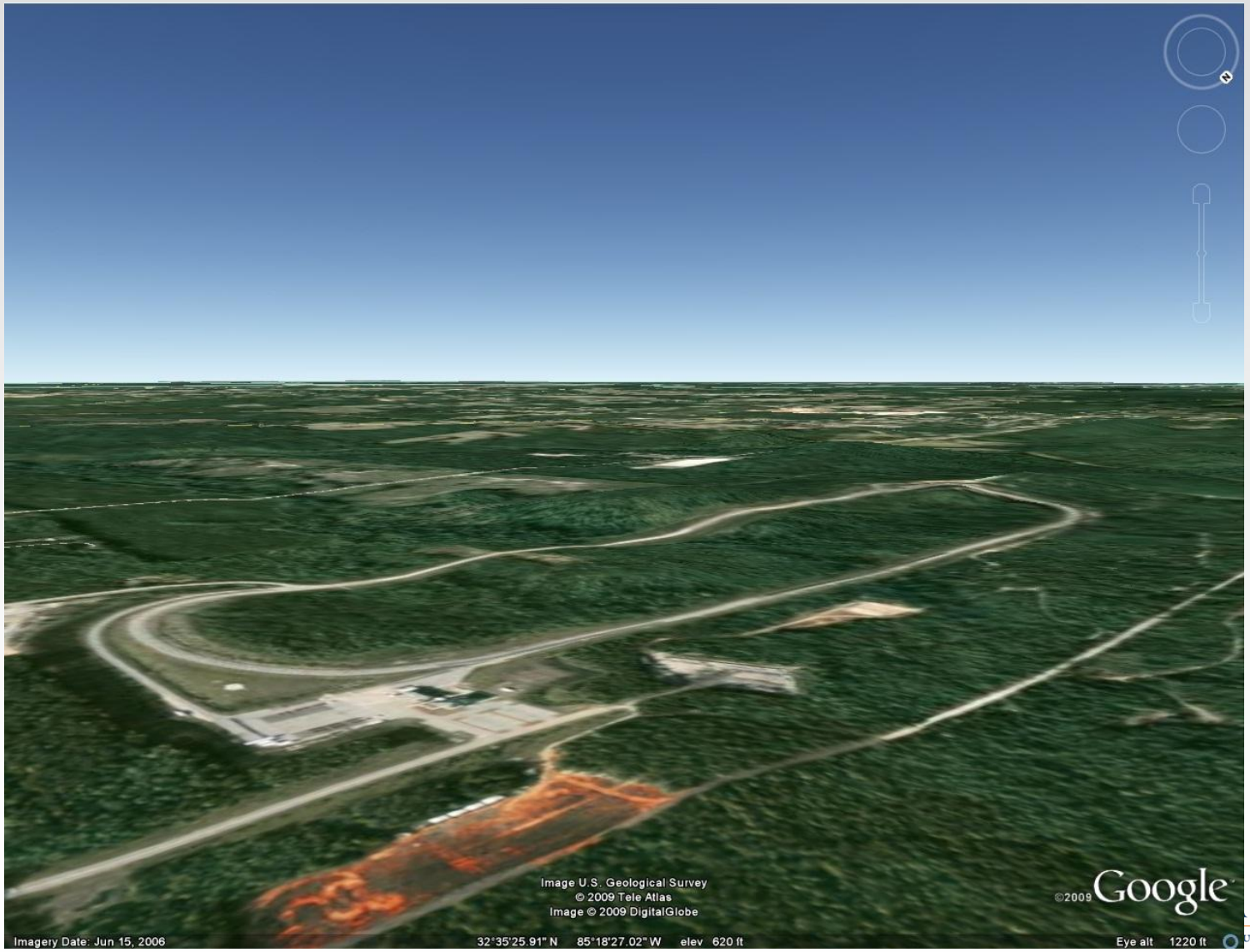

AUBURN UNIVERSITY
SAMUEL GINN COLLEGE OF ENGINEERING

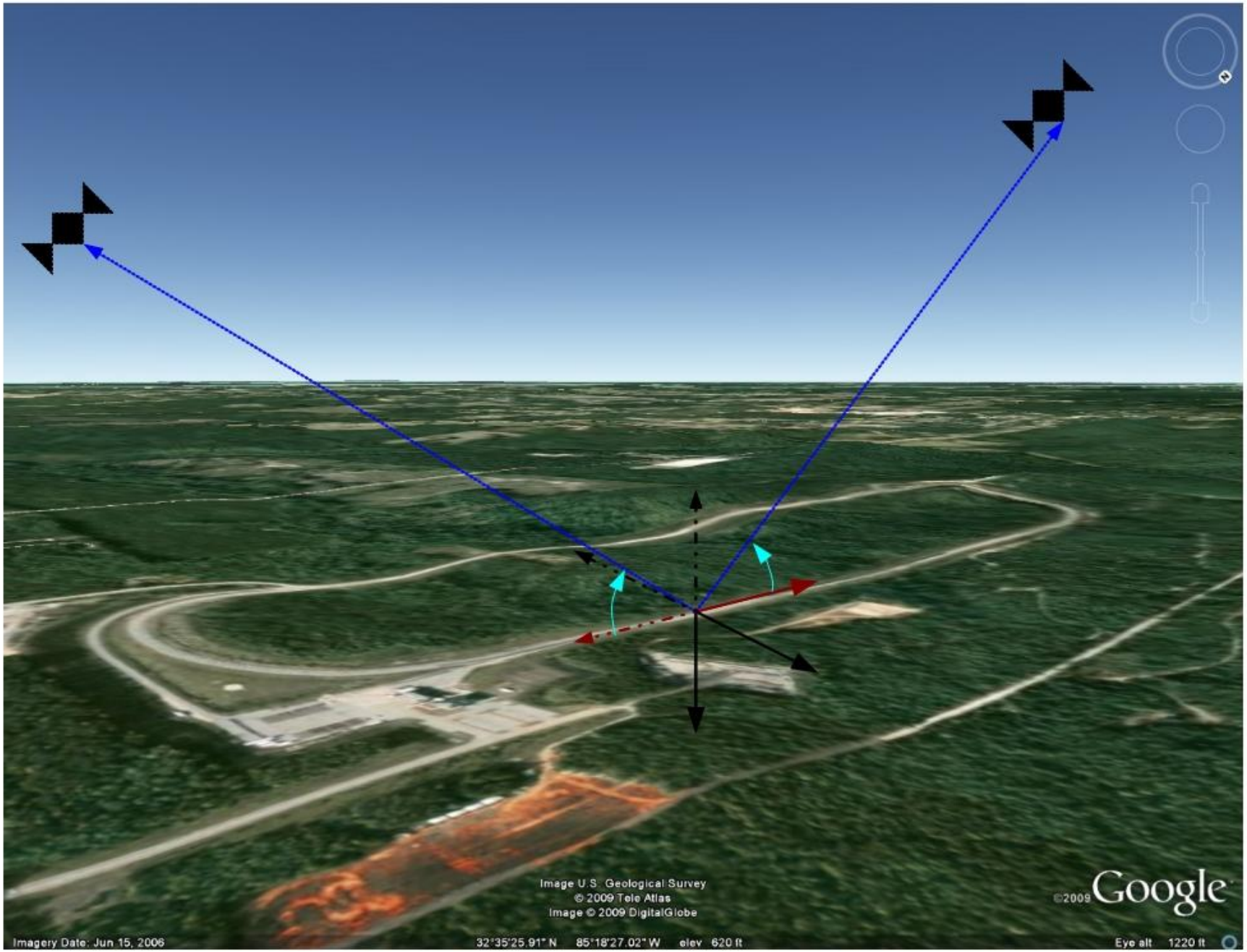
Image U.S. Geological Survey
© 2009 Tele Atlas
Image © 2009 DigitalGlobe
©2009 Google
Imagery Date: Jun 15, 2006
32°35'25.91" N 85°18'27.02" W elev 620 ft
Eye alt 1220 ft

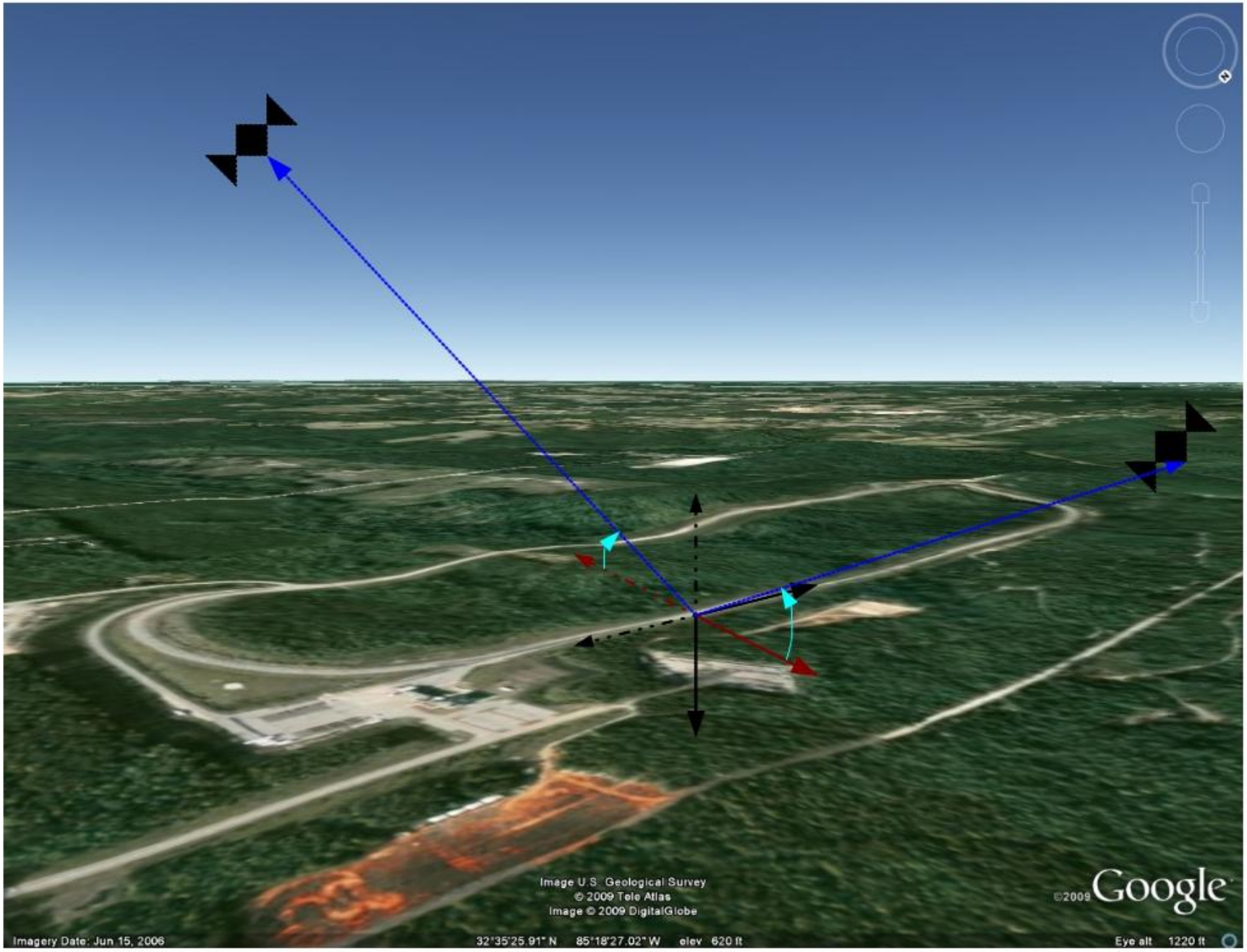
Image U.S. Geological Survey
© 2009 Tele Atlas
Image © 2009 DigitalGlobe
©2009 Google
Imagery Date: Jun 15, 2006
32°35'25.91" N 85°18'27.02" W elev 620 ft
Eye alt 1220 ft

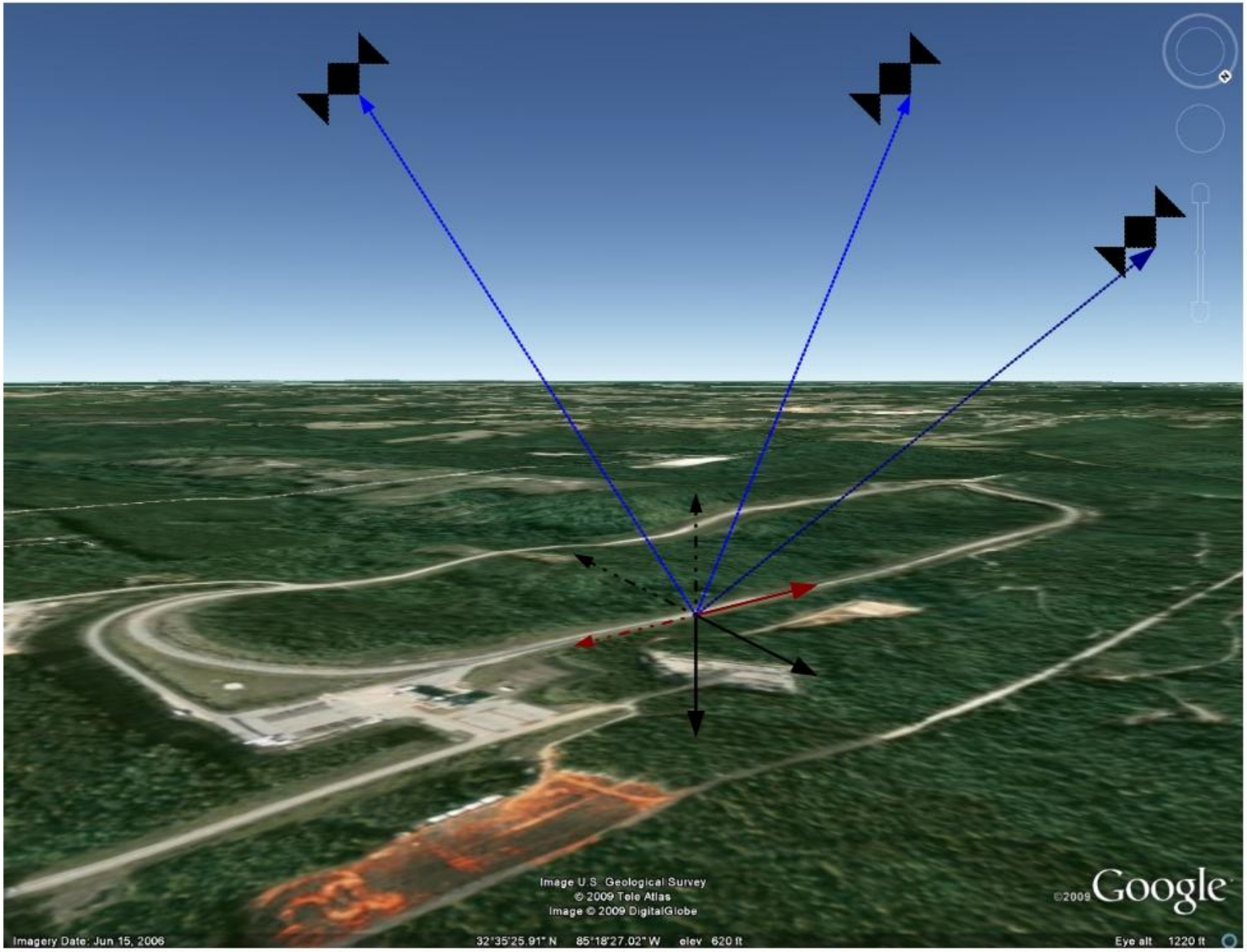
Image U.S. Geological Survey
© 2009 Tele Atlas
Image © 2009 DigitalGlobe
©2009 Google
Imagery Date: Jun 15, 2006
32°35'25.91" N 85°18'27.02" W elev 620 ft
Eye alt 1220 ft

Results

	Elevation	Azimuth
SV5	19°	63°
SV9	16°	151°
SV15	80°	100°
SV18	38°	-80°
SV21	52°	-39°
SV26	44°	47°
SV27	25°	129°
SV29	49°	148°

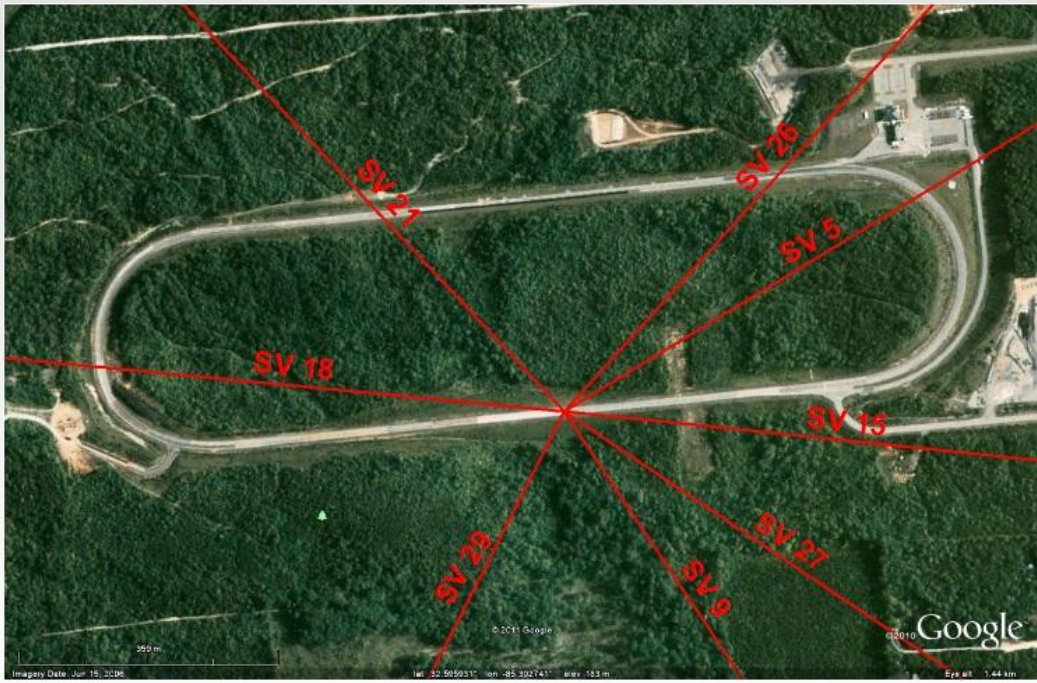

AUBURN UNIVERSITY
SAMUEL GINN COLLEGE OF ENGINEERING

Results

- Velocity error directly corresponds to number of observations available
- Using vision during satellite outages results in better overall velocity estimation
- There is no benefit when using only 1 GPS observation

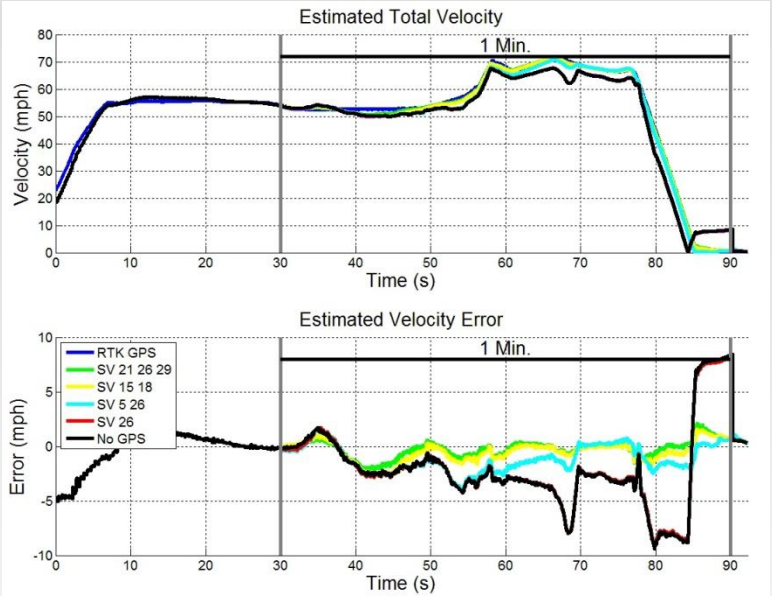

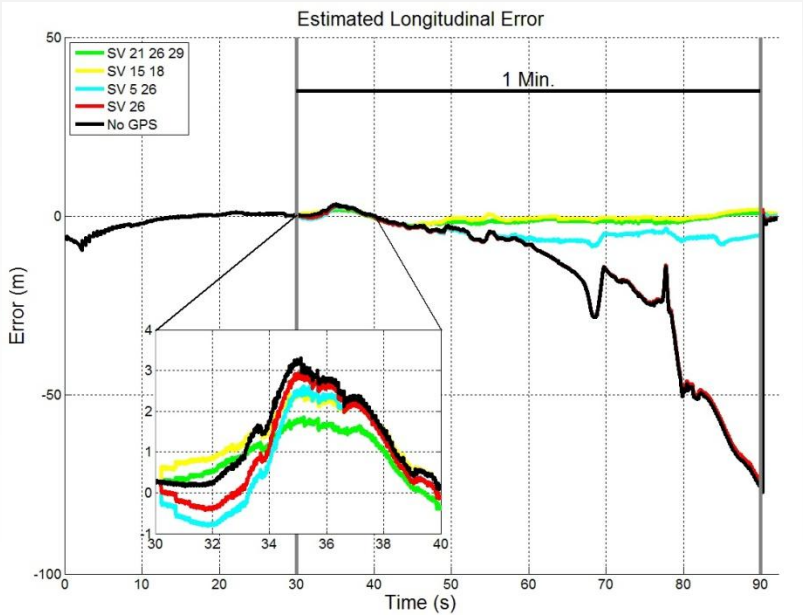

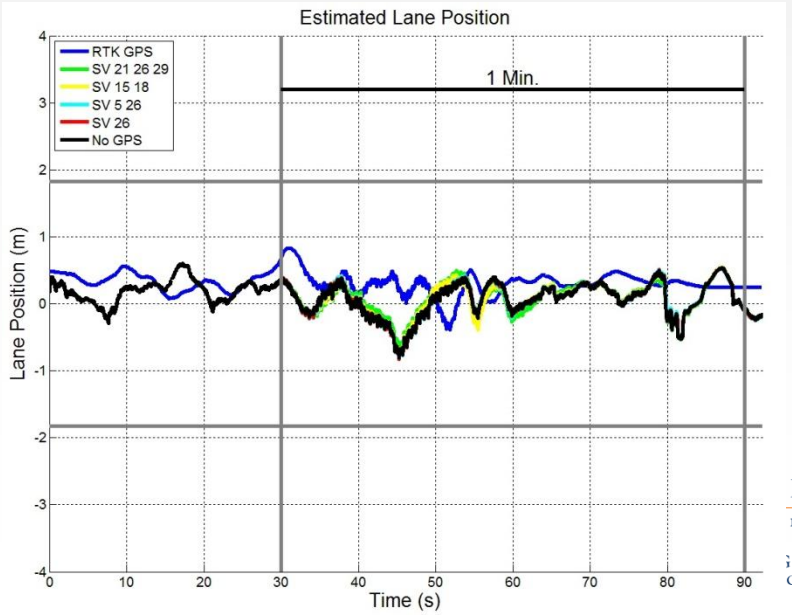

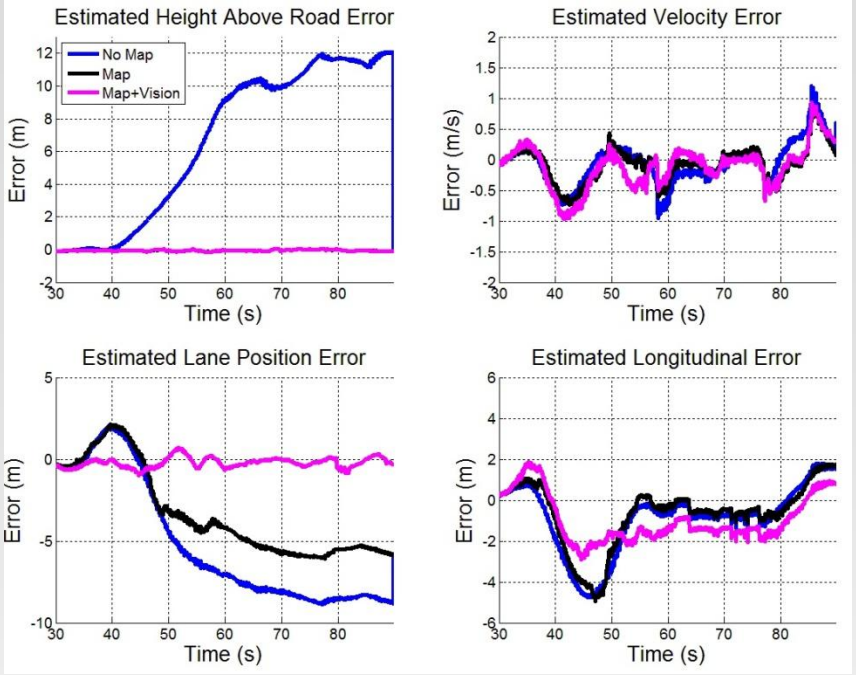

SV 21 26 29

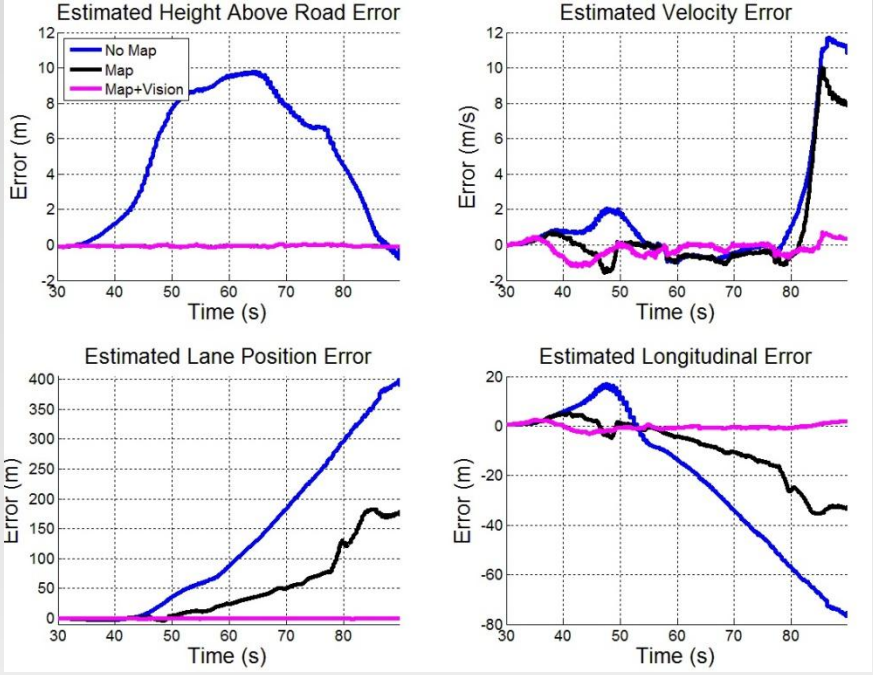

SV 15 18

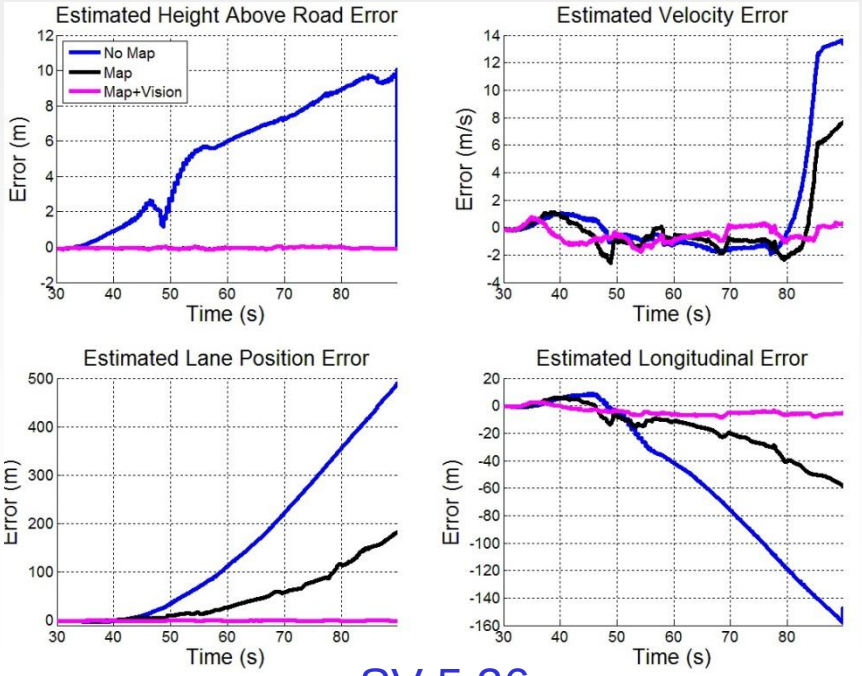

SV 5 26

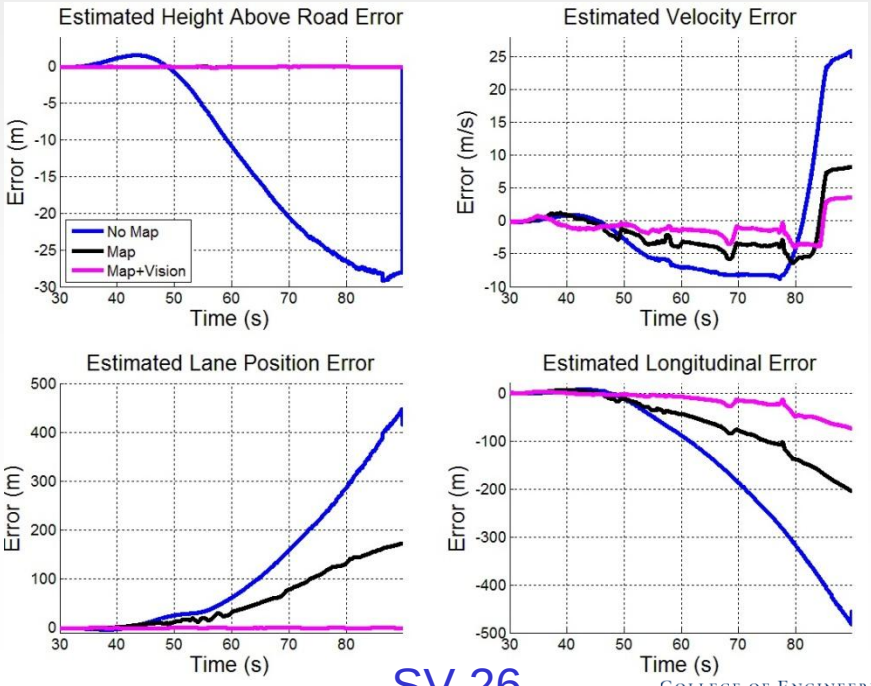

SV 26

Results

	C2N
SV5	48
SV9	48
SV15	54
SV18	53
SV21	52
SV26	48
SV27	42
SV29	51

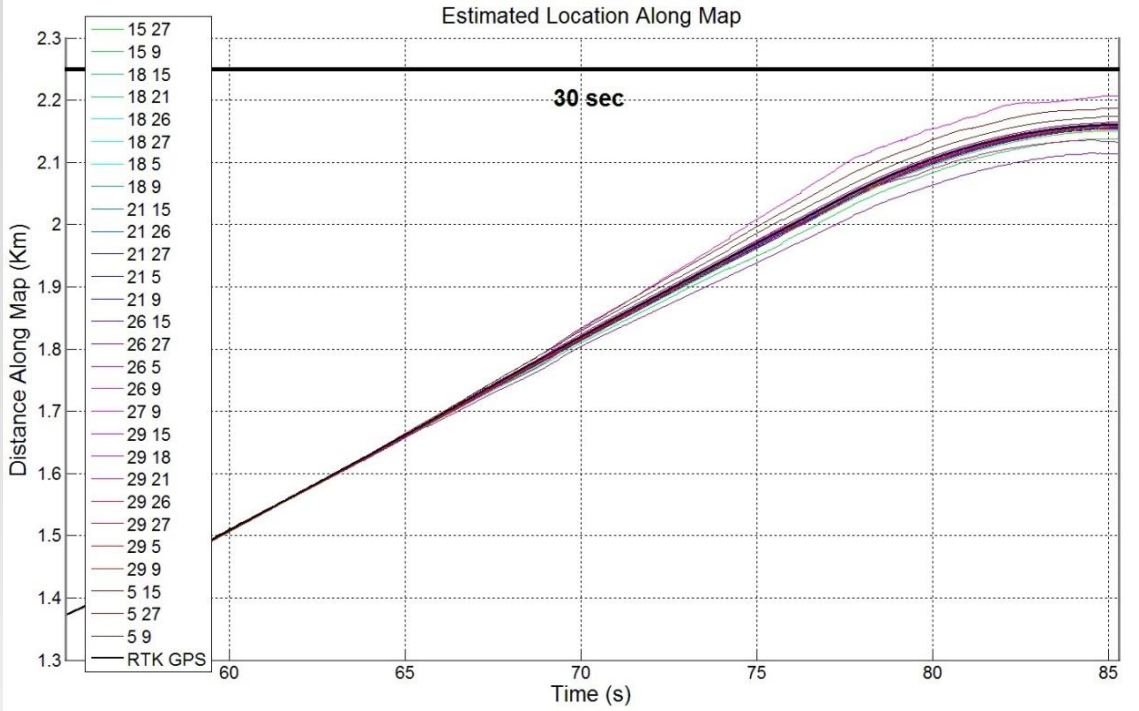

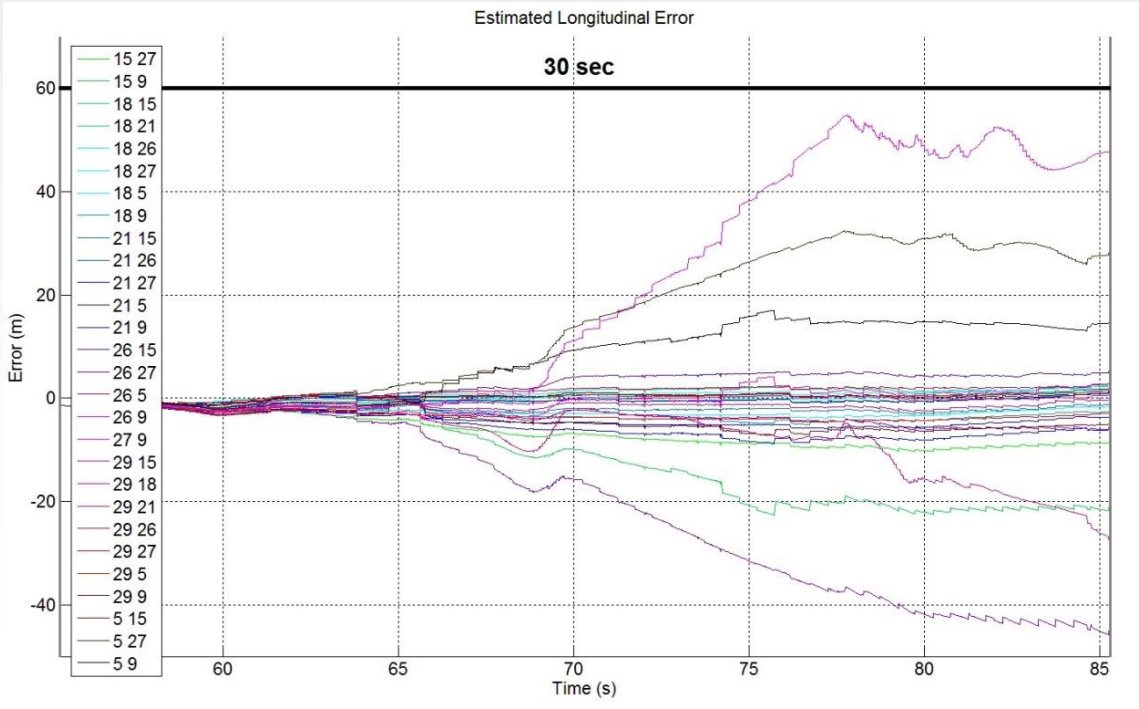

Conclusions

- It is possible to use measurements in a coordinate frame that is not aligned with the navigation coordinate frame.
- This technique can be applied to any situation where the measurement coordinate frame and navigation coordinate frame do not align.
- Using an accurate map along with vision based lane position measurements will improve global accuracy in 2 dimensions.
- It is possible to have a fully observable navigation filter only using 2 GPS satellites as long as supplemental measurements are provided. Using only 2 GPS satellites will result in more estimate error than using a full GPS satellite constellation.
- Effects of satellite geometry will increase as the number of GPS observations used decreases.

Future Work

- Use multiple waypoint maps to create a filter that can track lane changes and track the current lane the vehicle resides
- Use DSRC ranging, visual odometry, and road signature maps to further improve robustness
- Develop maps that incorporate road bank
- Develop maps that are equation based instead of way-point based.
- Use of SLAM or other techniques simultaneous positioning and mapping.